INVESTIGATING THE EXTRACELLULAR MATRIX IN PULMONARY FIBROSIS

INVESTIGATING THE EXTRACELLULAR MATRIX'S ROLE IN PULMONARY FIBROSIS TO APPROPRIATELY MODEL DISEASE AND TEST ANTIFIBROTIC THERAPIES

By

CHANDAK UPAGUPTA, Hon. B.Sc.

A Thesis Submitted to the School of Graduate Studies in Partial Fulfillment of the Requirements for the Degree Doctor of Philosophy

McMaster University

DOCTOR OF PHILOSOPHY (2019) McMaster University
Department of Medical Sciences Hamilton, Ontario, Canada

TITLE: Investigating the extracellular matrix's role in pulmonary fibrosis to appropriately model disease and test antifibrotic therapies

AUTHOR: Chandak Upagupta, Hon. B.Sc. in Biochemistry (McMaster University)

SUPERVISOR: Dr. Martin Kolb

NUMBER OF PAGES: xiv, 168

LAY ABSTRACT

Idiopathic pulmonary fibrosis (IPF) (idiopathic - unknown cause; pulmonary - lungs; fibrosis - scarring) is characterized by progressive scarring of the lung extracellular matrix (ECM). The ECM is an organ's backbone that provides structural and biochemical support to surrounding cells. Continued ECM scarring can lead to difficulty breathing, cough, and ultimately death. The cause of IPF is unknown, however, studies suggest that the scarred ECM can promote further scarring, and cause disease progression. In this thesis, we summarized the current knowledge of how the ECM interacts with cells. Using a 3D model we see that depending on the ECM's structure and composition, it can promote both disease and healthy cellular changes. Lastly, we evaluate if researchers are appropriately using the bleomycin model (most common preclinical model for pulmonary fibrosis) by testing interventions after ECM fibrosis is established. We propose changes to improve its usefulness as a preclinical tool for IPF.

ABSTRACT

IPF is a progressive disease, characterized by dysregulated fibrosis of the extracellular matrix (ECM). The pathobiology of the disease is still unknown, and the median survival post-diagnosis is about 3-5 years. The two current US FDA approved drugs for IPF (nintedanib and pirfenidone) slow, but fail to reverse, disease progression.

There is cumulating research that suggests the ECM is an active player in fibrosis. In this thesis, we summarized the current knowledge of ECM-cell interactions in the context of pulmonary fibrosis. To gain more mechanistic insight into the ECM characteristics that dictate cell behavior, we established a 3D ECM *ex vivo* system to assess the nonfibrotic and fibrotic ECM's effect on fibroblasts. The ECM appears to promote both pathological and physiological cellular changes, depending on its structural and compositional properties. We also used this 3D *ex vivo* system as a preclinical tool to test the effect of directly inhibiting mechanotransduction in the fibrotic ECM – fibroblast profibrotic relationship. Lastly, since the fibrotic ECM seems to play a key role in progressive fibrosis, we evaluate if researchers are appropriately using the bleomycin model by starting interventions after ECM fibrosis is established. Over the past decade in the field, there has been an overall improvement in the appropriate therapeutic timing. In the preventative studies, however, there is still an inadequate characterization of inflammation. There is also poor transparency of preclinical-bleomycin data for clinically tested interventions for IPF. Addressing these shortcomings may improve the utility of the model at predicting an intervention's success in clinical trials.

These findings illustrate the ECM's role in driving pulmonary fibrosis. Therefore, the ECM should be further investigated to understand disease progression, and reproduced in preclinical models to test interventions. This will improve the transition of pathobiological findings into efficient drug development for this devastating disease.

AKNOWLEDGMENTS

It takes a village to raise a child – African proverb

I was a bewildered child when I started my Masters, and if it wasn't for the many people that so supportively took me under their wing, I would still be lost today. I would like to first thank my supervisor, Dr. Martin Kolb, for taking a chance on me and being understanding and supportive of my goals in and outside of research. Thank you for always believing in me and encouraging me to strive for success. You offered me so many unique opportunities throughout my Ph.D., which helped me grow and make memories beyond my wildest dreams. I would also like to thank Dr. Kjetil Ask who always had an open door to for me to go in for a chat. Together, Dr. Kolb and Dr. Ask taught me how to foster a collaborative research environment, and instilled in me skills of resilience and teamwork which will prove beneficial for both my academic and personal life. I would like to also thank Dr. Marin Stämpfli and Dr. Jeremy Hirota who provided guidance and helped me be a more effective researcher and thinker.

One of my first mentors in the lab was Dr. Pierre Simon-Bellaye. He was always selfless and patient, regardless of how busy he was with his work, or how many times I would ask him to repeat himself. He taught me to be patient and keep a level head in research. Dr. Chiko Shimbori was my second mentor, and she showed me how to be a hard worker. Together they would listen to my struggles and without them, my first few years as a graduate student would have been unfathomable. I would be remiss if I did not mention Dr. Ehab Ayaub and Dr. Jewel Imani. Though they were not in my lab, the amount of help they

offered me throughout my graduate degree was beyond measure. The late nights you spent in the lab listening to my committee presentations, reading my reports, helping me bounce ideas meant so much. You are like my older brothers, and never once hesitated to help me be a better student and researcher.

I would like to also thank the Japanese duo: Dr. Seidai Sato and Dr. Toyoshi Yanagihara. I had so much fun working with Dr. Sato, and his witty humor always lightened the mood, especially during the frequent 12 hr workdays we would have together. Dr. Yanagihara is one of the hardest workers I have had the privilege of working alongside. He taught me how to balance my work and personal life, and offered me the skills to be productive. I am so grateful for having had the opportunity to work with you both and am excited to collaborate with you in the future. I would also like to thank our lab technician, Dr. Fuqin Duan. You were the mother of the lab and without your help, running our experiments would have been a lot harder than it needed to be.

Thank you to Phil Kolb, Karun Tandon, Safaa Naiel, Tina Nham, and Victor Tat and all my other dear lab mates and friends. You were tasked with keeping me sane and I think you guys did a pretty decent job. To my close friends Darren Thai and Sal Macaluso, though you were not in science, you always helped me weather the stress of being a researcher and were always willing to offer whatever type of help you could. Most importantly, I would like to thank my parents. You have held my hand, supported me and believed in my dreams. I don't say it enough, but I love you with all my heart, and your support means the world to me.

TABLE OF CONTENTS

List of figures and Tables

None

List of abbreviations

AdTGF-β1	Adenoviral Vector Containing Active TGF-Beta 1
AdDL	Adenoviral Vector containing Delete Vector
α-SMA	Alpha Smooth Muscle Actin
AEC	Alveolar epithelial cells
CCL	C-C Motif Chemokine Ligand
EndMT	Endothelial-to-mesenchymal transition
EMT	Epithelial-to-Mesenchymal Transition
ECM	Extracellular Matrix
FAP	Fibroblast Activation Protein
f-actin	Filamentous-actin
FAK	Focal adhesion kinases
FVC	Forced vital capacity
GPCRs	G-protein-coupled receptors
GAPDH	Glyceraldehyde 3-phosphate dehydrogenase
H&E	Hematoxylin and Eosin
IPF	Idiopathic Pulmonary Fibrosis
iPSCs	Induced Pluripotent Stem Cells
IL	Interleukin
ILD	Interstitial lung disease
LLC	Large latent complex
LT	Lysis treatment
LOX	Lysyl oxidase
LOXL	Lysyl oxidase Like enzymes
MMPs	Matrix metalloproteinases
MKL1	Megakaryoblastic leukemia factor-1
PSR	Picrosirius red
ROCK	Rho-associated protein kinase
SDC	Sodium deoxycholate
SDS	Sodium dodecyl sulfate
TAZ	Transcriptional co-activator with the PDZ-binding motif
TGF-β1	Transformation Growth Factor-Beta1
TGs	Transglutaminases
TRPV4	Transient receptor potential vanilloid 4
YAP	Yes-associated protein

Preface

This Ph.D. thesis is presented in a "Sandwich" format. It follows the instructions outlined in the "Guide for the Preparation of Master's and Doctoral Theses" from the School of Graduate Studies at McMaster University.

Chapter 1: Briefly introduces the field of study, objectives, and general concepts needed to understand the papers presented.

Chapter 2-4: Includes the three independent, yet related projects completed during the Ph.D. Together they first summarize the current understanding of ECM-cell interaction, followed by establishing and using a model system to further assess this relationship in the context of pulmonary fibrosis. Finally, understanding the importance of the pathological ECM in driving pulmonary fibrosis, we assess how this is incorporated when using the preclinical – bleomycin model for pulmonary fibrosis. Below I outline the duration, current status, and my contribution for each project:

Chapter 2: Encyclopedia of Respiratory Medicine, 2nd Edition Chapter: The Extracellular Matrix-Cell Interaction in ILD.

Chandak Upagupta[1], Toyoshi Yanagihara[1], Martin Kolb[1]

This book chapter was written between January 2019 – April 2019. Writing this manuscript required a robust understanding of the current field of ECM-cell interaction, and the role of this relationship in driving pulmonary fibrosis. This expertise was developed over the course of my Ph.D. work, and from the insight gathered while writing a review article titled Matrix abnormalities in Pulmonary fibrosis, published in the European Respiratory

Review. Also, my work as the second author of the book chapter: The Role of Mast Cells in the Pathophysiology of Pulmonary Fibrosis, published in SpringerLink's Fibrosis in Disease, taught me how to use scientific data to effectively translate complex information. As the first author of this book chapter, I reviewed the literature and presented the current understanding of how the lung ECM interacts with cells in the context of ILD. TY and MK assisted with editing the manuscript. This manuscript is under revision.

Chapter 3: Structure and Composition of Decellularized Extracellular Matrix scaffolds from nonfibrotic and Ad-TGFβ1-induced fibrotic lungs have opposing effects on fibroblast to myofibroblast differentiation in 2 and 3 dimensional settings.

Chandak Upagupta[1], Seidai Sato[1], Toyoshi Yanagihara[1], Pierre-Simon Bellaye[1], Chiko Shimbori[1], Shannon Gui[2], Kjetil Ask[1] and Martin Kolb[1]

This project was completed between October 2015 – January 2019, beginning at the start of my Masters and continued throughout the course of my Ph.D. As the primary author, I designed and performed the majority of experiments, analysis, interpretation and presentation of the generated date in a manuscript. SS, TY, PSB, CS and SG assisted in experiments. KA and MK supervised the project and edited the manuscript. This manuscript is ready for submission to Matrix Biology.

Chapter 4: The Importance of Interventional Timing in the Bleomycin Model of Pulmonary Fibrosis.

Philipp Kolb[1*], Chandak Upagupta[1*], Kjetil Ask[1], Ehab Ayaub[1], Pierre-Simon Bellaye[1], Jack Gauldie[1], Chiko Shimbori[1], Martin RJ Kolb[1]
*These authors contributed equally to this work.

This project was completed between October 2014 – March 2019. A fellow student (PK) started the initial project in 2014, before I started my Master's. After I joined the team in 2015, PK graduated, and I oversaw the rest of the project. This included collecting data from the majority of publications included in this study, and working with PK to analyze and present the collected information. I also prepared the final manuscript and revisions for publication. PK, EA, PSB and CS helped with the data collection. PK, KJ, JG and MK assisted in preparing and editing the manuscript.

Chapter 5: Includes a discussion section for the three projects included in this thesis. It highlights the major findings and their implications to improve the pathobiological understanding and drug development pipeline for pulmonary fibrosis. Potential future directions are also included.

Chapter 1

Introduction

Pulmonary fibrosis

Interstitial lung disease (ILD) is an umbrella term for a group of lung pathologies characterized by lung scarring, which contribute to disease progression and mortality [1]. The 4 major disorders under ILD are sarcoidosis, idiopathic pulmonary fibrosis (IPF), hypersensitivity pneumonitis, and asbestosis. IPF is a chronic disease with irreversible scarring of lung tissue, commonly the peripheral (subpleural) lung parenchyma. IPF has a median survival post-diagnosis of about 3-5 years, with a mortality rate higher than common cancers [2, 3]. IPF presents around 60-70 years of age, and in the United States, has a prevalence of 42.7 per 100,000 people and an incidence rate of 16.3 per 100,000 people per year [4].

Shortness of breath, caused by excessive lung scarring and stiffening is one of the first symptoms patient's experience. Therefore, by the time IPF is diagnosed, significant pathological changes have already occurred. This late diagnosis has made understanding IPF etiology difficult [5]. There are currently two FDA-approved drugs: nintedanib and pirfenidone, which *in vitro* inhibit pathways in the wound healing response, and in patients slow the decline of lung function. These drugs, however, fail at stopping or reversing IPF progression [6]. This leaves lung transplantation as the only remaining treatment, but due to shortages in organ donors, this option is not accessible to most patients [7]. Therefore more insightful studies into disease pathobiology and drug discovery are needed. This requires improvements to how IPF progression is studied, modeled, and how interventions are preclinically tested. This will improve the use of available resources and may facilitate the development of more successful therapeutics for this progressive disease.

Pathological changes and cellular contributors to Pulmonary fibrosis

The extracellular matrix (ECM) provides structural and biochemical support for resident cells and serves as an organ's backbone. In the lung, this backbone creates the intricate microstructure and provides the mechanical rigidity and elastic recoil required for respiratory function. The ECM is comprised of a network of macromolecules such as collagen, elastin, glycoproteins, and proteoglycans. The ECM structure is constantly changing and maintained by a balance between deposition and degradation. "Controlled" ECM scarring/fibrosis is an indispensable wound healing response that facilitates contraction and prompts recovery of the wound. Following repair, the scarred matrix is resolved to re-establish the soft microenvironment needed for healthy lung function. In IPF and other ILDs, the scarring is persistent and irreversible and it destroys the parenchyma, epithelial barrier, and alveolar architecture. This leads to increased lung rigidity, dysfunction, and ultimately death [8]. Different cells have been implicated in the pathological ECM fibrosis, with myofibroblasts being one of the major contributors.

Under physiological conditions, mesenchymal cells called fibroblasts are responsible for the constant ECM remodeling, through both ECM protein deposition and degradation [9]. In response to an injury, the mechanical and chemical stimuli from the surrounding microenvironment trigger the assembly of stress fibers composed of cytoplasmic actin to activate fibroblasts. Once in the activated form, fibroblasts have increased cell-to-cell and cell-to-matrix interactions, increased contractility, and produce more ECM proteins. With enough profibrotic stimulation, fibroblasts can fully differentiate into myofibroblasts, which have elevated α-smooth muscle actin (α- SMA) expression [10].

Compared to other actin isoforms, α-SMA has significantly increased contraction, which offers myofibroblast's characteristically high contractile activity. During an injury, fibroblasts and myofibroblasts play an integral role in scarring and the normal wound healing response. Resident fibroblasts in the perivascular and peribronchiolar adventitia or circulating fibrocytes (progenitors of fibroblasts) in the plasma are recruited to the site of injury via chemotaxis [9, 11]. Here, these cells are stimulated to differentiate into activated fibroblasts or fully differentiated myofibroblasts, and cluster to form regions called fibroblastic foci. During the active phase of repair, the increased contractility of myofibroblasts in these fibroblastic foci stiffens the surrounding microenvironment. Myofibroblasts also produce large amounts of ECM proteins such as collagen and fibronectin, which facilitates the scarring process [10]. Once the repair process is complete, myofibroblasts are removed via apoptosis [12], and most of the scarred matrix is subsequently degraded and resolved by matrix metalloproteinases (MMPs) [13]. Collectively, these processes are crucial for a healthy wound healing response. In IPF and other ILDs, however, myofibroblasts are resistant to apoptosis [14]. Histological analysis of IPF patients shows a marked elevation of myofibroblast percentage, accumulating in fibroblastic foci in the lung [15]. These myofibroblasts produce large amounts of ECM proteins that facilitate the characteristic ECM thickening and scarring seen in ILD.

A study performed by Zhang et al. in 1994 demonstrated that perivascular and peribronchiolar adventitial fibroblasts were the major precursors for myofibroblasts, which increased collagen deposition in bleomycin-induced pulmonary fibrosis [16]. Until the last decade, fibroblasts were therefore believed to be the main and only precursor for

myofibroblasts. Through further investigation, it is now accepted that myofibroblasts can originate from a few different sources such as epithelial cells [17, 18], endothelial cells, pericytes and fibrocytes [19, 20].

Epithelial cells

Aside from fibroblasts, epithelial cells are another major source for myofibroblasts via epithelial to mesenchymal transition (EMT). Cells exposed to profibrotic mediator such as transforming growth factor beta (TGF-β) undergo EMT [21]. TGF-β induces SMAD activation, which causes disassembly of epithelial-specific morphology and molecular markers such as E-cadherin, to give way for mesenchymal specific markers such as α-SMA, and increased cellular motility. Inhibition of TGF-β–induced EMT, using the TGF-β signaling antagonist: BMP-7 protects mice against kidney, liver, biliary tract, lung, and intestinal fibrosis [22, 23]. In the alveoli of lungs, there are two classes of epithelial cells: alveolar type 1 (AEC I) and type 2 (AEC II) epithelial cells [24]. AEC I make up about 90% of the alveolar epithelial cells and are responsible for forming a barrier that can sense microbial products, generate inflammatory responses, and participate in gaseous exchange. AEC II are less abundant than AEC I, however, they play an important role in repairing the epithelium when injured. Due to AEC II's role in wound healing, they are investigated as potential players in fibrosis. In IPF patients, isolated AECs have been seen to express collagen 1 [25]. AECs which express both mesenchymal and epithelial cell markers are also important for the formation of fibroblastic foci, and therefore the progression of IPF [21]. Furthermore, studies have also shown that epithelial injury can trigger fibrogenic processes in the lung [26]. Specifically, injury increases ER stress markers and the unfolded

protein response, which subsequently induces EMT in AECs, potentially initiating and driving pulmonary fibrosis [27–29].

Endothelial cells

Endothelial cells form the continuous monolayer on the luminal surface of the lung vasculature, and provide a surface for the exchange of gases, water, and macromolecules [30]. The pulmonary endothelium is also metabolically active and participates in immunological and inflammatory responses. Though a bit more controversial, like epithelial cells, endothelial cells have also been seen to differentiate into myofibroblasts via a process called endothelial-to-mesenchymal transition (EndMT). Profibrotic stimuli can promote endothelial cells to undergo EndMT, during which cells lose their endothelial phenotype such as CD31 expression, and express mesenchymal markers such as α-SMA and collagen. In a mouse model of cardiac fibrosis, TGF-β-induced EndMT was important for the development of fibrosis [31, 32]. Systemic administration of recombinant human BMP-7 significantly inhibited EndMT, and the progression of cardiac fibrosis. Furthermore, labeled endothelial cells in transgenic mice were shown to undergo EndMT to give rise to collagen 1 and α-SMA positive cells in the bleomycin model of pulmonary fibrosis [33].

Pericytes

As the search for pathological sources of myofibroblasts in fibrosis continued, researchers identified pericytes as a potentially significant precursor in 2010. Pericytes are periendothelial cells with a rounded cell body and cytoplasmic process that surround endothelial cells [34, 35]. Pericytes are responsible for vascular development, stabilization,

and integrity. Using genetic cell-labeling techniques, pericytes were seen to be a major myofibroblast progenitor in various organ fibrosis including the lung, liver, and kidneys [35, 36]. Interestingly, in this study, pericytes were a more important source for myofibroblasts than EMT. Furthermore, human pericytes have also been shown to adopt myofibroblast properties in the microenvironment of IPF lungs [37].

Fibrocytes

Fibrocytes are bone marrow-derived circulating mesenchymal progenitor cells [38]. These cells have both hematopoietic and mesenchymal cell characteristics such as CD45 and collagen 1 expression. Fibrocytes express many chemokine receptors such as C-C chemokine receptor 3, 5, and 7, and are rapidly recruited during injury via chemokines [39]. Once at the site of injury, fibrocytes facilitate wound healing by differentiating into fibroblasts and myofibroblasts and contributing to ECM scarring [38]. Fibrocytes are also elevated in the lungs and blood of IPF patients and are further increased during episodes of acute exacerbation [40]. Circulating fibrocyte levels have therefore shown some efficacy as a prognostic biomarker for IPF severity and progression [11]. Despite these findings, the overall impact of fibrocytes in pulmonary fibrosis is still not completely understood, and more research is needed to fully establish them as key players in progressive pulmonary fibrosis.

These are some of the different myofibroblast precursors, which all seem to play a role in the development and progression of pulmonary fibrosis. The therapeutic potential of targeting cellular pathways to inhibit differentiation of these cells into myofibroblasts have been tested in preclinical and clinical settings, however, none have proven effective

at stopping/reversing disease progression in patients [41]. Furthermore, the diversity in precursors highlights the need for a more holistic approach, one that influences the different cells types and is able to more robustly target the different molecular drivers of pulmonary fibrosis.

The ECM's effect on cell phenotype

The aberrant ECM changes during the progression of ILD creates a unique microenvironment with structural and compositional cues that influence cell behavior and phenotype. There is a growing body of research that suggests this ECM-cell interaction may play a notable role in progressive fibrosis. Specifically, accumulation and persistence of myofibroblasts lead to ECM fibrosis. The microenvironment of this fibrotic ECM stimulates profibrotic behavior and myofibroblast differentiation of surrounding cells. This creates a positive feedback loop that causes further ECM fibrosis and subsequent disease progression. For a more in-depth overview of the ECM-cell interaction in the context of ILD please see chapter 2. The major concepts covered in this chapter are summarized here in this section of the introduction.

The ECM is comprised of over 300 proteins that make up the matrisome core. This includes polysaccharides, glycosaminoglycans, ECM-binding growth factors, and ECM-modifying enzymes. Under both physiological and pathological conditions, the ECM structure is dynamically remodeled and constantly changing. In ILD, this remodeling is dysregulated and overtime causes accumulation of ECM proteins such as proteoglycans, collagen, elastin, and fibronectin. Proteoglycans are made up of ECM core proteins bound

to a highly charged glycosaminoglycan. This forms the integral hydrated gel, which binds to collagen and elastin fibers to establish the lung's alveolar structure and mechanical stability. Fibrillar collagen is the most abundant type of collagen in the lung and is crucial for tensile strength and functionality. Elastin fibers attach to collagen and contribute to the lung's elastic recoil. Glycoproteins such as fibronectin are responsible for mediating cell-matrix adhesions by binding ECM proteins such as collagen and cell-surface integrins.

In fibrotic lungs, dysregulated expression causing accumulation of these ECM components which have profibrotic effects. For example, increased proteoglycan-glycosaminoglycan complexes in IPF lungs causes destruction of lung architecture [42]. Accumulating collagen around myofibroblasts within fibroblastic foci causes increased stiffness within these regions [43]. Elastin is also elevated in bleomycin-treated mouse lungs [44]. Furthermore, studies have shown that elastin enhances TGF-β1-induced myofibroblast differentiation. Fibronectin and other glycoproteins are also abundantly found in the lungs of IPF patients [45]. Similar to elastin, fibronectin is also essential in driving myofibroblast differentiation. These are some of the compositional changes that underpin the characteristically elevated stiffness and rigidity seen in pulmonary fibrosis.

Effect of ECM Stiffness on cell phenotype

Studies have shown that various cell types have the capacity to sense mechanical cues from their surrounding microenvironments [46, 47]. There are two major working theories proposed to understand this: the tethered and the membrane model [48][49]. Briefly, the tethered model states that cells sense mechanical cues by anchoring directly to

the ECM through integrins and forming focal adhesions. These anchors allow mechanical cues from the ECM to quickly move intracellularly and induce downstream changes, much faster than ligand-stimulated second-messenger based pathways [50, 51]. On the other hand, the membrane model states that changes in membrane tension in response to mechanical cues activate integral membrane proteins such as G-protein coupled receptors (GPCRs) [52]. *In vitro* studies have shown that mechanical cues can activate GPCRs in the absence of its receptor-specific agonist. GPCRs are expressed in almost all cell types and induce a cascade of intracellular effects.

In light of these findings, it is not surprising that numerous cell types change their behavior and undergo differentiation in response to mechanical cues [46, 47]. *In vitro* studies have clearly shown that fibroblast to myofibroblast differentiation is strongly correlated with substrate stiffness [53–55]. Specifically, increased stiffness stimulates fibroblasts to produce profibrotic mediators (e.g. TGF-β1) and ECM proteins, while a physiological stiffness inactivates myofibroblasts and favor their apoptosis [53–55]. In line with the tethered model of mechanosensing, one potential mechanism for fibroblasts to respond to stiffness is via f-actin polymerization and focal adhesions. This causes nuclear translocation of megakaryoblastic leukemia factor-1, which induces the expression of fibrotic genes, including α-SMA. On softer matrices, less force is exerted, and actin cables and focal adhesions are less well developed [56]. Fibroblasts are not the only cells that undergo profibrotic changes in response to mechanical cues. Studies have shown that increased substrate stiffness also induces epithelial cells to undergo EMT [53, 57–59]. In addition to these structural pulmonary cells, inflammatory cells, such as macrophages and

mast cells are also sensitive to mechanical stress [46, 47, 60, 61]. Using a decellularization model, our group recently showed that the 3D fibrotic ECM alone is able to induce mast cell degranulation [62]. Degranulation of mast cells release profibrotic mediators such as TGF-β1 and is linked to the progression of IPF. For a more in-depth understanding of mechanosensing and stiffness induced cellular changes please see chapter 2.

Effect of ECM Composition on cell phenotype

MMPs cleave full-length ECM proteins during remodeling and can generate bioactive fragments [63]. Recent findings suggest that these soluble ECM fragments can also influence cell behavior. ECM fragments can bind to integral membrane proteins, such as integrins and EGFR receptors, to initiate intracellular changes. In the case of angiogenesis, bioactive ECM fragments can induce both pro- and anti-angiogenic effects [63]. As mentioned, the compositional makeup of the fibrotic ECM is markedly different than the physiological ECM. Collagen and hyaluronan are two examples of ECM proteins that are drastically upregulated. In liver fibrosis, MMP mediated degradation of Type VI collagen has been strongly linked to disease progression [64]. Similarly, in a study published by Collins et al., low molecular weight hyaluronan was shown to promote inflammation and fibrosis by downregulating the adenosine A2a receptor [65]. *In vitro,* supplementation of sonicated hyaluronan was also shown to induce EMT in alveolar type II epithelial cells [58].

ECM fragments are not the only bioactive components present in the ECM. Along with providing structural stability, the ECM also serves as a reservoir for the storage of growth factors. In response to appropriate stimuli, these growth factors are quickly

activated and released so they can execute their function on surrounding cells [66]. Interestingly, work published by our group and others have uncovered the role of mechanical cues in activating certain ECM bound growth factors, specifically TGF-β [67, 68]. Briefly, various cells such as fibroblasts, epithelial and endothelial cells produce TGF-β, which influences essential cellular processes such as cell growth, proliferation, differentiation, and apoptosis [69]. TGF-β is secreted as an inactive homodimer, and after binding to proteins to form complexes, it attaches to the ECM where it is stored until activation and release. The inactive TGF-β in the ECM binds to cells via integrins. Through stretching and mechanical cues during movement, the growth factor is wedged open from its ECM bound complex, releasing active TGF-β. TGF-β then goes on to induce significant profibrotic effects on different cell types in the lung. The increased TGF-β stored in fibrotic lungs, along with the increased mechanical cues in stiff lungs, may together explain the increased overall TGF-β activity seen in experimental models of fibrosis and IPF patient lungs [70, 71]. This process represents just one of the possible many in which the ECM composition and structure work together to influence the behavior of resident cells.

These findings highlight how the fibrotic ECM can promote a profibrotic behavior in cells, and how the ECM may play a key role in driving pulmonary fibrosis. The precise mechanisms of how the ECM influences cells, and to what extent is still largely unknown. This line of inquiry requires more accurate modeling systems to assess how the ECM interacts with cells to influence their behavior and differentiation. This can uncover key targetable pathways in the ECM-cell relationship, which may ultimately lead to viable therapies for pulmonary fibrosis.

Model systems to study the pathobiology of pulmonary fibrosis

Systems are needed to study the underlying mechanisms responsible for the development and progression of pulmonary fibrosis. It is important that these systems appropriately reproduce pathological and physiological conditions so that accurate insight can be gathered to empower future drug development. 2D *in vitro* plates are one of the most commonly used systems to culture and study cells. These systems are relatively inexpensive, and they offer rapid growth of cells and controlled conditions to study cellular changes. However, as we understand more of the complexities of the *in vivo* system and the diverse role they play in regulating cell behavior, it is important that our model systems also advance to improve the quality of our basic science research.

Tissue culture plates made of plastic are the most commonly used culture conditions for *in vitro* studies. The stiff conditions on plastic plates offer an easy surface for cells such as fibroblasts to attach to and grow. As discussed earlier, this stiffness induces morphological and physiological changes such as increased proliferation and cell contractility [53–55]. The rapid cell proliferation allows for easy culturing, however, it is important to note that this cellular behavior is characteristic of a pathological state. Numerous studies have shown soft plates with a physiological substrate stiffness of 1kPa to markedly attenuate proliferation of fibroblasts [53–55]. This is a sensitive relationship, where small increases in stiffness as low as 2, 25 or 50 kPa can induce notable increases in proliferation. Surprisingly, these stiffness conditions are all still vastly softer than the commonly used plastic plates which are about 10^6 kPa [72]. Furthermore, numerous *in vitro* studies have shown that increased substrate stiffness promotes fibroblasts to produce

profibrotic mediators, ECM deposition, and differentiation to myofibroblasts [53–55]. The importance of this issue is heightened by the findings of Balestrini et al. who noted that substrate stiffness imparts a persistent cell memory, which influences cell behavior even after cells are introduced into different stiffness conditions [54]. Therefore, when using these plastic plates to grow and study cells, the stiff conditions can have prolonged effects on cell phenotype. It is therefore important that these culturing limitations are considered, and cells are studied under substrate conditions that more appropriately resemble the physiological or pathological state of interest.

Gels made of polyacrylamide or silicone are commercially available, and can be used to homogeneously control substrate stiffness in 2D culture plates. Though stiffness can be controlled, there is still an issue of what exactly constitutes as a pathologically stiff condition. In pulmonary fibrosis, like other fibrotic diseases, fibrosis is heterogeneous and stiffness is unevenly distributed throughout the organ. Therefore, depending on the stage of the disease, the fibrotic lung will still have regions of physiological stiffness, marked by varying levels of fibrotic and rigid pockets usually in fibroblastic foci. Recreating this environment while maintaining the same level of heterogeneity and complexity can be very difficult; especially in an intricate organ system such as the lung.

One interesting approach to address these challenges is removing cellular material via decellularization to create 3D ECM scaffolds. Cells can then be recellularized into these scaffolds and used to study cell behavior under pathological or physiological conditions. These scaffolds maintain both the structural and chemical characteristics and natural binding sites present in native lungs. Booth et al. were one of the first to use acellular ECM

scaffolds from donor and IPF lungs to study ECM's effect on fibroblast behavior [73]. Sodium dodecyl sulfate (SDS), sodium deoxycholate (SDC), and 3-[(3-cholamidopropyl) dimethylammonio]-1- propanesulfonate (CHAPS) are three commonly used decellularization detergents, however, the concentration, and decellularization and recellularization techniques vary greatly between protocols. Furthermore, many recellularization techniques use a dropwise method to seed cells onto thin (~1 mm) ECM slices, which loses much of the ECM's 3D architecture. Therefore, a complete 3D model system that ensures optimal decellularization and recellularization, while also offering control over the scaffold's fibrosis is still needed. This model will improve currently available tools to study ECM – cell interaction, and advance our understanding of the lung ECM's role in pulmonary fibrosis.

Preclinical models for pulmonary fibrosis

Basic science models such as the ones discussed above provide key insights into disease pathology, however moving forward, appropriate preclinical *in vivo* models that reproduce patient pulmonary fibrosis are needed to translate these findings into effective drug development. Different approaches have been used in the literature to create *in vivo* models of pulmonary fibrosis, however, each have their unique advantages and disadvantages [74].

One example are viral vectors, which increase the expression of a recombinant gene in airway epithelial cells when administered directly into the lungs. Overexpression of various profibrotic genes such as TNFα, TGF-β and IL-1 have been used to establish models of pulmonary fibrosis [75]. Once introduced into the lungs, these transgenes persist

for up to 21 days and induce significant fibrotic lung injury in mice and rats. Adenoviral vectors thus provide valuable models to study pathogenesis, and serve as a preclinical model to test the anti-fibrotic efficacy of novel drugs. Recently, we investigated the effect of macitentan, a dual endothelial receptor antagonist approved for the treatment of pulmonary arterial hypertension, in an adenoviral TGF-β1 (adTGF-β1) vector model of fibrosis [76]. Unlike other models, the adTGF-β1 model induces significant pulmonary fibrosis accompanied by pulmonary hypertension, which is seen in a subset of patients with IPF. Therefore, this model offers a closer reproduction of the pulmonary abnormalities present in these patients and serves as a useful preclinical model for this disease subtype. Despite these advantages, adenoviral vectors have limitations such as a notable initial inflammatory response, and the organisms' adaptive immunity which prevents repeated dosing of the vector. Furthermore, adenoviral vectors have tropism mainly to epithelial cells, which along with the overexpression of one particular gene, creates a relatively specific fibrotic process; which is probably not the case in the complex patient pathobiology [74]. To account for the complex fibrogenesis, researchers have investigated injury-induced fibrosis. These models may more accurately resemble the consistent assault and injury present in patients, which creates the patchy and temporal heterogeneous fibrosis seen in their lungs.

One example of injury-induced fibrosis is the bleomycin model of pulmonary fibrosis. This model is one of the best characterized, and most commonly used preclinical model for pulmonary fibrosis. Multiple administration techniques and dosages of bleomycin have been shown to induce lung fibrosis in different animal systems including

mice, rats, dogs, and primates [74]. Single intratracheal administration of bleomycin damages the alveolar epithelial cells, by causing DNA strand breakage and oxidant injury [74, 75]. The injured lung releases chemokines such as CCL2 and CCL12 to recruit fibrocytes and other inflammatory cells. These cells induce profibrotic cellular changes, some of which are TGF-β dependent, to promote myofibroblast differentiation. This inflammatory phase lasts for approximately 7 days before subsiding into a fibrotic phase which is marked by drastic ECM deposition and lung scarring. The fibrotic phase in the bleomycin model is progressive and resembles the progressive fibrogenesis present in IPF patients [77]. However, spontaneous reversal of fibrosis, particularly in young mice, has been noted to occur 3-4 weeks post intratracheal bleomycin administration [78–81]. Therefore, since the fibrotic phase is typically no longer than two weeks [77], the "window" during which fibrogenic mechanisms can be studied and anti-fibrotic drugs should be tested is relatively short.

Despite these limitations, the bleomycin model of pulmonary fibrosis remains the best characterized and most commonly used preclinical model for this disease. Therefore, identifying and advocating for ways in which the model can be more effectively used will facilitate improved translation of basic science findings into fruitful drug development and therapeutic strategies for pulmonary fibrosis.

Central Aim and Thesis Objectives

The central hypothesis of this thesis is: the ECM plays a governing role in directing cell behavior, and the fibrotic ECM can induce profibrotic cellular changes to create a positive-feedback loop that can drive progressive fibrosis. Therefore, the fibrotic ECM needs to be appropriately assessed and modeled to understand the pathobiology of fibrosis and reproduce progressive fibrosis in preclinical models.

The thesis objective is to assess the current understanding of ECM-cell interaction in fibrosis, and then establish an *ex vivo* system to further elucidate the extent and mechanisms by which the ECM influences cell phenotype to drive pulmonary fibrosis. Next, we evaluate the use of a common preclinical model to see if researchers are appropriately timing interventions when fibrosis is established and adequately modeled. We identify shortcomings in the use of this preclinical model and propose changes to improve disease modeling and drug development for pulmonary fibrosis.

These objectives are separated by chapter below:

1. Assess the current understanding of ECM-cell interactions in interstitial lung disease (Chapter 2).
2. Establish a complete 3D *ex vivo* ECM scaffold system to directly study the nonfibrotic and fibrotic ECM's influence on cell phenotype (Chapter 3).
3. Assess the extent and mechanisms of the ECM's influence on fibroblast phenotype, in a 2D and 3D context (Chapter 3).

4. Evaluate the use of the bleomycin model, and assess if researchers are appropriately timing interventions to test antifibrotic efficacy (Chapter 4).
5. Identify shortcomings and propose changes to improve the utilization of the bleomycin model (Chapter 4).

Chapter 2

Encyclopedia of Respiratory Medicine, 2nd Edition Chapter: The Extracellular Matrix-Cell Interaction in ILD

Summary and Significance

Fibrotic diseases are not unique to the lung and are found in the liver, heart, and kidneys. Myofibroblasts are one of the major cell type known to cause fibrosis and ECM scarring. Myofibroblasts have various precursors, and inhibiting their differentiation to myofibroblasts has shown some antifibrotic efficacy *in vitro* and *in vivo*, however, have proven ineffective in patients. This highlights the need for a more holistic approach for targeting the different pathways and cellular drivers of fibrosis. There is a growing body of research suggesting that the fibrotic ECM works in conjunction with surrounding cells to create a vicious positive feedback loop that can drive rapid and persistent fibrosis. Since the ECM serves as a backbone for resident cells, the ECM can mechanically and chemically influence the behavior and differentiation of various cell types; all of which can potentially drive fibrosis. In this chapter we present the work done by researchers investigating how the ECM interacts with cells in the context of interstitial lung disease. We hope that this will establish the ECM as a key therapeutic target as we move forward in developing more effective therapies for fibrotic diseases, which have thus far been largely untreatable.

Encyclopedia of Respiratory Medicine, 2nd Edition Chapter:

The Extracellular Matrix-Cell Interaction in ILD

Chandak Upagupta[1], Toyoshi Yanagihara[1], Martin Kolb[1]

1. Firestone Institute for Respiratory Health, Department of Medicine, McMaster University, Hamilton, ON, Canada

Running title: The Extracellular Matrix-Cell Interaction in ILD.

Conflict of interest: All authors declared no conflicts of interest.

Status of the work: Book Chapter accepted for publication in "Encyclopedia of Respiratory Medicine, 2E".

Author contributions: Conception and design: CU, TY, MK. Performed review of current literature: CU, TY, MK; Drafting the manuscript: CU, TY, MK.

Corresponding author: Dr. Martin Kolb, Department of Medicine, McMaster University and The Research Institute of St. Joe's Hamilton, Firestone Institute for Respiratory Health, 50 Charlton Ave East, Room T2120, Hamilton, Ontario, Canada L8N 4A6, Ph. (905) 522.1155 ext. 33683; Fax (905) 521.6183; E-mail: kolbm@mcmaster.ca

ABSTRACT

Interstitial lung disease (ILD) is an umbrella term for a group of disorders characterized by lung inflammation and progressive fibrosis. The extracellular matrix (ECM) is a structural scaffold for cells, which provides mechanical stability and elastic recoil necessary for proper lung function. In ILD, the ECM undergoes aberrant structural and chemical changes, creating a uniquely pathological microenvironment for cells. Here we explore these changes, and how they interact with cells to facilitate progressive lung fibrosis in ILD.

KEY WORDS

Extracellular Matrix, Extracellular Matrix Composition, Fibrosis, Idiopathic Pulmonary Fibrosis, Interstitial Lung Disease, Mechanosensing, Mechanotransduction, Pulmonary Fibrosis

INTRODUCTION

The human body is a dynamic system with many delicate balances working in concert to maintain homeostasis. A deficiency in any one of these balances can lead to dysfunction and disease; importantly, in response to these imbalances, the body quickly tries to compensate by skewing other factors, which can either lead to a new balance or to the progression of the problem. This is the case in many diseases, and also true for Interstitial lung disease (ILD). ILD is an umbrella term for a group of disorders characterized by variable degrees of inflammation and scarring or fibrosis of the lung. In most cases, ILD is a chronic disease with progressive scarring of lung tissue (Selman and Pardo, 2014). Idiopathic pulmonary fibrosis (IPF) is the most common form of ILD and has a median survival of 3-5 years, a mortality rate that is higher than most common cancers (Hopkins et al., 2016; Raghu et al., 2014). For IPF, two FDA approved antifibrotic drugs are currently available: Nintedanib and Pirfenidone, which have shown promise in reducing the decline of lung function in IPF (Raghu and Selman, 2015). Although these drugs slow disease progression, they fail to stop or reverse the structural damage and loss of lung function. Therefore, we need to develop novel therapeutic strategies to effectively target the progressive fibrosis that characterizes ILD. This requires a deeper understanding of the mechanisms that drive progressive fibrosis.

The lung extracellular matrix (ECM) is comprised of collagens, elastin, glycoproteins, and proteoglycans, which serve as structural scaffolding for cells, and also provide the mechanical stability and elastic recoil necessary for proper lung function. “Controlled” fibrosis is an indispensable wound healing response of the host to protect from

injury. During normal wound healing, the scarring of the ECM facilitates contraction and recovery of the wound. Once the repair process is complete, the scared matrix is subsequently resolved to re-establish the soft microenvironment. In IPF and other ILDs however, persistent scarring leads to increasing lung rigidity and dysfunction (Bellaye and Kolb, 2015). Through this extensive ECM deposition, the parenchyma, epithelial barrier, and alveolar architecture are destroyed. These structural changes are profibrotic, and direct cell behavior to further accelerate fibrosis in the surrounding regions. This process is likely similar between the different ILD fibrotic diseases, and not only applicable to IPF (Wells et al., 2018). These changes cause a relentless decline in lung function that ultimately leads to respiratory failure and death. In this chapter, we will discuss the intricate ECM-cell interaction in the context of ILD, and how this relationship may be at the heart of progressive lung stiffening and organ dysfunction (figure 1).

Structural ECM changes in ILD

Under physiological conditions, the ECM structure is constantly changing and maintained by a balance between synthesis, deposition, and degradation. Fibroblasts produce factors for both deposition and degradation and are one of the major cells responsible for the continuous remodeling of the ECM (Baum and Duffy, 2011). Mechanical and chemical profibrotic stimuli from the surrounding microenvironment can activate fibroblasts by triggering the assembly of stress fibers composed of cytoplasmic actin. Once in the activated form, fibroblasts have enhanced contractility and produce substantial amounts of ECM proteins. With enough profibrotic stimulation, fibroblasts can fully differentiate into myofibroblasts, which are characterized by the expression of α-

smooth muscle actin (α- SMA) (Hinz et al., 2007). This allows myofibroblasts a characteristic two-folded increase in contractile activity upon differentiation from fibroblasts. During an injury, fibroblasts and myofibroblasts play an integral role in scarring and the normal wound healing response. Resident fibroblasts in the perivascular and peribronchiolar adventitia or circulating fibrocytes (progenitors of fibroblasts) in the plasma are recruited to the site of injury via chemotaxis (Baum and Duffy, 2011; Moeller et al., 2009). Here these cells are stimulated to differentiate into activated fibroblasts or myofibroblasts. During the active phase of repair, the increased contractility in myofibroblasts causes stiffening of the surrounding microenvironment. Myofibroblasts also produce large amounts of ECM proteins such as collagen and fibronectin, which further alters the microenvironment surrounding these cells (Hinz et al., 2007). Once the repair process is complete, myofibroblasts are quickly removed via apoptosis (Desmoulière et al., 1995). Most of the scarred matrix is subsequently resolved by matrix metalloproteinases (MMPs), which are the main enzymes involved in cleaving and degrading the ECM (Cox and Erler, 2011). These processes are crucial for a healthy wound healing response. In IPF and other ILDs, however, myofibroblasts are resistant to apoptosis (Thannickal and Horowitz, 2006). Histological analysis of IPF lungs shows a marked increase of myofibroblast in the tissue, accumulating in clusters called fibroblastic foci (King et al., 2001). These myofibroblasts produce large amounts of ECM proteins that facilitate the characteristic ECM thickening and scarring seen in ILD. As mentioned, usually MMPs degrade the ECM to maintain a healthy ECM structure, however, in ILD, the rate of degradation is largely outweighed by the rate of deposition (Kulkarni et al.,

2016). Over time, this leads to a persistent and sustained ECM scarring. One reason for this imbalance may be increased crosslinking between ECM proteins, which stabilizes the ECM structure and makes it more resistant to degradation.

ECM crosslinking enzymes in ILD

Crosslinking enzymes play an important role in maintaining lung structure and ECM homeostasis. The biomechanical properties of the ECM are dependent on the biochemical composition of the matrix and post-translational modifications, such as glycosylation, trans-glutamination and crosslinking (Erler and Weaver, 2009). Crosslinking enzymes include prolyl hydroxylase, transglutaminases (TGs), lysyl oxidases and lysyl oxidases like (LOXL1-4) congeners. These enzymes regulate the stability, maturation, and turnover of ECM proteins, and orient the ECM assembly for correct function (Kadler et al., 2008). In the lung, highly fibrotic regions can hinder oxygen perfusion and creates hypoxic conditions. These hypoxic conditions have been seen to increase LOX, LOXL2 and LOXL4 secretion from normal human fibroblasts *in vitro* (Aumiller et al., 2017). Recent experiments in LOXL1 deficient mice have also shown protection against pulmonary fibrosis, via reduced collagen crosslinking and decreased tissue stiffening (Bellaye et al., 2017). Similarly, transglutaminase 2 deficient mice were also protected against bleomycin-induced pulmonary fibrosis (Janoštiak et al., 2014; Olsen et al., 2011). A recent study investigating the role of both TG and LOXL enzymes concluded that the pathological cross-linking of the ECM in IPF increases fibroblast growth and resistance to normal ECM turnover (Philp et al., 2018). High serum LOXL2 levels have also been associated with an increased risk of disease progression in IPF patients (Chien et

al., 2014). Neutralizing antibodies against LOXL2 prevented against bleomycin-induced pulmonary fibrosis (Barry-Hamilton et al., 2010). Despite these promising experimental studies, a recent phase II clinical trial targeting LOXL2 with the monoclonal antibody Simtuzumab had no effect on progression-free survival in patients with IPF (Raghu et al., 2017). This contrast between experimental and clinical results highlights the need for further research into understanding the role of crosslinking mechanisms in the persistence and progression of fibrosis.

Lung Stiffness in ILD

These structural ECM changes in the fibrotic lung translate to abnormally altered biomechanical characteristics. Scarring of the lung parenchyma causes cough and shortness of breath, which are usually the first clinical symptom of IPF (Lederer and Martinez, 2018). Increasing lung stiffness can be measured by a decline in forced vital capacity (FVC), which correlates with mortality and is the best parameter to determine IPF progression in patients (Martinez and Flaherty, 2006). The relationship between stiffness and peripheral/basal fibrosis pattern in IPF was nicely outlined by a mathematical model of lung maximal stiffness, which suggests that the distribution of IPF lesions correspond to areas of greatest mechanical distension during breathing (Carloni et al., 2013). Compliance, a more direct parameter of stiffness measures the elastic properties of the lung. Reduced lung compliance is observed in IPF patients, which constantly declines throughout the course of the disease (Zielonka et al., 2010). Interestingly, in the context of liver fibrosis, there are reports of tissue stiffness preceding the fibrotic response (Georges et al., 2007). These findings indicate that disease progression might, at least in part, be driven by

increased rigidity in the abnormally remodeled (or fibrotic) tissues. There is a growing body of research highlighting the dynamic interaction between the ECM and cells, and the significant role the ECM may play in directing cell behavior and phenotype. It is well known that the microenvironment in the fibrotic ECM can promote myofibroblast differentiation. This differentiation causes further profibrotic changes in the ECM, creating a positive feedback loop. Therefore, understanding how exactly the ECM interacts with the cell is important for developing effective strategies to uncouple this vicious ECM-cell relationship, which may be driving fibrosis and the rapid progression profile in ILD.

Mechanosensing

Aberrant ECM deposition and crosslinking lead to notable changes in the biomechanical cues experienced by tissue-resident cells. Before investigating how these changes influence cell behavior to promote ILD, we must first understand if and how cells sense mechanical cues. Two potential models have been proposed to explain how integral proteins on the cell membrane can perceive mechanical force. The "tethered" model suggests that intra- or extracellular attachment to proteins act as springs to transfer mechanical stimuli to the cell (Kung, 2005). The "membrane model" on the other hand states that changes in membrane tension provoke conformational changes in integral proteins (Cantor, 1997). Here we will discuss one example for each of these models, specifically: integrins, focal adhesions, and the cytoskeleton for the tethered mode, and mechanosensitive membrane proteins for the membrane model.

Integrins are heterodimeric cell-surface receptors made up of α and β chains and play an important role in the adhesion of cells to the ECM (Hynes, 1992). There are a total

of 24 types of integrin heterodimers, comprised of one α and several types of β chains. The extracellular portion of the α chain binds selectively to RGD sequences of ECM proteins and serves as the anchor to the ECM (Barczyk et al., 2010; Hynes, 1992). Once the α chain binds to the ECM, it is activated and undergoes a conformational change. This change induces another conformational change in the intracellular tail of the β chain (Geiger et al., 2009). Once activated, the β chain binds to cytoskeletal proteins called talins, which marks the activation of the heterodimer. Once in this state, the integrin-talin complex readily binds to the filamentous-actin (f-actin) cytoskeleton. The activation of one integrin facilitates a positive feedback loop where other surrounding integrins are activated to form activated integrin clusters. This causes the recruitment of proteins such as vinculin and focal adhesion kinases (FAK), which further promote the formation of F-actin-rich stress fibers (Geiger et al., 2009). This activated integrin, talin, vinculin, FAK complex is collectively referred to as focal adhesions. Mechanical forces from the ECM such as elasticity, stress, or strain are transmitted via these integrin-focal adhesions into the cell, and they serve as the direct link between the ECM and the intracellular contractile actomyosin system.

The cytoskeleton is the backbone of a cell and is responsible for maintaining its structure, motility and overall function (Fletcher and Mullins, 2010). The cytoskeleton is comprised of three major classes of filaments: f-actin, microtubules and intermediate filaments. By attaching to integrins via focal adhesions, the cytoskeleton functions as a mechanosensor of external mechanical cues. In epithelial cells, microtubules interact with focal adhesions and the actomyosin cytoskeleton to change the cellular structure in response to changes in ECM stiffness (Myers et al., 2011). F-actin polymerization and

length have also been seen to rapidly change in response to load and ECM stiffness, and alter cell contractility (Humphrey et al., 2014). The cytoskeleton and focal adhesions work in concert to allow the cell to appropriately respond to mechanical cues. Therefore, the cytoskeleton is considered a major regulator and transducer of mechanical stimuli.

The other major way cells respond to mechanical cues is via integral proteins such as ion channels and G-protein-coupled receptors (GPCRs) (Sukharev and Sachs, 2012). In 1987, mechanosensitive ion channels were first characterized in Escherichia Coli using patch clamp experiments (Martinac et al., 1987). These mechanosensitive ion channels are present in almost all species and in all cell types; highlighting their importance for cell survival. Mechanosensitive ion channels follow the membrane model of mechanosensing. They are responsible for sensing tension experienced by the plasma membrane and change in its ion permeability. Potassium gated ion channels are the best investigated, and are found in mammalian neurons (Krepkiy et al., 2009). Mechanosensitive ion channels, PIEZO1 and PIEZO2 have also been identified in the lung (Coste et al., 2010, p. 2). These channels may play a role in the mechanical stiffness induced cellular changes observed in ILD. GPCRs are another integral protein with many important canonical signaling responsibilities. GPCRs are commonly found in various cell types and play crucial roles in inflammation, cell growth, and differentiation. Briefly, the activation of GPCR occurs once a specific agonist binds to the receptor. The receptor then undergoes a conformation change, which causes diverse intracellular signaling cascades. Recent findings, however, have shown that GPCR can undergo mechanosensitive activation, irrespective of its agonist, which was first identified in angiotensin-II type-1 receptors (Storch et al., 2012).

Mechanical stimuli alone can, therefore, activate GPCRs and enact the various downstream effects of this multifaceted receptor.

Together these findings highlight the cellular machinery to sense mechanical cues from their surroundings. Furthermore, various *in vitro* studies have shown that cells respond much more rapidly to substrate stiffness via the cytoskeleton, than ligand-stimulated second-messenger based pathways (Mitrossilis et al., 2010; Na et al., 2008). This is understandable since cells need to quickly respond to mechanical cues if they want to survive sudden changes in tension and stress. Next, we will see how cells interpret these mechanical cues and induce long-term changes in their phenotype and behavior.

Mechanotransduction

Cells also quickly respond to mechanical stimuli chemically, by changing their gene expression profiles. In a study using magnetic beads to apply mechanical force to osteoblasts via integrins, α-SMA expression was increased within 5 min of stimulation (Wang et al., 2002). In the same study, phosphorylation and activity of other mechanotransduction mediators such as Rho kinase (ROCK) were measured within 10 min of mechanical stimulation. In a separate study, activated integrins in focal adhesions activated ROCK and phosphorylation of focal adhesion kinase (Janoštiak et al., 2014). These proteins promote the polymerization and stabilization of f-actin, therefore changing the structure and further enhancing the cell's mechanosensitivity. Furthermore, ROCK and FAK potently stimulate the differentiation of fibroblasts into myofibroblasts *in vitro* (Akhmetshina et al., 2008). Inhibition of ROCK using Y-27632 has been shown to inhibit stiff matrix-induced actin stress fiber formation in lung fibroblasts (Liu et al., 2010). FAK

inhibitors (Kinoshita et al., 2013) and the ROCK inhibitor fasudil (Froese et al., 2016; Zhou et al., 2013) have demonstrated therapeutic efficacy in preclinical models of pulmonary fibrosis. This may explain the success of KD025 - a ROCK inhibitor that recently passed through a phase IIA clinical trial (Averill et al., 2018).

ROCK also plays an important role in the nuclear localization of Yes-associated protein (YAP) and transcriptional co-activator with the PDZ-binding motif (TAZ). YAP/TAZ are known profibrotic mediators, and they regulate the transcription of cell-proliferative and anti-apoptotic genes. Immortalized fibroblasts, conditionally expressing YAP/TAZ mutant proteins have been shown to promote fibrosis *in vivo* when adoptively transferred into mouse lungs (Liu et al., 2015). Various other profibrotic genes such as collagen, fibronectin, laminin, and transformation growth factor-β1 (TFG-β1) have also been shown to be upregulated in response to increasing stiffness (T Yasuda et al., 1996; T. Yasuda et al., 1996). Together, these findings briefly highlight the various chemical changes a cell undergoes during the mechanotransduction of environmental cues. Next, we will explore how these changes influence cell behavior and may potentially be a driver in progressive fibrosis in ILD.

ECM structure and cell phenotype in ILD

We have discussed the ability of cells to sense stiffness and some of the ways they respond structurally and chemically to these changes. Here we will directly explore how the mechanical stiffness in fibrotic lungs can be a driving factor for profibrotic cellular changes, specifically myofibroblast differentiation, which causes further scarring and disease progression. *In vitro,* the differentiation of fibroblasts to myofibroblasts is strongly

correlated with substrate stiffness: stiff substrates promote the production of profibrotic mediators and ECM deposition, whereas substrates of physiological stiffness inactivate myofibroblasts and favor their apoptosis (Balestrini et al., 2012; Eisenberg et al., 2011; Marinković et al., 2013). Fibroblasts are sensitive to stiffness through actin dynamics that promote f-actin polymerization. One result of actin polymerization is the nuclear translocation of megakaryoblastic leukemia factor-1 (MKL1) (Huang et al., 2012). MKL1 is an actin dynamics sensor that plays a central role in regulating the expression of fibrotic genes, including α-SMA. On softer matrices, less force is exerted, and actin cables and focal adhesions are less well developed.

An elegant study by Booth et al. showed that the acellular ECM scaffolds from IPF lungs induces myofibroblast differentiation, but not the acellular ECM scaffolds from donor lungs (Booth et al., 2012). IPF fibroblasts have also been shown to be sensitive to durotaxis; low to high stiffness gradients. Stiff regions amplify tissue fibrosis by promoting fibroblast recruitment through cell durotaxis in an α-tubulin acetylation-dependent manner (Liu et al., 2010). Furthermore, Balestrini et. al. have shown myofibroblasts to retain their profibrotic activity up until 2 weeks in soft culturing plates, when they are primed previously on stiff plates for 3 weeks (Balestrini et al., 2012). Priming fibroblasts on soft plates for 3 weeks, imparted some protection from myofibroblast differentiation in the cell population when transferred into stiff conditions (Balestrini et al., 2012). This priming and resistance to change suggest a form of mechanical memory, which has been linked to changes in DNA methylation, histone modification, and relative miRNA. miRNA-29 is one example of such a modification, and establishes fibroblast memory, by regulating fibrosis-

related genes such as lamins, integrins and the formation of focal adhesions. Decreased miRNA-29 levels in fibrotic lungs are associated with the increased expression of profibrotic genes, therefore suggesting miRNA-29 roles in inhibiting a profibrotic phenotype (Cushing et al., 2011).

Recent studies have also shown that increased tissue stiffness can induce epithelial-mesenchymal transition (EMT), which is another potential but disputed origin of myofibroblasts (Brown et al., 2013; Eisenberg et al., 2011; Heise et al., 2011; Leight et al., 2012). The mechanical properties of the matrix induces EMT in higher stiffnesses, via an effect on PI3K/Akt signaling and a switch between TGF-β induced apoptosis, which occurs in lower stiffnesses (Leight et al., 2012). Stress-induced activation of the mechanosensitive integral protein transient receptor potential vanilloid 4 (TRPV4) channel, has also been seen to induce fibroblast to myofibroblast differentiation, and TRPV4 knockout mice are protected from bleomycin-induced pulmonary fibrosis (Rahaman et al., 2014). In addition to the structural pulmonary cells, macrophages and mast cells are also sensitive to mechanical stress (Fowlkes et al., 2013; Patel et al., 2012). Using a decellularization model, our group recently highlighted the 3D fibrotic ECM's ability to induce mast cell degranulation (Shimbori et al., 2019). Degranulation of mast cells release profibrotic mediators such as TGF-β1 and is linked to the progression of IPF. Others have also shown that increased stiffness promotes a profibrotic phenotype in macrophages, endothelial cells, and mesenchymal cells (Blakney et al., 2012; Wells, 2008).

Together these findings highlight how the stiff mechanical cues can promote profibrotic cells and myofibroblast differentiation. This illustrates potential ways how the

ECM interacts with cells in a fibrotic lung, and how this can drive disease progression. Along with structure, however, the fibrotic ECM also has drastic changes in composition that make it a very different microenvironment for cells. Next, we will explore the fibrotic ECM composition in ILD lungs, and assess its potential in directing cell behavior.

ECM composition and cell phenotype in ILD

The ECM is comprised of more than 300 proteins that make up the "matrisome core". Polysaccharides, glycosaminoglycans, ECM-binding growth factors, and ECM-modifying enzymes are attached to this core, and together they serve as the tissue scaffold. The ECM structure is highly dynamic and is constantly remodeled. In fibrosis, this remodeling is dysregulated which overtime causes accumulation of proteoglycans, collagen, elastin, and fibronectin. Proteoglycans consist of a core protein that binds to a highly charged glycosaminoglycan. Together they make up the integral hydrated gel, which binds collagen and elastin fibers to provide mechanical stability for the alveolar structure. Dysregulated remodeling of the lung causes abnormal expression of the proteoglycan-glycosaminoglycan complexes and leads to the destruction of the architecture (Kulkarni et al., 2016). Fibrillar collagen is the most abundant type of collagen in the lung and is crucial for tensile strength and functionality. In IPF, collagen accumulates around myofibroblasts and fibroblastic foci, resulting in increased stiffness within these regions (Kuhn et al., 1989). Elastin fibers attach to collagen and contribute to the lung elastic recoil. Elastin is increased in the bleomycin-treated mouse lungs (Blaauboer et al., 2014) and can enhance TGF-β1-induced myofibroblast differentiation. Glycoproteins such as fibronectin are responsible for mediating cell-matrix adhesions by binding ECM proteins. Fibronectin and

other glycoproteins are abundant in IPF lungs (Serini et al., 1998). Similar to elastin, fibronectin is also essential in driving myofibroblast differentiation. These are some of the compositional changes that underlay the increased stiffness seen in ILD, and here we see how they promote a profibrotic cell phenotype. Therefore, proteomic studies are needed to better understand the dynamics of the matrix and improve ECM diagnostics to develop effective treatments for fibrotic diseases.

Furthermore, there is research to suggest that soluble ECM fragments also have profibrotic effects. Specifically, MMPs generate fragments by cleaving full-length ECM proteins to produce bioactive molecules. These fragments bind to integrins and EGFR receptors, and in the case of angiogenesis can induce both pro- and anti-angiogenic effects (Neve et al., 2014). In ILD, proteins such as collagen and hyaluronan are drastically upregulated in the ECM. MMP mediated degradation of Type VI collagen has been strongly linked to progressive fibrosis in the liver (Veidal et al., 2011). Low molecular weight hyaluronan has been seen to promote inflammation and fibrosis by downregulating the adenosine A2a receptor (Collins et al., 2011). In another study, supplementation of sonicated hyaluronan induced EMT in alveolar type II epithelial cells *in vitro* (Heise et al., 2011). We are only beginning to understand the bioactive capabilities of these ECM fragments, and since the ECM structure is rich in proteins and is constantly degraded during remodeling, they represent a potentially important facet of ECM-cell interaction. ECM fragments, however, are not the only bioactive components found in the ECM. Along with providing structural support for cells, the ECM is also a ligand reservoir for growth factors which have potent effects on cell behavior (Schultz and Wysocki, 2009). Interestingly,

mechanical stimuli seem to be involved in the activation of these growth factors. Next, we will explore one example of how the compositional and structural changes in the fibrotic ECM work together to create a profibrotic microenvironment.

A complex profibrotic microenvironment in ILD

So far we have discussed how individually, structural and chemical changes in the fibrotic ECM of ILD lungs interact with cells in a profibrotic nature. In the *in vivo* system, however, these ECM-cell interactions are seldom independent. As mentioned above, the ECM stores many inactive growth factors, including TGF-β1. Briefly, TGF-β is a growth factor known to regulate numerous essential cellular processes such as cell growth, proliferation, differentiation, and apoptosis (Border and Noble, 1994). Three major mammalian isoforms of this growth factor have been identified: TGF-β1, 2, and 3, with TGF-β1 being the most closely related to the development of pulmonary fibrosis (Sime et al., 1997; Xaubet et al., 2003). TGF-β1 content and activity are increased in lungs from experimental fibrosis models and IPF (Khalil et al., 1991; Westergren-Thorsson et al., 1993). Inactive TGF-β1 is synthesized by many parenchymal and infiltrating cells. After binding to the latency associated peptide and latent TGF-β-binding protein, TGF-β1 forms a complex called the large latent complex (LLC) and is secreted and stored bound to the ECM (Leppäranta et al., 2012; Upagupta et al., 2018). In fibrotic lungs, the amount of TGF-β1 attached to the ECM is significantly increased. As discussed, the stiff fibrotic ECM also has more mechanical stimulation. Interestingly, *in vitro* studies have shown that mechanical stress contributes to TGF-β1 activation (Wipff et al., 2007). Therefore, this dual compositional and structural change in fibrotic lungs may play a notable role in facilitating

TGF-β1-induced fibrosis in ILD. To further investigate this relationship, our group assessed the potential of mechanical stretch to induce activation and release of latent TGF-β1 in living tissues (rat and human) (Froese et al., 2016). In this study, fibrotic and normal lung strips were subjected to cyclic mechanical stimuli, and activation and release of TGF-β1 from the lung strips were measured. We determined that the mechanical stress induces active TGF-β1 release and also activates TGF-β1 downstream signaling pathways in fibrotic lungs (Froese et al., 2016). Furthermore, increased Young's modulus-measured tissue stiffness was also positively correlated with the amount of active TGF-β1 released from tissues following mechanical stretch (Froese et al., 2016). One potential mechanism for this may be integrin mediated. *In vitro* studies indicate that integrin subtypes containing αv and β1, 3, 5 and 6 isoforms physically link the LLC attached to the ECM with the cell's cytoskeleton. Of these isoforms, αvβ6 are specifically known to bind and activate latent TGF-β1 (Annes et al., 2004). Antibodies for integrin αvβ6 protects mice against bleomycin-induced pulmonary fibrosis (Horan et al., 2008). Recently in IPF patients, BG00011 a humanized monoclonal antibody against integrin αvβ6 showed inhibition of phospho-SMAD2 levels, a key signal transducer for TGF-β1, in bronchoalveolar lavage cells (Raghu et al., 2018). In light of these results, BG00011 is currently being tested in a larger clinical trial for IPF patients (NCT03573505).

Once activated, TGF-β1 mediates many fibrogenic responses, including myofibroblast activation and differentiation (Evans et al., 2003). TGF-β1 also induces EMT (Xu et al., 2009) and myofibroblast-like differentiation of mesenchymal stem cells (Mishra and Banerjee, 2011). In addition to myofibroblast differentiation, TGF-β1 also regulates

M2 macrophage polarization, a known profibrotic phenotype that produces more TGF-β1 (Gong et al., 2012). Altogether, it is clear that TGF-β1 plays a key profibrotic role in ECM structure and composition. Here we see how both the chemical and structural ECM components of the fibrotic lung can work in concert to create a profibrotic microenvironment for cells. This is but one example of many such relationships in the fibrotic lung, highlighting the significance of ECM-cell interaction in understanding ILD progression.

CONCLUSION

In this chapter, we discuss the marked structural and compositional changes of the ECM in fibrotic lungs in ILD. We explore the different machinery cells utilize to sense mechanical cues, and how they undergo both short and long-term changes in response to their microenvironments. Structure and composition of the fibrotic lungs seem to create a profibrotic environment, which facilitates cellular changes that promote further scarring. This ECM-cell interaction can create a vicious cycle that plays a key role in the progression of ILD. More insight into the ECM-cell interactions in ILD will allow for holistic approaches to correct the imbalances that drive fibrosis, and therefore uncover effective therapeutic avenues for this progressive disease.

FIGURE LEGEND

Figure 1: Schematic overview of how the ECM-cell interaction fits into progressive lung fibrosis in ILD.

Figure 1:

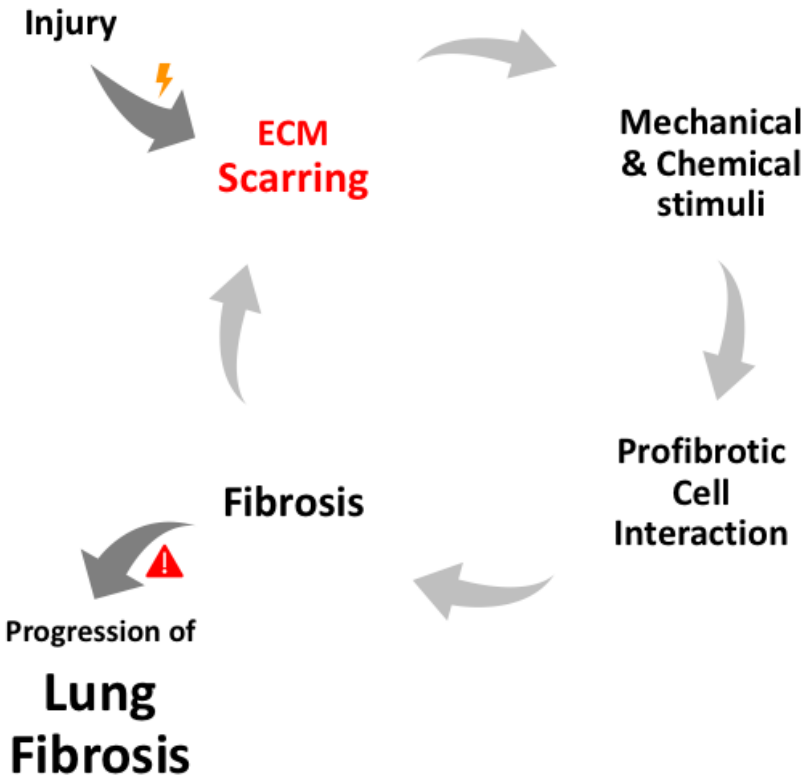
Injury
ECM
Scarring
Mechanical
& Chemical
stimuli
Profibrotic
Cell
Interaction
Fibrosis
Progression of
Lung
Fibrosis

REFERENCES

Akhmetshina, A., Dees, C., Pileckyte, M., Szucs, G., Spriewald, B.M., Zwerina, J., Distler, O., Schett, G., Distler, J.H.W., 2008. Rho-associated kinases are crucial for myofibroblast differentiation and production of extracellular matrix in scleroderma fibroblasts. Arthritis Rheum. 58, 2553–2564. https://doi.org/10.1002/art.23677

Annes, J.P., Chen, Y., Munger, J.S., Rifkin, D.B., 2004. Integrin alphaVbeta6-mediated activation of latent TGF-beta requires the latent TGF-beta binding protein-1. J. Cell Biol. 165, 723–734. https://doi.org/10.1083/jcb.200312172

Aumiller, V., Strobel, B., Romeike, M., Schuler, M., Stierstorfer, B.E., Kreuz, S., 2017. Comparative analysis of lysyl oxidase (like) family members in pulmonary fibrosis. Scientific Reports 7, 149. https://doi.org/10.1038/s41598-017-00270-0

Averill, F., Albertson, T. e., Baratz, D. m., Chaudhary, S., Mobin, S., O'Brien, T., Scholand, M. b., Whelan, T. p. m., Poyurovsky, M., Schueller, O., Ryan, J., Gibson, K. f., 2018. A Phase 2 Trial of KD025 to Assess Efficacy, Safety and Tolerability in Patients with Idiopathic Pulmonary Fibrosis, in: C97. DIFFUSE PARENCHYMAL LUNG DISEASES: EVALUATION, OUTCOMES, AND TRIALS, American Thoracic Society International Conference Abstracts. American Thoracic Society, pp. A5927–A5927. https://doi.org/10.1164/ajrccm-conference.2018.197.1_MeetingAbstracts.A5927

Balestrini, J.L., Chaudhry, S., Sarrazy, V., Koehler, A., Hinz, B., 2012. The mechanical memory of lung myofibroblasts. Integr Biol (Camb) 4, 410–421. https://doi.org/10.1039/c2ib00149g

Barczyk, M., Carracedo, S., Gullberg, D., 2010. Integrins. Cell and Tissue Research 339, 269–280. https://doi.org/10.1007/s00441-009-0834-6

Barry-Hamilton, V., Spangler, R., Marshall, D., McCauley, S., Rodriguez, H.M., Oyasu, M., Mikels, A., Vaysberg, M., Ghermazien, H., Wai, C., Garcia, C.A., Velayo, A.C., Jorgensen, B., Biermann, D., Tsai, D., Green, J., Zaffryar-Eilot, S., Holzer, A., Ogg, S., Thai, D., Neufeld, G., Van Vlasselaer, P., Smith, V., 2010. Allosteric inhibition of lysyl oxidase-like-2 impedes the development of a pathologic microenvironment. Nat. Med. 16, 1009–1017. https://doi.org/10.1038/nm.2208

Baum, J., Duffy, H.S., 2011. Fibroblasts and Myofibroblasts: What are we talking about? J Cardiovasc Pharmacol 57, 376–379. https://doi.org/10.1097/FJC.0b013e3182116e39

Bellaye, P.-S., Kolb, M., 2015. Why do patients get idiopathic pulmonary fibrosis? Current concepts in the pathogenesis of pulmonary fibrosis. BMC Med 13, 176. https://doi.org/10.1186/s12916-015-0412-6

Bellaye, P.-S., Shimbori, C., Upagupta, C., Sato, S., Shi, W., Gauldie, J., Ask, K., Kolb, M., 2017. Lysyl Oxidase-like 1 Protein Deficiency Protects Mice from AdTGF-β1 Induced Pulmonary Fibrosis. Am. J. Respir. Cell Mol. Biol. https://doi.org/10.1165/rcmb.2017-0252OC

Blaauboer, M.E., Boeijen, F.R., Emson, C.L., Turner, S.M., Zandieh-Doulabi, B., Hanemaaijer, R., Smit, T.H., Stoop, R., Everts, V., 2014. Extracellular matrix proteins: A positive feedback loop in lung fibrosis? Matrix Biology 34, 170–178. https://doi.org/10.1016/j.matbio.2013.11.002

Blakney, A.K., Swartzlander, M.D., Bryant, S.J., 2012. The effects of substrate stiffness on the in vitro activation of macrophages and in vivo host response to poly(ethylene glycol)-based hydrogels. J Biomed Mater Res A 100, 1375–1386. https://doi.org/10.1002/jbm.a.34104

Booth, A.J., Hadley, R., Cornett, A.M., Dreffs, A.A., Matthes, S.A., Tsui, J.L., Weiss, K., Horowitz, J.C., Fiore, V.F., Barker, T.H., Moore, B.B., Martinez, F.J., Niklason, L.E., White, E.S., 2012. Acellular Normal and Fibrotic Human Lung Matrices as a Culture System for In Vitro Investigation. Am J Respir Crit Care Med 186, 866–876. https://doi.org/10.1164/rccm.201204-0754OC

Border, W.A., Noble, N.A., 1994. Transforming growth factor beta in tissue fibrosis. N. Engl. J. Med. 331, 1286–1292. https://doi.org/10.1056/NEJM199411103311907

Brown, A.C., Fiore, V.F., Sulchek, T.A., Barker, T.H., 2013. Physical and chemical microenvironmental cues orthogonally control the degree and duration of fibrosis-associated epithelial-to-mesenchymal transitions. J. Pathol. 229, 25–35. https://doi.org/10.1002/path.4114

Cabrera-Benitez, N.E., Laffey, J.G., Parotto, M., Spieth, P.M., Villar, J., Zhang, H., Slutsky, A.S., 2014. Mechanical Ventilation–associated Lung Fibrosis in Acute Respiratory Distress Syndrome: A Significant Contributor to Poor Outcome. Anesthesiology 121, 189–198. https://doi.org/10.1097/ALN.0000000000000264

Cantor, R.S., 1997. Lateral Pressures in Cell Membranes: A Mechanism for Modulation of Protein Function. The Journal of Physical Chemistry B 101, 1723–1725. https://doi.org/10.1021/jp963911x

Carloni, A., Poletti, V., Fermo, L., Bellomo, N., Chilosi, M., 2013. Heterogeneous distribution of mechanical stress in human lung: a mathematical approach to evaluate abnormal remodeling in IPF. J. Theor. Biol. 332, 136–140. https://doi.org/10.1016/j.jtbi.2013.04.038

Chien, J.W., Richards, T.J., Gibson, K.F., Zhang, Y., Lindell, K.O., Shao, L., Lyman, S.K., Adamkewicz, J.I., Smith, V., Kaminski, N., O'Riordan, T., 2014. Serum lysyl

oxidase-like 2 levels and idiopathic pulmonary fibrosis disease progression. Eur. Respir. J. 43, 1430–1438. https://doi.org/10.1183/09031936.00141013

Collins, S.L., Black, K.E., Chan-Li, Y., Ahn, Y.-H., Cole, P.A., Powell, J.D., Horton, M.R., 2011. Hyaluronan Fragments Promote Inflammation by Down-Regulating the Anti-inflammatory A2a Receptor. Am J Respir Cell Mol Biol 45, 675–683. https://doi.org/10.1165/rcmb.2010-0387OC

Coste, B., Mathur, J., Schmidt, M., Earley, T.J., Ranade, S., Petrus, M.J., Dubin, A.E., Patapoutian, A., 2010. Piezo1 and Piezo2 Are Essential Components of Distinct Mechanically Activated Cation Channels. Science 330, 55–60. https://doi.org/10.1126/science.1193270

Cox, T.R., Erler, J.T., 2011. Remodeling and homeostasis of the extracellular matrix: implications for fibrotic diseases and cancer. Dis Model Mech 4, 165–178. https://doi.org/10.1242/dmm.004077

Cushing, L., Kuang, P.P., Qian, J., Shao, F., Wu, J., Little, F., Thannickal, V.J., Cardoso, W.V., Lü, J., 2011. miR-29 is a major regulator of genes associated with pulmonary fibrosis. Am. J. Respir. Cell Mol. Biol. 45, 287–294. https://doi.org/10.1165/rcmb.2010-0323OC

Desmoulière, A., Redard, M., Darby, I., Gabbiani, G., 1995. Apoptosis mediates the decrease in cellularity during the transition between granulation tissue and scar. Am J Pathol 146, 56–66.

Eisenberg, J.L., Safi, A., Wei, X., Espinosa, H.D., Budinger, G.S., Takawira, D., Hopkinson, S.B., Jones, J.C., 2011. Substrate stiffness regulates extracellular matrix deposition by alveolar epithelial cells. Res Rep Biol 2011, 1–12. https://doi.org/10.2147/RRB.S13178

Erler, J.T., Weaver, V.M., 2009. Three-dimensional context regulation of metastasis. Clin. Exp. Metastasis 26, 35–49. https://doi.org/10.1007/s10585-008-9209-8

Evans, R.A., Tian, Y.C., Steadman, R., Phillips, A.O., 2003. TGF-beta1-mediated fibroblast-myofibroblast terminal differentiation-the role of Smad proteins. Exp. Cell Res. 282, 90–100.

Fletcher, D.A., Mullins, R.D., 2010. Cell mechanics and the cytoskeleton. Nature 463, 485–492. https://doi.org/10.1038/nature08908

Fowlkes, V., Wilson, C.G., Carver, W., Goldsmith, E.C., 2013. Mechanical loading promotes mast cell degranulation via RGD-integrin dependent pathways. J Biomech 46, 788–795. https://doi.org/10.1016/j.jbiomech.2012.11.014

Froese, A.R., Shimbori, C., Bellaye, P.-S., Inman, M., Obex, S., Fatima, S., Jenkins, G., Gauldie, J., Ask, K., Kolb, M., 2016. Stretch-induced Activation of Transforming Growth Factor-β1 in Pulmonary Fibrosis. Am. J. Respir. Crit. Care Med. 194, 84–96. https://doi.org/10.1164/rccm.201508-1638OC

Geiger, B., Spatz, J.P., Bershadsky, A.D., 2009. Environmental sensing through focal adhesions. Nature Reviews Molecular Cell Biology 10, 21–33. https://doi.org/10.1038/nrm2593

Georges, P.C., Hui, J.-J., Gombos, Z., McCormick, M.E., Wang, A.Y., Uemura, M., Mick, R., Janmey, P.A., Furth, E.E., Wells, R.G., 2007. Increased stiffness of the rat liver precedes matrix deposition: implications for fibrosis. Am. J. Physiol. Gastrointest. Liver Physiol. 293, G1147-1154. https://doi.org/10.1152/ajpgi.00032.2007

Gong, D., Shi, W., Yi, S., Chen, H., Groffen, J., Heisterkamp, N., 2012. TGFβ signaling plays a critical role in promoting alternative macrophage activation. BMC Immunol. 13, 31. https://doi.org/10.1186/1471-2172-13-31

Heise, R.L., Stober, V., Cheluvaraju, C., Hollingsworth, J.W., Garantziotis, S., 2011. Mechanical stretch induces epithelial-mesenchymal transition in alveolar epithelia via hyaluronan activation of innate immunity. J. Biol. Chem. 286, 17435–17444. https://doi.org/10.1074/jbc.M110.137273

Hinz, B., Phan, S.H., Thannickal, V.J., Galli, A., Bochaton-Piallat, M.-L., Gabbiani, G., 2007. The myofibroblast: one function, multiple origins. Am. J. Pathol. 170, 1807–1816. https://doi.org/10.2353/ajpath.2007.070112

Hopkins, R.B., Burke, N., Fell, C., Dion, G., Kolb, M., 2016. Epidemiology and survival of idiopathic pulmonary fibrosis from national data in Canada. Eur. Respir. J. 48, 187–195. https://doi.org/10.1183/13993003.01504-2015

Horan, G.S., Wood, S., Ona, V., Dan, J.L., Lukashev, M.E., Weinreb, P.H., Simon, K.J., Hahm, K., Allaire, N.E., Rinaldi, N.J., Goyal, J., Feghali-Bostwick, C.A., Matteson, E.L., O'Hara, C., Lafyatis, R., Davis, G.S., Huang, X., Sheppard, D., Violette, S.M., 2008. Partial inhibition of integrin αvβ6 prevents pulmonary fibrosis without exacerbating inflammation. American journal of respiratory and critical care medicine 177, 56–65. https://doi.org/10.1164/rccm.200706-805OC

Huang, X., Yang, N., Fiore, V.F., Barker, T.H., Sun, Y., Morris, S.W., Ding, Q., Thannickal, V.J., Zhou, Y., 2012. Matrix stiffness-induced myofibroblast differentiation is mediated by intrinsic mechanotransduction. Am. J. Respir. Cell Mol. Biol. 47, 340–348. https://doi.org/10.1165/rcmb.2012-0050OC

Humphrey, J.D., Dufresne, E.R., Schwartz, M.A., 2014. Mechanotransduction and extracellular matrix homeostasis. Nature Reviews Molecular Cell Biology 15, 802–812. https://doi.org/10.1038/nrm3896

Hynes, R.O., 1992. Integrins: versatility, modulation, and signaling in cell adhesion. Cell 69, 11–25.

Janoštiak, R., Pataki, A.C., Brábek, J., Rösel, D., 2014. Mechanosensors in integrin signaling: the emerging role of p130Cas. Eur. J. Cell Biol. 93, 445–454. https://doi.org/10.1016/j.ejcb.2014.07.002

Kadler, K.E., Hill, A., Canty-Laird, E.G., 2008. Collagen fibrillogenesis: fibronectin, integrins, and minor collagens as organizers and nucleators. Curr. Opin. Cell Biol. 20, 495–501. https://doi.org/10.1016/j.ceb.2008.06.008

Khalil, N., O'Connor, R.N., Unruh, H.W., Warren, P.W., Flanders, K.C., Kemp, A., Bereznay, O.H., Greenberg, A.H., 1991. Increased production and immunohistochemical localization of transforming growth factor-beta in idiopathic pulmonary fibrosis. Am. J. Respir. Cell Mol. Biol. 5, 155–162.

King, T.E., Schwarz, M.I., Brown, K., Tooze, J.A., Colby, T.V., Waldron, J.A., Flint, A., Thurlbeck, W., Cherniack, R.M., 2001. Idiopathic pulmonary fibrosis: relationship between histopathologic features and mortality. Am. J. Respir. Crit. Care Med. 164, 1025–1032. https://doi.org/10.1164/ajrccm.164.6.2001056

Kinoshita, K., Aono, Y., Azuma, M., Kishi, J., Takezaki, A., Kishi, M., Makino, H., Okazaki, H., Uehara, H., Izumi, K., Sone, S., Nishioka, Y., 2013. Antifibrotic effects of focal adhesion kinase inhibitor in bleomycin-induced pulmonary fibrosis in mice. Am. J. Respir. Cell Mol. Biol. 49, 536–543. https://doi.org/10.1165/rcmb.2012-0277OC

Krepkiy, D., Mihailescu, M., Freites, J.A., Schow, E.V., Worcester, D.L., Gawrisch, K., Tobias, D.J., White, S.H., Swartz, K.J., 2009. Structure and hydration of membranes embedded with voltage-sensing domains. Nature 462, 473–479. https://doi.org/10.1038/nature08542

Kuhn, C., Boldt, J., King, T.E., Crouch, E., Vartio, T., McDonald, J.A., 1989. An immunohistochemical study of architectural remodeling and connective tissue synthesis in pulmonary fibrosis. Am. Rev. Respir. Dis. 140, 1693–1703. https://doi.org/10.1164/ajrccm/140.6.1693

Kulkarni, T., O'Reilly, P., Antony, V.B., Gaggar, A., Thannickal, V.J., 2016. Matrix Remodeling in Pulmonary Fibrosis and Emphysema. Am J Respir Cell Mol Biol 54, 751–760. https://doi.org/10.1165/rcmb.2015-0166PS

Kung, C., 2005. A possible unifying principle for mechanosensation. Nature 436, 647–654. https://doi.org/10.1038/nature03896

Lederer, D.J., Martinez, F.J., 2018. Idiopathic Pulmonary Fibrosis. N. Engl. J. Med. 378, 1811–1823. https://doi.org/10.1056/NEJMra1705751

Leight, J.L., Wozniak, M.A., Chen, S., Lynch, M.L., Chen, C.S., 2012. Matrix rigidity regulates a switch between TGF-β1-induced apoptosis and epithelial-mesenchymal transition. Mol. Biol. Cell 23, 781–791. https://doi.org/10.1091/mbc.E11-06-0537

Leppäranta, O., Sens, C., Salmenkivi, K., Kinnula, V.L., Keski-Oja, J., Myllärniemi, M., Koli, K., 2012. Regulation of TGF-β storage and activation in the human idiopathic pulmonary fibrosis lung. Cell and Tissue Research 348, 491–503. https://doi.org/10.1007/s00441-012-1385-9

Liu, F., Lagares, D., Choi, K.M., Stopfer, L., Marinković, A., Vrbanac, V., Probst, C.K., Hiemer, S.E., Sisson, T.H., Horowitz, J.C., Rosas, I.O., Fredenburgh, L.E., Feghali-Bostwick, C., Varelas, X., Tager, A.M., Tschumperlin, D.J., 2015. Mechanosignaling through YAP and TAZ drives fibroblast activation and fibrosis. Am. J. Physiol. Lung Cell Mol. Physiol. 308, L344-357. https://doi.org/10.1152/ajplung.00300.2014

Liu, F., Mih, J.D., Shea, B.S., Kho, A.T., Sharif, A.S., Tager, A.M., Tschumperlin, D.J., 2010. Feedback amplification of fibrosis through matrix stiffening and COX-2 suppression. J Cell Biol 190, 693–706. https://doi.org/10.1083/jcb.201004082

Marinković, A., Liu, F., Tschumperlin, D.J., 2013. Matrices of physiologic stiffness potently inactivate idiopathic pulmonary fibrosis fibroblasts. Am. J. Respir. Cell Mol. Biol. 48, 422–430. https://doi.org/10.1165/rcmb.2012-0335OC

Martin, C., Papazian, L., Payan, M.J., Saux, P., Gouin, F., 1995. Pulmonary fibrosis correlates with outcome in adult respiratory distress syndrome. A study in mechanically ventilated patients. Chest 107, 196–200.

Martinac, B., Buechner, M., Delcour, A.H., Adler, J., Kung, C., 1987. Pressure-sensitive ion channel in Escherichia coli. Proc. Natl. Acad. Sci. U.S.A. 84, 2297–2301.

Martinez, F.J., Flaherty, K., 2006. Pulmonary function testing in idiopathic interstitial pneumonias. Proc Am Thorac Soc 3, 315–321. https://doi.org/10.1513/pats.200602-022TK

Mishra, P.J., Banerjee, D., 2011. Activation and Differentiation of Mesenchymal Stem Cells, in: Kalyuzhny, A.E. (Ed.), Signal Transduction Immunohistochemistry. Humana Press, Totowa, NJ, pp. 245–253. https://doi.org/10.1007/978-1-61779-024-9_14

Mitrossilis, D., Fouchard, J., Pereira, D., Postic, F., Richert, A., Saint-Jean, M., Asnacios, A., 2010. Real-time single-cell response to stiffness. Proceedings of the National Academy of Sciences 107, 16518–16523. https://doi.org/10.1073/pnas.1007940107

Moeller, A., Gilpin, S.E., Ask, K., Cox, G., Cook, D., Gauldie, J., Margetts, P.J., Farkas, L., Dobranowski, J., Boylan, C., O'Byrne, P.M., Strieter, R.M., Kolb, M., 2009. Circulating fibrocytes are an indicator of poor prognosis in idiopathic pulmonary fibrosis. Am. J. Respir. Crit. Care Med. 179, 588–594. https://doi.org/10.1164/rccm.200810-1534OC

Myers, K.A., Applegate, K.T., Danuser, G., Fischer, R.S., Waterman, C.M., 2011. Distinct ECM mechanosensing pathways regulate microtubule dynamics to control endothelial cell branching morphogenesis. The Journal of Cell Biology 192, 321–334. https://doi.org/10.1083/jcb.201006009

Na, S., Collin, O., Chowdhury, F., Tay, B., Ouyang, M., Wang, Y., Wang, N., 2008. Rapid signal transduction in living cells is a unique feature of mechanotransduction. Proceedings of the National Academy of Sciences 105, 6626–6631. https://doi.org/10.1073/pnas.0711704105

Neve, A., Cantatore, F.P., Maruotti, N., Corrado, A., Ribatti, D., 2014. Extracellular Matrix Modulates Angiogenesis in Physiological and Pathological Conditions. Biomed Res Int 2014. https://doi.org/10.1155/2014/756078

Olsen, K.C., Sapinoro, R.E., Kottmann, R.M., Kulkarni, A.A., Iismaa, S.E., Johnson, G.V.W., Thatcher, T.H., Phipps, R.P., Sime, P.J., 2011. Transglutaminase 2 and its role in pulmonary fibrosis. Am. J. Respir. Crit. Care Med. 184, 699–707. https://doi.org/10.1164/rccm.201101-0013OC

Patel, N.R., Bole, M., Chen, C., Hardin, C.C., Kho, A.T., Mih, J., Deng, L., Butler, J., Tschumperlin, D., Fredberg, J.J., Krishnan, R., Koziel, H., 2012. Cell Elasticity Determines Macrophage Function. PLOS ONE 7, e41024. https://doi.org/10.1371/journal.pone.0041024

Philp, C.J., Siebeke, I., Clements, D., Miller, S., Habgood, A., John, A.E., Navaratnam, V., Hubbard, R.B., Jenkins, G., Johnson, S.R., 2018. Extracellular Matrix Cross-Linking Enhances Fibroblast Growth and Protects against Matrix Proteolysis in Lung Fibrosis. Am. J. Respir. Cell Mol. Biol. 58, 594–603. https://doi.org/10.1165/rcmb.2016-0379OC

Raghu, G., Brown, K.K., Collard, H.R., Cottin, V., Gibson, K.F., Kaner, R.J., Lederer, D.J., Martinez, F.J., Noble, P.W., Song, J.W., Wells, A.U., Whelan, T.P.M., Wuyts, W., Moreau, E., Patterson, S.D., Smith, V., Bayly, S., Chien, J.W., Gong, Q., Zhang, J.J., O'Riordan, T.G., 2017. Efficacy of simtuzumab versus placebo in patients with

idiopathic pulmonary fibrosis: a randomised, double-blind, controlled, phase 2 trial. Lancet Respir Med 5, 22–32. https://doi.org/10.1016/S2213-2600(16)30421-0

Raghu, G., Chen, S.-Y., Yeh, W.-S., Maroni, B., Li, Q., Lee, Y.-C., Collard, H.R., 2014. Idiopathic pulmonary fibrosis in US Medicare beneficiaries aged 65 years and older: incidence, prevalence, and survival, 2001-11. Lancet Respir Med 2, 566–572. https://doi.org/10.1016/S2213-2600(14)70101-8

Raghu, G., Mouded, M., Culver, D. a., Hamblin, M. j., Golden, J. a., Veeraraghavan, S., Enelow, R. i., Lancaster, L. h., Goldberg, H. j., Frost, A. e., Ginns, L. c., Maroni, B. j., Sheppard, D., Kaminski, N., Rosas, I. o., Arjomandi, M., Prasse, A., Stebbins, C., Zhao, G., Song, G., Arefayene, M., Christmann de Souza, R., Violette, S. m., Gallagher, D. c., Gibson, K. f., 2018. Randomized, Double-Blind, Placebo-Controlled, Multiple Dose, Dose-Escalation Study of BG00011 (Formerly STX-100) in Patients with Idiopathic Pulmonary Fibrosis (IPF), in: D14. ILD: CLINICAL RESEARCH, American Thoracic Society International Conference Abstracts. American Thoracic Society, pp. A7785–A7785. https://doi.org/10.1164/ajrccm-conference.2018.197.1_MeetingAbstracts.A7785

Raghu, G., Selman, M., 2015. Nintedanib and Pirfenidone. New Antifibrotic Treatments Indicated for Idiopathic Pulmonary Fibrosis Offer Hopes and Raises Questions. Am J Respir Crit Care Med 191, 252–254. https://doi.org/10.1164/rccm.201411-2044ED

Rahaman, S.O., Grove, L.M., Paruchuri, S., Southern, B.D., Abraham, S., Niese, K.A., Scheraga, R.G., Ghosh, S., Thodeti, C.K., Zhang, D.X., Moran, M.M., Schilling, W.P., Tschumperlin, D.J., Olman, M.A., 2014. TRPV4 mediates myofibroblast differentiation and pulmonary fibrosis in mice. J. Clin. Invest. 124, 5225–5238. https://doi.org/10.1172/JCI75331

Sakamoto, S., Homma, S., Mun, M., Fujii, T., Kurosaki, A., Yoshimura, K., 2011. Acute exacerbation of idiopathic interstitial pneumonia following lung surgery in 3 of 68 consecutive patients: a retrospective study. Intern. Med. 50, 77–85.

Schultz, G.S., Wysocki, A., 2009. Interactions between extracellular matrix and growth factors in wound healing. Wound Repair and Regeneration 17, 153–162. https://doi.org/10.1111/j.1524-475X.2009.00466.x

Selman, M., Pardo, A., 2014. Revealing the Pathogenic and Aging-related Mechanisms of the Enigmatic Idiopathic Pulmonary Fibrosis. An Integral Model. American Journal of Respiratory and Critical Care Medicine 189, 1161–1172. https://doi.org/10.1164/rccm.201312-2221PP

Serini, G., Bochaton-Piallat, M.L., Ropraz, P., Geinoz, A., Borsi, L., Zardi, L., Gabbiani, G., 1998. The fibronectin domain ED-A is crucial for myofibroblastic phenotype induction by transforming growth factor-beta1. J. Cell Biol. 142, 873–881.

Shimbori, C., Upagupta, C., Bellaye, P.-S., Ayaub, E.A., Sato, S., Yanagihara, T., Zhou, Q., Ognjanovic, A., Ask, K., Gauldie, J., Forsythe, P., Kolb, M.R.J., 2019. Mechanical stress-induced mast cell degranulation activates TGF-β1 signalling pathway in pulmonary fibrosis. Thorax. https://doi.org/10.1136/thoraxjnl-2018-211516

Sime, P.J., Xing, Z., Graham, F.L., Csaky, K.G., Gauldie, J., 1997. Adenovector-mediated gene transfer of active transforming growth factor-beta1 induces prolonged severe fibrosis in rat lung. J. Clin. Invest. 100, 768–776. https://doi.org/10.1172/JCI119590

Storch, U., Schnitzler, M.M. y, Gudermann, T., 2012. G protein-mediated stretch reception. American Journal of Physiology-Heart and Circulatory Physiology 302, H1241–H1249. https://doi.org/10.1152/ajpheart.00818.2011

Sukharev, S., Sachs, F., 2012. Molecular force transduction by ion channels – diversity and unifying principles. Journal of Cell Science 125, 3075–3083. https://doi.org/10.1242/jcs.092353

Thannickal, V.J., Horowitz, J.C., 2006. Evolving Concepts of Apoptosis in Idiopathic Pulmonary Fibrosis. Proc Am Thorac Soc 3, 350–356. https://doi.org/10.1513/pats.200601-001TK

Upagupta, C., Shimbori, C., Alsilmi, R., Kolb, M., 2018. Matrix abnormalities in pulmonary fibrosis. European Respiratory Review 27, 180033. https://doi.org/10.1183/16000617.0033-2018

Veidal, S.S., Karsdal, M.A., Vassiliadis, E., Nawrocki, A., Larsen, M.R., Nguyen, Q.H.T., Hägglund, P., Luo, Y., Zheng, Q., Vainer, B., Leeming, D.J., 2011. MMP Mediated Degradation of Type VI Collagen Is Highly Associated with Liver Fibrosis – Identification and Validation of a Novel Biochemical Marker Assay. PLoS ONE 6, e24753. https://doi.org/10.1371/journal.pone.0024753

Wang, J., Su, M., Fan, J., Seth, A., McCulloch, C.A., 2002. Transcriptional Regulation of a Contractile Gene by Mechanical Forces Applied through Integrins in Osteoblasts. Journal of Biological Chemistry 277, 22889–22895. https://doi.org/10.1074/jbc.M203130200

Watanabe, A., Kawaharada, N., Higami, T., 2011. Postoperative Acute Exacerbation of IPF after Lung Resection for Primary Lung Cancer. Pulm Med 2011, 960316. https://doi.org/10.1155/2011/960316

Wells, A.U., Brown, K.K., Flaherty, K.R., Kolb, M., Thannickal, V.J., 2018. What's in a name? That which we call IPF, by any other name would act the same. European Respiratory Journal 51, 1800692. https://doi.org/10.1183/13993003.00692-2018

Wells, R.G., 2008. The role of matrix stiffness in regulating cell behavior. Hepatology 47, 1394–1400. https://doi.org/10.1002/hep.22193

Westergren-Thorsson, G., Hernnäs, J., Särnstrand, B., Oldberg, A., Heinegård, D., Malmström, A., 1993. Altered expression of small proteoglycans, collagen, and transforming growth factor-beta 1 in developing bleomycin-induced pulmonary fibrosis in rats. J. Clin. Invest. 92, 632–637. https://doi.org/10.1172/JCI116631

Wipff, P.-J., Rifkin, D.B., Meister, J.-J., Hinz, B., 2007. Myofibroblast contraction activates latent TGF-beta1 from the extracellular matrix. J. Cell Biol. 179, 1311–1323. https://doi.org/10.1083/jcb.200704042

Xaubet, A., Marin-Arguedas, A., Lario, S., Ancochea, J., Morell, F., Ruiz-Manzano, J., Rodriguez-Becerra, E., Rodriguez-Arias, J.M., Inigo, P., Sanz, S., Campistol, J.M., Mullol, J., Picado, C., 2003. Transforming growth factor-beta1 gene polymorphisms are associated with disease progression in idiopathic pulmonary fibrosis. Am. J. Respir. Crit. Care Med. 168, 431–435. https://doi.org/10.1164/rccm.200210-1165OC

Xu, J., Lamouille, S., Derynck, R., 2009. TGF-beta-induced epithelial to mesenchymal transition. Cell Res. 19, 156–172. https://doi.org/10.1038/cr.2009.5

Yasuda, T., Akai, Y., Kondo, S., Becker, B.N., Homma, T., Owada, S., Ishida, M., Harris, R.C., 1996. Alteration of cellular function in rat mesangial cells in response to mechanical stretch relaxation. Contrib Nephrol 118, 222–228.

Yasuda, T, Kondo, S., Homma, T., Harris, R.C., 1996. Regulation of extracellular matrix by mechanical stress in rat glomerular mesangial cells. Journal of Clinical Investigation 98, 1991–2000. https://doi.org/10.1172/JCI119003

Zhou, Y., Huang, X., Hecker, L., Kurundkar, D., Kurundkar, A., Liu, H., Jin, T.-H., Desai, L., Bernard, K., Thannickal, V.J., 2013. Inhibition of mechanosensitive signaling in myofibroblasts ameliorates experimental pulmonary fibrosis. J. Clin. Invest. 123, 1096–1108. https://doi.org/10.1172/JCI66700

Zielonka, T., Demkow, U., Radzikowska, E., Bialas, B., Filewska, M., Zycinska, K., Obrowski, M., Kowalski, J., Wardyn, K., Skopinska-Rozewska, E., 2010. Angiogenic activity of sera from interstitial lung disease patients in relation to pulmonary function. Eur J Med Res 15, 229–234. https://doi.org/10.1186/2047-783X-15-S2-229

Chapter 3

Structure and Composition of Decellularized Extracellular Matrix Scaffolds from Nonfibrotic and Ad-TGFβ1-induced Fibrotic Lungs have Opposing effects on Fibroblast to Myofibroblast differentiation in 2 and 3 dimensional settings.

Summary and Significance

The etiology and progression of IPF are still largely unknown. Various cell types have been associated with fibrosis, however, therapeutically targeting these cells has proven ineffective at reversing or stopping disease progression. Aside from these profibrotic cells, there is a growing body of research highlighting the fibrotic ECM's role in driving fibrosis. ECM stiffening is known to promote fibroblast to myofibroblast differentiation *in vitro*, however, the precise ECM factors and the extent to which the 3D ECM can drive profibrotic cellular changes have not been fully investigated. To address this gap in knowledge, we established an *ex vivo* decellularization model to directly study the ECM-cell interaction in a complete 3D setting, in both nonfibrotic and fibrotic ECMs. Using this model, we found that the 3D fibrotic ECM activates recellularized healthy fibroblasts and promotes their differentiation to myofibroblasts. Interestingly, nonfibrotic ECM scaffolds attenuate the profibrotic activity (α-SMA) in recellularized fibrotic fibroblasts and myofibroblasts. Furthermore, modulating stiffness and supplementing soluble ECM proteins into the media also had pro- and anti-fibrotic effects on fibroblast phenotype in 2D settings. In addition to this, using our *ex vivo* system we showed that inhibiting the mechanotransduction pathway had antifibrotic efficacy, by directly interfering with the fibrotic ECM-fibroblast relationship. This is one of the first studies to directly assess the 3D ECM's effect on fibroblast phenotype, and highlight the ECM's pro- and anti-fibrotic potential, which is present at the structural and compositional levels. This study proposes a novel *ex vivo* system to assess nonfibrotic and fibrotic ECM effects on fibroblasts, and potentially other cell types. It also highlights the usefulness of this *ex vivo*

system as a preclinical model, to assess intervention efficacy directly within the profibrotic 3D ECM-cell context.

Structure and Composition of Decellularized Extracellular Matrix Scaffolds from Nonfibrotic and Ad-TGFβ1-induced Fibrotic Lungs have Opposing Effects on Fibroblast to Myofibroblast differentiation in 2 and 3 Dimensional settings.

Chandak Upagupta[1], Seidai Sato[1], Toyoshi Yanagihara[1], Pierre-Simon Bellaye[1], Chiko Shimbori[1], Shannon Gui[2], Kjetil Ask[1] and Martin Kolb[1]

1. Firestone Institute for Respiratory Health, Department of Medicine, McMaster University, Hamilton, ON, Canada
2. McMaster University, Department of Health sciences, Hamilton, ON, Canada

Running title: Structure and composition of Lung Extracellular Matrix Dictates Fibroblast Phenotype.

Conflict of interest: All authors declared no conflicts of interest.

Status of the work: Prepared for submission to "Matrix Biology"

Author contributions: Conception and design: CU, SS, TY, PSB, CS, SG, KA, MK; Performed experiments: CU, SS, TY, PSB, CS, SG; Analysis and interpretations: CU, SS, TY, PSB, CS, SG, KA, MK; Drafting the manuscript: CU, SS, TY, PSB, KA, MK.

Corresponding author: Dr. Martin Kolb, Department of Medicine, McMaster University and The Research Institute of St. Joe's Hamilton, Firestone Institute for Respiratory Health, 50 Charlton Ave East, Room T2120, Hamilton, Ontario, Canada L8N 4A6, Ph. (905) 522.1155 ext. 33683; Fax (905) 521.6183; E-mail: kolbm@mcmaster.ca

ABSTRACT

Rational: Idiopathic Pulmonary fibrosis (IPF) is a chronic disease, characterized by progressive scarring of lung tissue. Accumulation of myofibroblasts is a key characteristic of IPF, which causes excessive deposition of extracellular matrix (ECM) proteins. This is believed to create a positive-feedback loop, where the aberrant ECM promotes further myofibroblast differentiation, and drives disease progression in an exponential manner. The full extent and precise ECM components (composition and structure) that influence cell phenotype, however, are still largely unknown. **Methods:** We first established an *ex vivo* model via whole rat lung decellularization, to create 3D fibrotic and nonfibrotic ECM scaffolds. These scaffolds were recellularized with normal and fibrotic fibroblasts to assess the 3D ECMs effect on cell phenotype and differentiation. Next, the mechanical and compositional cues from the ECM were assessed individually under 2D conditions, by culturing fibroblasts on different stiffness plates (1, 50, 10^7 kPa), and in media supplemented with normal and fibrotic soluble ECM homogenates. The role of mechanotransduction, specifically Rho-associated kinase (ROCK), and the therapeutic efficacy of inhibiting ROCK were also investigated in the 3D fibrotic ECM-cell relationship. **Results:** The 3D fibrotic scaffolds increased the α-SMA expression in normal fibroblasts. The 3D nonfibrotic scaffolds notably attenuated the initially elevated α-SMA expression in fibrotic fibroblasts. This bidirectional effect was also observed at the 2D stiffness and compositional levels. Mechanotransduction plays a significant role in the 3D fibrotic scaffold's profibrotic effect, which is *blocked* by the administration of the ROCK inhibitor Y-27632. **Conclusion:** The omnipotent effect of the ECM is present at both the

composition and structural levels, and highlights the ECM's governing role on fibroblast phenotype and myofibroblast differentiation.

KEY WORDS

Idiopathic Pulmonary Fibrosis, Pulmonary Fibrosis, Extracellular Matrix, Decellularization, *ex vivo* Scaffold Model System, Fibroblast, Myofibroblast.

INTRODUCTION

IPF is a chronic disease characterized by progressive lung scarring [1]. It usually presents in patients between 60-70 years of age and has a poor prognosis with a median survival of about 3 to 5 years; comparable to some aggressive forms of cancer [2]. In the United States, IPF has a prevalence of 42.7 per 100,000 people and an incidence rate of 16.3 per 100,000 people per year [3]. Currently, there are two available FDA-approved drugs: nintedanib and pirfenidone [4]. These drugs inhibit pathways in the wound healing response to reduce scarring, which slows, however fails to stop or reverse IPF progression. We need to therefore elucidate key pathways in IPF progression to effectively target and treat this fibrotic disease.

The etiology of IPF remains elusive, in part due to the typically late diagnosis [1]. IPF progression has been linked with the differentiation and accumulation of myofibroblasts in lung tissues [5]. Fibroblasts are one of the main precursors of myofibroblasts, and after differentiation these cells produce large amounts of collagen and other structural proteins. This increases the surrounding rigidity and causes drastic thickening of the extracellular matrix (ECM); a hallmark of IPF [1]. The ECM is an insoluble scaffold that provides structural support and defines the shape and architecture of all complex organs in the body [6]. It is composed of two classes of macromolecules: interlocking fibrous proteins, mainly collagen and elastin, and glycoproteins such as fibronectin, proteoglycans, and laminin. For the past few decades cellular changes were believed to be the only drivers in IPF progression, and were targeted as potential therapeutic strategies. The ECM on the other hand was believed to only play structural and basic

biomechanical roles for these cells. Recent findings, however, have highlighted the intricate and dynamic role the ECM has in dictating cell phenotype in various systems: from vascular smooth muscle cells to fibroblasts and also inflammatory cells [7, 8]. Therefore, the ECM may be a more active participant in IPF progression than initially anticipated [9–11]. One potential mechanism for this may be: ECM changes in the fibrotic lung creates a profibrotic microenvironment that promotes increased myofibroblast differentiation of resident cells. This differentiation causes further profibrotic changes in the ECM, creating a positive feedback loop. This cyclical relationship may explain the lack of success seen in many cell-targeted therapeutic strategies, and the exponential disease progression observed in IPF patients. In this current study, we investigate the ECM's role in influencing fibroblast phenotype using a novel 3D *ex vivo* model system. We observe the ECM's clear governing effect on fibroblast phenotype, which is present at both the ECM's structural and chemical levels. This study establishes a unique model system to directly study the ECM-cell interaction in a complete 3D setting. Furthermore, it highlights the ECM's notable role in disease progression, and its potential as a therapeutic target for IPF.

MATERIALS AND METHODS

Rat model of TGF-β1 adenovirus vector-induced pulmonary fibrosis

Female Sprague-Dawley rats (225-250 g; Charles River, Wilmington, MA, USA) were maintained in 12-hours light, 12-hours dark cycles with free access to food and water. Rats were given intratracheal instillation of TGF-β1 adenovirus (AdTGF-β1223/225) or control virus (AdDL) as previously described [12]. Rats intratracheally received 5.0 $x10^8$ plaque-forming units (PFU) of virus in 300 µl sterile saline and lungs were harvested on days 7, 21, or 49 after vector administration. Lungs were either decellularized to prepare ECM scaffolds or used for primary culturing fibroblasts. All work was conducted under the Canadian Council on Animal Care guidelines and approved by the Animal Research Ethics Board of McMaster University under protocol #13.12.48.

Antibodies and regents

For western blots we use α-smooth muscle actin (α-SMA) (ab7817, Abcam) and Glyceraldehyde 3-phosphate dehydrogenase (GAPDH) (#5174, Cell signalling Technology). Anti-rabbit HRP linked IgG (#7074, Cell Signaling Technology) and Anti-mouse IgG HRP-linked Antibody (#7076, Cell Signaling Technology). For fluorescence microscopy, we used goat or donkey secondary antibody conjugated with Alexa Fluor-488 and Alexa Fluor-555 (Abcam).

Primary culturing fibroblasts from rat lungs

Single cell suspensions were created by mincing and 1 hr collagenase treatment of harvested rat lungs. Cells were cultured in 10% Fetal Bovine Serum and 1% pen-strep (Gibco, Life Technologies) in Dulbecco's modified Eagle Medium (Biowhittaker

Reagents, Lonza) and cultured at 37°C, 5% CO_2 in T150 Falcon flasks for 7 days or till confluency and used for experiments/analysis. Due to the stiff culturing conditions and plasticity of primary cultured fibroblasts, cells were used within 14 days or passage 3. Fibroblast populations harvested at 7, 21 and 49 days following AdTGF-β1 treatment were considered Early, Intermediate, and Late fibrotic fibroblast populations, respectively, as they spent increasing time in the TGF-β1 rich lungs. 1kPa and 50 kPa collagen coated hydrogel plates (Softwell, Matrigel) were used for the *in vitro* 2D stiffness experiments.

Decellularization and Recellularization of Rat Lungs

Decellularization was performed through manual lung perfusion (10 ml each time) and incubation with 50 ml of: TritonX (1%; overnight), Sodium Deoxycholate (2%; overnight), NaCl (1 M; 1 hr), and stored in PBS supplemented with Penicillin Streptomycin (1%; max 3 months). Lungs were washed with sterile H_2O between each solution during decellularization to ensure there was no mixing of wash solutions. To investigate fibrosis in a kinetic manner, lungs were harvested at three different times points: 7, 21 and 49 days after AdTGF-β1 administration. Lungs from the different timepoints were termed Early (day 7), Intermediate (day 21), and Late (day 49) fibrotic ECMs, and were selected since in the AdTGF-β1 model they represent the initial, active and persistent fibrosis, respectively. Left lobe recellularization was performed by first tying off the right lobes leaving only the left lobe open. The left lobe was perfused with 5 ml of fibroblasts ($1*10^6$ cells/ml) in 2% low melting agarose. Lungs were briefly left to solidify at room temperature and the left lobe was sectioned into horizontal slices of ~3 cm and immersed in 10% Fetal Bovine Serum and 1% pen-strep (Gibco, Life Technologies) in Dulbecco's modified Eagle

Medium (Biowhittaker® Reagents, Lonza) and incubated at 37°C, 5% CO^2 for 7 and 21 days. The remaining right lobes were stored for hydroxyproline and histological analysis.

Preparation of ECM homogenate solutions

Normal and fibrotic lungs were harvested at day 49 following vector administration. Lungs were decellularized to produce ECM scaffolds, which were then lyophilized and lysed. The lyses buffer was removed from the resulting ECM solutions via 3.5K dialysis cassettes (Slide-A-lyzer Dialysis Cassette G2, Thermo Scientific), and supplemented into the culturing media at 1 µg/ml.

Western blotting

See online supplement for details.

Histology and immunofluorescence

Lung slides were stained with haematoxylin and eosin (H&E) or Picrosirius red (PSR). Images were collected using the Olympus microscope (Olympus BX41, Olympus, ON, Canada) equipped with DP Controller software (Olympus, ON, Canada). PSR pictures were taken using polarized detection. Immunofluorescence staining of α-SMA (Abcam, ON, Canada) and FAP (ab53066, Abcam) was performed on formalin-fixed cells or rat lung tissue sections. Pictures were taken using an epifluorescence microscope (Olympus IX81, Olympus) with the same setting and exposure time for all images. See online supplement for more details.

ELISA

Active TGF-β1 levels in normal and fibrotic ECM solutions were detected using

mouse/rat/porcine/canine TGF-β1-specific ELISA kit (R&D Systems, Minneapolis, MN), according to the manufacturer's recommendations.

Isolation of mRNA and gene expression

Total RNA was extracted from frozen rat lung tissue and *in vitro* cultured cells using TRIzol® reagent (Invitrogen). 1 μg of total RNA was reverse-transcribed using qScript cDNA Super Mix (Quanta Bioscience, Gaithersburg, MD, USA). The cDNA was amplified by a Fast 7500 real-time PCR system (AB Applied Biosystems) using TaqMan® Universal PCR Master Mix and predesigned primer pairs: *Gapdh* (Rn01775763_g1), *Acta2* (Rn01759928_g1), *Col1a1* (Rn00801649_g1), and *Tgfb1* (Rn00572010_m1) (Thermo Fisher Scientific, ON, Canada).

Alamar blue assay

Cell viability and proliferation was assessed for primary cultured fibroblasts before and after ECM recellularization using the Alamar blue dye (Invitrogen) according to the manufacturer's guidelines.

Hydroxyproline assay

Hydroxyproline content in decellularized rat lung samples was determined by a colorimetric assay as described previously [13]. See online supplement for details.

Young's modulus

Using a similar set up as described previously by our group [14], a force transducer and a servo-control arm used in tandem with a digital controller interface (Models 400A, 322C, 604C; Aurora Scientific Inc., Aurora, Canada) were used to exert 5 mN of force onto transversely cut normal (AdDL) and fibrotic (AdTGF-β1) scaffold strips of 10 x 2 x 2 mm

sections for 10 to 15 seconds. These parameters were selected as they allowed for effective measurement of changes in lung scaffold length in response to a controlled force without damaging the scaffolds. Using change in length the respective Young's modulus of the scaffolds were calculated by the formula:

$$E = \frac{F/Ao}{\Delta L/Lo}$$

E = Young's Modulus

F = force exerted on strip;

A_0 = original cross-sectional area of strip;

ΔL = change in length of strip;

L_0 = original length of strip

Due to the standardized strip dimensions and exerted force:

F = 5 mN, A_0 = 4 mm^2 and L_0 = 10 mm

Statistical analysis

The statistically significant differences were determined using a Student's *t*-test for paired samples or a one-way ANOVA followed by a Bonferroni post-hoc test for multiple comparisons. Data sets were normally distributed as determined by the Shapiro-Wilk test. The strength of association between continuous variables was tested with the Pearson correlation (*P*). *P* values of less than 0.05 were considered to be significant. GraphPad Prism program Ver. 8.02 (*GraphPad* Software Inc.) was used for statistical analyses.

RESULTS

Optimization of lung decellularization protocol

Before starting our experiments we needed to first establish a decellularization technique to adequately remove cellular material while preserving the ECM's delicate 3D architecture. Different decellularization protocols (solutions and perfusion techniques) have been investigated by researchers to produce lung scaffolds [15, 16]. Various ionic and non-ionic detergents have been assessed, each with their unique advantages and disadvantages. We, therefore first tested and optimized a currently used protocol: Triton X and sodium deoxycholate, which utilizes both the non-ionic and ionic methods of decellularization in our model system [16]. We also tested manual and gravity powered perfusion techniques. Finally, due to superior lung perfusion and cell clearance, we decided to use 1% Triton X and 2% sodium deoxycholate via manual perfusion for our experiments. Each step in this protocol made the lungs visibly more transparent (figure 1A) and, Hematoxylin and Eosin (H&E) staining showed clear removal of cellular material in both normal and fibrotic lungs (figure 1B). This was further supported by the loss of α-tubulin bands in western blots (figure 1C).

Drastic changes in ECM structure and composition characterize the difference between a normal and fibrotic lung [9]. Our group has previously established and reported the intratracheal administration of an adenovirus encoding active TGF-β1 (AdTGF-β1) to induce transient synthesis of transgenic active TGF-β1 in the lungs [12, 14]. This induces controlled and increasing lung fibrosis in this model. Normal (AdDL) and fibrotic (AdTGF-β1) lungs were harvested at 21 days following vector administration and subsequently

decellularized to create ECM scaffolds. To assess the quality of decellularization we stained scaffolds with H&E and PSR. Staining visualized the maintenance of the microstructural environment and the elevated collagen deposition, characteristic of fibrotic lungs (figure 1B). This increase in collagen embedded in the fibrotic ECMs was also measured by western blot (figure 1C). Fibrosis in the scaffold was measured using a colorimetric assay for hydroxyproline. The hydroxyproline to dry tissue weight ratio of fibrotic scaffolds was 83.1 ± 8.4 µg/mg, compared to the 31.2 ± 6.2 µg/mg in normal scaffolds (figure 1D). The fibrotic scaffolds also exhibited significantly increased rigidity with a Young's modulus of 13.4 ± 2.5 N/mm^2; nearly double that of normal scaffolds at 7.3 ± 1.6 N/mm^2 (figure 1E). Together this data suggests that our decellularization protocol effectively removes cellular material while preserving the structure of both normal and fibrotic ECMs. Through this technique we can produce complete 3D lung scaffolds to investigate the influence of the ECM on cell phenotype.

Phenotypic assessment of fibroblasts harvested from fibrotic vs nonfibrotic lungs

To understand how the ECM affects fibroblast differentiation, we needed to first establish a clear phenotypic starting point between fibroblasts harvested from fibrotic vs nonfibrotic lungs. Rats were treated with AdTGF-β1 or AdDL, and fibroblasts were harvested 21 days after vector administration. Fibrotic fibroblasts (AdTGF-β1 lungs) exhibited a more spindle shaped morphology, with increased expression of the profibrotic, myofibroblast marker: α-smooth muscle actin (α-SMA) than normal fibroblasts (AdDL lungs) (figure 2A, B). Fibrotic fibroblasts also had a decrease in the activated fibroblast specific marker: fibroblast activation protein (FAP) single positive cells (20.5 ± 2.4 vs. 48.8 ± 2.8 cells). Instead, the

fibrotic fibroblast populations had more FAP and α-SMA double positive (70.7 ± 6.2 vs. 51.2 ± 2.8 cells) and α-SMA single positive cells (8.8 ± 4.1 cells vs. none) (figure 2C). Both normal and fibrotic fibroblast populations exhibited high cell viability and proliferation (figure 2D, E). Fibroblasts were also harvested from AdTGF-β1 lungs 7, 21 and 49 days after vector administration, to investigate AdTGF-β1's temporal effect on fibroblast phenotype. A statistically significant increase in the protein expression of α-SMA was seen in fibroblast populations from 7 days (figure 2F). This profibrotic phenotype was most pronounced in cells from 49 days, an elevation that was statistically significant from the other two fibrotic populations as well. These findings highlight the cellular changes between fibroblasts harvested from fibrotic and nonfibrotic lungs, along with the clear increased profibrotic phenotype in fibroblasts 49 days after AdTGF-β1 administration.

Assessing fibroblast recellularization and growth in lung scaffolds

To study the ECM's influence on fibroblast phenotype we needed to first assess the efficacy of recellularization. Immunofluorescence (IF) staining showed removal of cells during decellularization (figure 2G, H), and the effective attachment of fibroblasts after recellularization (figure 2I). For our experiments, fibroblasts were cultured in the scaffolds for up to 21 days. This extended culturing can potentially cause cell senescence or apoptosis [17]. Therefore, we re-harvested the recellularized fibroblasts 21 days after recellularization to evaluate cell viability as outlined in figure 2J. The Alamar blue assay of these cells indicated robust fibroblast health despite the extended culturing period (figure 2K). These results suggest that this recellularization protocol can effectively seed

fibroblasts into 3D fibrotic and normal scaffolds, and maintain adequate cell viability up to 21 days of culturing.

Assessing the role of fibrotic and nonfibrotic scaffolds on fibroblast fate

Having established the efficacy of decellularization and the cell viability pre- and post-recellularization, we were ready to use the *ex vivo* model to investigate the ECM's effect on fibroblast phenotype. To assess the profibrotic potential of the ECM, we recellularized normal fibroblasts into the three (Early, Intermediate, Late) fibrotic scaffolds. In this experiment, fibroblast populations were culture for 7 and 21 days as outlined in figure 3A. To control for variation between cell passages and scaffolds, changes in fibroblast phenotype were measured as a ratio of α-SMA protein expression between 21 and 7 days of culturing in the same scaffolds. In this experiment the 21 to 7 day α-SMA expression ratio increased from 0.7 ± 0.2 in normal fibroblasts in nonfibrotic scaffolds, to 7.0 ± 1.0 in normal fibroblasts cultured in Late (ECMs harvested 49 days after AdTGF-β1 administration) fibrotic scaffolds (figure 3B). This 10-fold increase suggests that the fibrotic scaffolds facilitate a notable profibrotic phenotype on the recellularized fibroblasts. Next, we were interested in investigating any anti-fibrotic capabilities of the ECM. Therefore, we recellularized the three (Early, Intermediate, Late) fibrotic fibroblast populations into nonfibrotic scaffolds as outlined in figure 3D. These scaffolds significantly attenuated the α-SMA protein expressions, with a 21 to 7 day α-SMA ratio lower than 1 (figure 3E). All three fibrotic fibroblast populations showed a statistically significant reduction in their profibrotic phenotype, with each group having a 21 to 7 day α-SMA ratio below 0.5. This was also true for the very fibrotic fibroblasts from the Late fibroblast group,

which initially had the greatest α-SMA expression (figure 2B). Recellularizing these fibrotic fibroblasts into a fibrotic ECM only preserved their profibrotic phenotype, with a ratio of 1.02 ± 0.19. These findings highlight the omnipotent influence of the ECM in dictating fibroblast phenotype, however, the question still remains as to what specific factors in these ECM scaffolds are responsible for this governing effect. The fibrotic and nonfibrotic ECMs have notable changes in both structure and composition, therefore, these aspects need to be investigated separately to appropriately understand this ECM dependent effect.

Assessing effect of stiffness on fibroblast phenotype

Significant increases in stiffness are a hallmark of IPF lungs [1, 9]. In our model too, AdTGF-β1 confers notable increases in lung rigidity to the scaffolds (figure 1E). Therefore, we assessed the impact of changing stiffness on fibroblast phenotype. Normal fibroblasts were cultured *in vitro* under increasing stiffness conditions: 1 kPa, 50 kPa and 10^6 kPa for 24 and 72 hrs. The cells exhibited a gradual increase in α-SMA protein expression, which was most pronounced at 72 hrs (figure 4B). These changes were also present at the mRNA level, where increased stiffness elevated *Acta2, Col1a1* and *Tgfb1* expression (figure 4 C, D, E). Interestingly, culturing Late (cells harvested from AdTGF-β1 lungs 49 days after vector administration) fibrotic fibroblasts under soft conditions decreased their mRNA *Acta2* expression, suggesting an attenuation of their fibrotic phenotype (figure 4F). Continued culturing of these cells under stiff conditions, however, further elevated this *Acta2* expression. These results highlight the effect of structural stiffness on fibroblast

phenotype. Therefore, investigating the transduction of these mechanical stimuli into the cells might be a potential target into decoupling the fibrotic ECM – fibroblast relationship.

Assessing ROCK in the fibrotic ECM's profibrotic effect on fibroblasts

Since 2D stiffness had a clear effect on fibroblast phenotype, we assessed mechanotransduction directly in our *ex vivo* model system. Rho-associated kinases (ROCK) are well known mediators of the mechanotransduction pathway, and we measured their mRNA expression levels in normal fibroblasts recellularized into fibrotic (ECMs harvested 21 days after AdTGF-β1 administration) scaffolds as outlined in figure 5A. Samples were collected at 7 and 21 days after recellularization. The fibrotic scaffolds clearly elevated the mRNA expression of both *Rock 1* and *2* isoforms at 21 days after recellularization (figure 5B). Since mechanotransduction seems to play a key role in the fibrotic ECM's profibrotic effect, we were interested to see the impact of inhibiting this pathway in our model. Similar to above, normal fibroblasts were recellularized into fibrotic (ECMs harvested 21 days after AdTGF-β1 administration) and nonfibrotic scaffolds (figure 5A). Recellularized scaffolds were cultured in media supplemented with or without the ROCK inhibitor: Y-27632 (10μM) and harvested at 7 and 21 days after recellularization. As expected, the fibrotic ECM scaffolds greatly increased the mRNA expression of *Acta2* in the normal fibroblasts between 7 to 21 days of culturing (figure 5D). Treatment with Y-27632, however, significantly attenuated this *Acta2* expression, with levels comparable to the fibroblasts cultured in nonfibrotic scaffolds (figure 5D). These findings again highlight the fibrotic scaffolds' profibrotic effect on fibroblasts, now at the mRNA level. More importantly, they establish the key role mechanotransduction plays in the fibrotic ECM –

fibroblast relationship, and the potential of ROCK inhibitors to decouple this cycle. Here we see the role of stiffness in the ECM's effects, however, drastic compositional changes are also present between the fibrotic and nonfibrotic ECMs.

Assessing effect of ECM composition on fibroblast phenotype

Having assessed the role of stiffness, the next step was to investigate the effect of composition. IPF lungs have significantly increased ECM deposition [9–11]. These changes have a large degree of variability: in the type and amount of proteins deposited [18]. To study the ECM's compositional effect on fibroblast fate, we homogenized the scaffolds and supplemented the soluble ECM proteins (1μM) into the media of fibroblasts. Cells were cultured on 1kPa plates to omit any stiffness dependent effects, and cells were assessed at 72 hrs after homogenate supplementation. The fibrotic ECM solutions increased the protein expression of α-SMA in normal fibroblasts (figure 6B). This was also supported by mRNA elevations of profibrotic markers such as *Acta2*, *Col1a1* and *Tgfb1* (figure 6C, D, E). To assess any anti-fibrotic potential of the ECM solutions, effects on fibrotic fibroblasts (cells harvested from AdTGF-β1 lungs 49 days after vector administration) were measured. Since here the fibrotic fibroblasts were cultured on 1kPa plates, and the soft plates attenuate the profibrotic expression of these cells (figure 4F), lysis treatment (LT) solution containing no ECM proteins were used as a control. When supplemented with the three different solutions, interestingly, exposure of fibrotic fibroblasts to the nonfibrotic ECM solutions decreased the initially elevated *Acta2* mRNA expression (figure 6F). The fibrotic ECM solution on the other hand further elevated the *Acta2* expression of the fibrotic fibroblasts. These findings suggest that both the profibrotic and also antifibrotic ECM

effects are present at the composition level. This may be explained by changes in the levels of ECM proteins, however, the ECM is also rich in growth factors. Specifically, the profibrotic mediator TGF-β1 is stored in an inactive form in the ECM, and is significantly increased in fibrotic lungs [18]. Therefore, we measured TGF-β1 levels in the ECM solutions. Interestingly, both nonfibrotic and fibrotic ECM solutions had undetectable levels of active TGF-β1 as measured by an ELISA (supplemental figure 2). Furthermore, inhibition of TGF-β1 signaling by SB431542 in the above ECM solution experiments did not block the ECM solutions effects as measured by *Acta2*, and a tendency is also seen in *Col1a1* expression (figure 6G, H). These findings suggest there is a notable compositional effect, irrespective of TGF-β1 signalling, in the soluble ECM solution driven pro-fibrotic and anti-fibrotic effect on fibroblasts.

DISCUSSION

The ECM's Profibrotic Capacity

In this study, we report the fibrotic ECM's profibrotic effect on fibroblast phenotype. Booth et al. were one of the first to highlight this relationship by seeding fibroblasts onto decellularized ECM scaffolds from human IPF lungs [19]. Their elegant study illustrated the ECM's profibrotic potential, however, the complete 3D effect of the ECM was not fully investigated. They used scaffolds of one mm in width and cells were seeded using a dropwise technique directly onto the scaffolds. Fibroblasts successfully attached to the ECM, however, due to the thin size, much of the 3D architecture was lost in this technique. The scaffolds were also derived from patient samples, which provide real *in vivo* conditions, however, are difficult to standardize; and without the whole lung architecture (trachea, bronchioles) difficult to achieve full lung/lobe recellularization. In this current study, by decellularizing whole rat lungs we successfully performed complete lobe recellularization and cultured cells in ~3 cm wide horizontal lung sections. Researchers have reported cell "memory" in fibroblasts, where prolonged exposure to a certain environment has lasting effects on phenotype that persist for up to 2 weeks [20]. Therefore, we also cultured cells in the ECM scaffolds for 7 and 21 days to ensure complete changes in fibroblast phenotype were observed in response to the new microenvironments. Using the AdTGF-β1 model we were able to create scaffolds that effectively recapitulate the fibrotic and nonfibrotic 3D ECMs. In this *ex vivo* system, the fibrotic scaffolds significantly increased the profibrotic phenotype of recellularized normal fibroblasts. To better understand this fibrotic ECM induced profibrotic effect, we assessed this individually at

the structural and compositional level. As it is well documented in the literature, here too increasing *in vitro* stiffness induced a clear fibrotic phenotype in normal fibroblasts [21, 22]. Interestingly, this profibrotic effect was also present at the compositional level. Soluble factors in the ECM solution prepared from fibrotic scaffolds promoted a fibrotic phenotype in normal fibroblasts. This ECM solution also further elevated the α-SMA expression of fibrotic fibroblasts. These findings are in accordance with the growing body of research that supports the notion of a vicious cyclical relationship between the fibrotic ECM and lung fibroblasts; which may drive progressive fibrosis [9–11]. Since our model investigates the ECM driven fibroblast phenotype, our results provide support for this theory. Furthermore, our group also recently published a paper illustrating the fibrotic ECM's ability to promote degranulation of Mast cells [23]. Degranulation of Mast cells release profibrotic mediators and is linked to IPF progression. Other researchers have also shown increasing stiffness to promote profibrotic phenotypes in macrophages, endothelial cells, and various mesenchymal cells [24, 25]. These and other cell types have been assessed in the context of IPF, and investigated as potential therapeutic targets. Despite these studies, very few cell types have been conclusively implicated in the pathogenesis or progression of IPF. The ECM on the other hand, as seen in this study and others, has a notable profibrotic capacity. This capacity also has widespread influence across various cell types, which highlights the key and active role the ECM plays in IPF progression. Therefore, by shifting our focus to the ECM we can holistically target the profibrotic microenvironment and potentially rescue the various cell types trapped in the vicious cycle driving progressive fibrosis.

The ECM's Anti-fibrotic Capacity

It was long believed that fibroblast to myofibroblast differentiation was an irreversible process, and therefore an unsuccessful avenue for IPF therapy [26, 27]. Recent data, however, indicates that myofibroblast dedifferentiation is possible, and can be induced by prostaglandin E2 or down-regulation of MyoD [28, 29]. Plating IPF fibroblasts on physiologically soft plates *in vitro* also decreases cell contractility, suggesting an attenuation in the cells' fibrotic function [30]. In this current study, we see that the nonfibrotic (physiological) scaffolds attenuate the fibrotic phenotype in recellularized fibrotic fibroblasts. Since these recellularized fibroblasts maintained a high degree of cell viability after the 21 days of culturing, we ruled out cell senescence and apoptosis. This anti-fibrotic effect was present at both the structural and compositional level, where *in vitro* physiological stiffness and ECM solution derived from nonfibrotic scaffolds both notably attenuated the *Acta2* expression of fibrotic fibroblasts. These findings highlight two key points: fibrotic fibroblasts maintain a high degree of plasticity despite spending 49 days in fibrotic lungs (Late fibrotic fibroblasts), and more importantly, the physiological ECM possesses a notable anti-fibrotic potential. These findings provide credence for current research that targets the ECM structure. One example is the Lysyl oxidase (LOX) family of enzymes, which catalyze the cross-linking of collagen and elastin [31, 32]. This is a growing body of research that still remains to be fully explored as an avenue for IPF therapy. By developing more effective drugs that restructure the fibrotic ECM, we can begin to utilize the ECM as a tool in the fight against fibrosis, rather than it being an active player in its progression.

Structure – The Mechanotransduction Pathway

Mechanotransduction is the propagation of external mechanical cues into the cell so that the cell can appropriately respond structurally and chemically to external stimuli [21, 33]. Many cell types are capable of responding to mechanical signals. In the case of induced pluripotent stem cells (iPSCs), an identical cell population can differentiate into district cell types based solely on substrate stiffness [34]. Therefore to avoid unnecessary iPSCs differentiation during culturing, many protocols use mechanotransduction inhibitors to limit this stiffness dependent effect [35]. Y27632 is one of the most commonly used mechanotransduction inhibitors and is a potent pan-inhibitor of Rho Associated coiled-coil forming Kinase (ROCK) [36]. ROCK is a serine-threonine kinase that acts on the cytoskeleton to regulate cell shape and movement and is a key mediator in the mechanotransduction pathway [37]. ROCK 1 and 2 are the two main isoforms of ROCK that have similar effects. Inhibiting both ROCK isoforms using the pan-ROCK inhibitor Y27632 (10 µM) has been shown to successful attenuate the stiffness dependent profibrotic effect in various *in vitro* and *in vivo* models of fibrosis and cancer [37–41]. In this current study, increased stiffness induces a profibrotic fibroblast phenotype at both the 2D and 3D level. The fibrotic scaffolds also elevated *Rock1* and *Rock2* in recellularized fibroblasts, which suggests mechanotransduction as a key contributor in this ECM scaffold – fibroblast relationship (figure 5 B, C). Inhibiting mechanotransduction using Y27632 in this *ex vivo* model significantly attenuated the fibrotic ECM induced *Acta2* expression in normal fibroblasts (figure D). This is one of the first studies to shown the efficacy of inhibiting mechanotransduction to directly impede the fibrotic ECM's ability to induce a fibrotic

fibroblast phenotype. This may explain the success of KD025 - a ROCK inhibitor that recently passed through phase IIA clinical trial [42]. These mechanotransduction inhibitors can, therefore, block the fibrotic ECM's profibrotic effect and intervene in the vicious positive feedback cycle, which may very well be at the heart of the rapid IPF/fibrosis progression profile.

Composition – ECM Homogenate Solution

One reason for the increased stiffness in the fibrotic ECM is changes in structural arrangement [9, 46]. Another key reason is the aberrant protein deposition by cells such as myofibroblasts, which augments the ECM composition. Under both physiological and pathological conditions, ECM composition is maintained by a dynamic balance between deposition and degradation. In IPF, increased deposition and decreased degradation facilitate the characteristic fibrous collagen-rich architecture. Fragments from the ECM can be generated by metalloproteins that cleave full-length ECM proteins to produce bioactive fragments. These fragments bind to integrins and EGFR receptors, and in the case of angiogenesis can induce both pro- and anti-angiogenic effects [43]. In fibrosis, ECM fragments such as fibrin, fibronectin, and hyaluronan are drastically upregulated in fibrotic ECMs, and have been seen to have profibrotic effects on cells. In this study, the ECM solutions generated from fibrotic ECM scaffolds induced a fibrotic response in fibroblasts. One explanation for this may be these bioactive ECM fragments that are upregulated in the fibrotic ECM. Another potential contributor may be growth factors attached to the ECM. Along with providing structural integrity, the ECM serves as a ligand reservoir for various growth factors such as TGF-β1 [44]. The fibrotic lung is also known to have increased

amounts of TGF-β1 attached to its ECM. Therefore, we measured active TGF-β1 levels by ELISA in the ECM solutions, however, both the nonfibrotic and fibrotic solutions in our study had undetectable levels. One explanation for this may be that most of the growth factors attached to the ECM were washed off during the decellularization and lyophilization process [16]. To further rule out any TGF-β dependent effects, we inhibited TGF-β mediated activation of SMAD proteins using SB431542. Despite inhibition, the fibrotic ECM solution's effects still persisted, suggesting an alternative pathway potentially induced by bioactive ECM fragments.

More interestingly, however, was the observation that the ECM solutions generated from a nonfibrotic (physiological) ECM scaffold attenuated α-SMA expression in fibrotic fibroblasts. Though a profibrotic effect of ECM fragments has been recognized in the literature, an anti-fibrotic effect has not been identified. A comprehensive list of ECM proteins in decellularized IPF and donor scaffolds was presented by Booth et al [19]. This list highlights the complexity in ECM composition and the large magnitude of changes between the physiological and pathological conditions. Therefore, the possibility of pinpointing one or even a handful of molecules sole responsible for the pro- or anti-fibrotic effects observed in the ECM solutions might be unreasonable. Instead, these effects may be the result of the amalgamation of various proteins that collectively make up the ECM composition. We believe that this ratio of proteins, may yield in ultimately either a pro- or anti-fibrotic effect on fibroblasts and potentially other cells. Therefore, instead of trying to pinpoint specific molecules, we need to develop effective methods to achieve a

physiological ECM state, as this may yield both the structural and compositional anti-fibrotic effects that will help halt and potentially reverse IPF/ fibrosis.

CONCLUSION

This study builds upon the current decellularization models to establish a system for complete full lung/ lobe recellularization to directly study the physiological and pathological ECM's effects on fibroblast phenotype. It can also be used to study the efficacy of drugs at directly targeting the ECM-cell relationship in the 3D context. The findings from this study highlight the opposing effects of the ECM scaffold. We see the ECM's profibrotic and antifibrotic effects present at both the structural and compositional levels, where mechanotransduction and bioactive ECM proteins are two potential factors at play. These findings highlight the corrective effect of the "physiological" ECM. By facilitating this physiological ECM state, we may be able to provide a more permanent treatment option for IPF and other fibrotic diseases.

FIGURE LEGENDS

Figure 1. Decellularization using 2% Sodium Deoxycholate is effective at clearing cells and maintaining ECM architecture in both normal and fibrotic lungs. (A) Lungs were first washed with water (Day 0) and then left in Triton X (1%) overnight (Day 1). Next, the lungs were placed in Sodium Deoxycholate (2%) overnight (Day 2). The following day the lungs were washed with NaCl (1%) and then stored in PBS supplemented with Penicillin Streptomycin (S). **(B)** Normal (AdDL) and fibrotic (AdTGF-β1) lungs were decellularized and cell clearance and ECM microenvironment were visualized via H&E and PSR staining. **(C)** Protein expression of Collagen I and α-tubulin were measured in these decellularized ECMs. **(D)** Hydroxyproline and **(E)** Young's modulus were measured for decellularized AdDL (n = 5) and AdTGF-β1 (n = 4) treated rat lungs 21 days after vector administration. Results are presented as mean ± SEM. Statistics was performed by Student's T-test. *$p < 0.05$.

Figure 2. Phenotypic changes in fibroblasts cultured from AdTGF-β1 treated lungs. Recellularization effectively seeds cells into ECM scaffolds, which maintains cell viability 21 days after recellularization. (A) Immunofluorescent staining for FAP (red), α-SMA (green), and DAPI (blue) of primary cultured fibroblasts from rats treated with **(A)** AdDL or **(B)** AdTGF-β1, 21 days after vector administration. **(C)** Quantitative analysis determined using 5 images similar to those in A & B from 3 different cell populations. **(D)** Cell viability of AdDL and AdTGF-β1 cells were determined using the Alamar blue assay. **(E)** Variation in α-SMA protein expression was assessed in different fibrotic fibroblast populations (n = 4), harvested: Early – 7 days; Intermediate – 21 days; Late – 49 days after

AdTGF-β1 administration. DAPI staining of ECM scaffolds before **(F)** and after **(G)** decellularization. **(H)** Recellularized cells were stained with FAP (red), α-SMA (green), and DAPI (blue) and imaged at 20X and 100X, 21 days after culturing in ECM scaffolds. Recellularized cells were also harvested after 21 days in ECM scaffolds, as **(I)** outlined, and assessed for cell viability using the **(J)** Alamar blue dye (n = 3). Results are presented as mean ± SEM. Statistic is one-way analysis of variance (ANOVA) and Tukey's post-test. * $p < 0.05$, ** $p < 0.01$, **** $p < 0.0001$.

Figure 3. ECM scaffolds dictate fibroblast phenotype and differentiation. (A) Diagram outlining the experimental setup for the normal fibroblasts in fibrotic ECM scaffolds experiment. **(B)** Relative fold increase of α-SMA presented as a ratio of protein expression measured between 7 and 21 following recellularization. Fibrotic ECM: Early – 7 days; Intermediate – 21 days; Late – 49 days after AdTGF-β1 administration, with normal ECM: AdDL as control. Protein expression was normalized to Gapdh; n=3. **(C)** Representative western blot for normal fibroblasts in normal ECM vs Late fibrotic ECM scaffolds. **(D)** Diagram outlining the experimental setup for the fibrotic fibroblasts in normal ECM scaffolds experiment. **(E)** Relative fold decrease of α-SMA presented as a ratio of protein expression measured between 7 and 21 days following recellularization. Fibrotic fibroblasts: Early – 7 days; Intermediate – 21 days; Late – 49 days after AdTGF-β1 administration in normal ECM scaffolds, with and Late fibrotic fibroblasts in Late fibrotic ECM scaffolds as control. Protein expression was normalized to Gapdh; n = 4. **(F)** Representative western blot for fibrotic fibroblasts in Late fibrotic ECM vs normal ECM scaffolds. **(G)** Representative IF images, staining for FAP (red), α-SMA (green), and DAPI

(blue) of these fibrotic fibroblasts at 21 days following recellularization into fibrotic and normal ECM scaffolds. Results are presented as mean ± SEM. Statistics are one-way ANOVA and Tukey's post-test. **p < 0.01, ***p < 0.001.

Figure 4. In vitro stiffness drives fibroblast phenotype. (A) Comparison of physiological organ systems to plate's stiffness as a measure of kilopascals (kPa). **(B)** Relative protein expression of α-SMA in normal rat fibroblasts cultured on different stiffness conditions: 1 kPa (blue), 50 kPa (red) and 10^6 kPa (Tissue Culture Plate) (Gray). The relative mRNA expression of **(C)** *Acta2*, **(D)** *Col1a1* and **(E)** *Tgf-β1* in these cells were also measured. Protein and mRNA expressions were normalized to Gapdh (n=3). **(F)** The relative *Acta2* mRNA expression was also measured in fibrotic fibroblasts (Late - harvested 49 days after AdTGF-β1 administration) cultured on 1 kPa (blue) and 10^6 kPa (Gray) stiffnesses plates. Expression normalized to Gapdh (n = 3). Results are presented as mean ± SEM. Statistic is one-way ANOVA and Tukey's post-test. *p < 0.05, ****p < 0.0001.

Figure 5. ROCK plays a key role in the ECM scaffold driven fibroblast differentiation. (A) Diagram outlining the experimental setup. The mRNA expression of **(B)** *Rock1* and **(C)** *Rock2* in normal fibroblasts cultured in normal (AdDL, n = 5) and fibrotic (AdTGF-β1, n = 4) ECM scaffolds at 7 and 21 days following recellularization. **(D)** mRNA expression of *Acta2* from normal fibroblasts cultured in normal (n = 4) and fibrotic (n = 5) ECM scaffolds at 7 and 21 days following recellularization. These cells were cultured with either no treatment (NT) or a rock inhibitor: Y-27632 - 10μM (ROC). Gene expression normalized to *Gapdh*. Results are presented as mean ± SEM. Statistics was performed using

one-way ANOVA and Bonferroni post-test. *p < 0.05, **p < 0.01, ****p < 0.0001, #p< 0.0001 difference compared to D7 NT in AdTGF-β1 group.

Figure 6. ECM composition alone is capable of directing fibroblast phenotype and differentiation. (A) Diagram outlining the experimental setup and ECM solution preparation from decellularized ECMs harvested 21 days after vector administration. **(B)** Relative protein expression of α-SMA in normal rat fibroblasts cultured in media supplemented with 1µg/ml of normal (AdDL) or fibrotic (AdTGF-β1) ECM solutions. The relative mRNA expression of **(C)** *Acta2*, **(D)** *Col1a1* and **(E)** *Tgf-β1* in these cells were measured.

(F) The relative mRNA expression of *Acta2* was also measured in fibrotic rat fibroblasts (Late - 49 days after AdTGF-β1 administration) cultured in media supplemented with normal or fibrotic ECM solutions. Lysis Treatment (LT) containing no ECM solution was used as control. Normal fibroblasts were exposed to normal and fibrotic ECM solutions with and without 100nM of SB431542 treatment and measured for **(G)** *Acta2* and **(H)** *Col1a1* mRNA expression. Cells for all experiments were harvested 72 hours after respective treatments. Protein and mRNA expressions were normalized to Gapdh (n = 3). Results are presented as mean ± SEM. Statistic was done using one-way ANOVA and Tukey's post-test. *p < 0.05, **p < 0.01, ****p < 0.0001. #p< 0.01 difference compared to Norm. ECM.

Figure 1

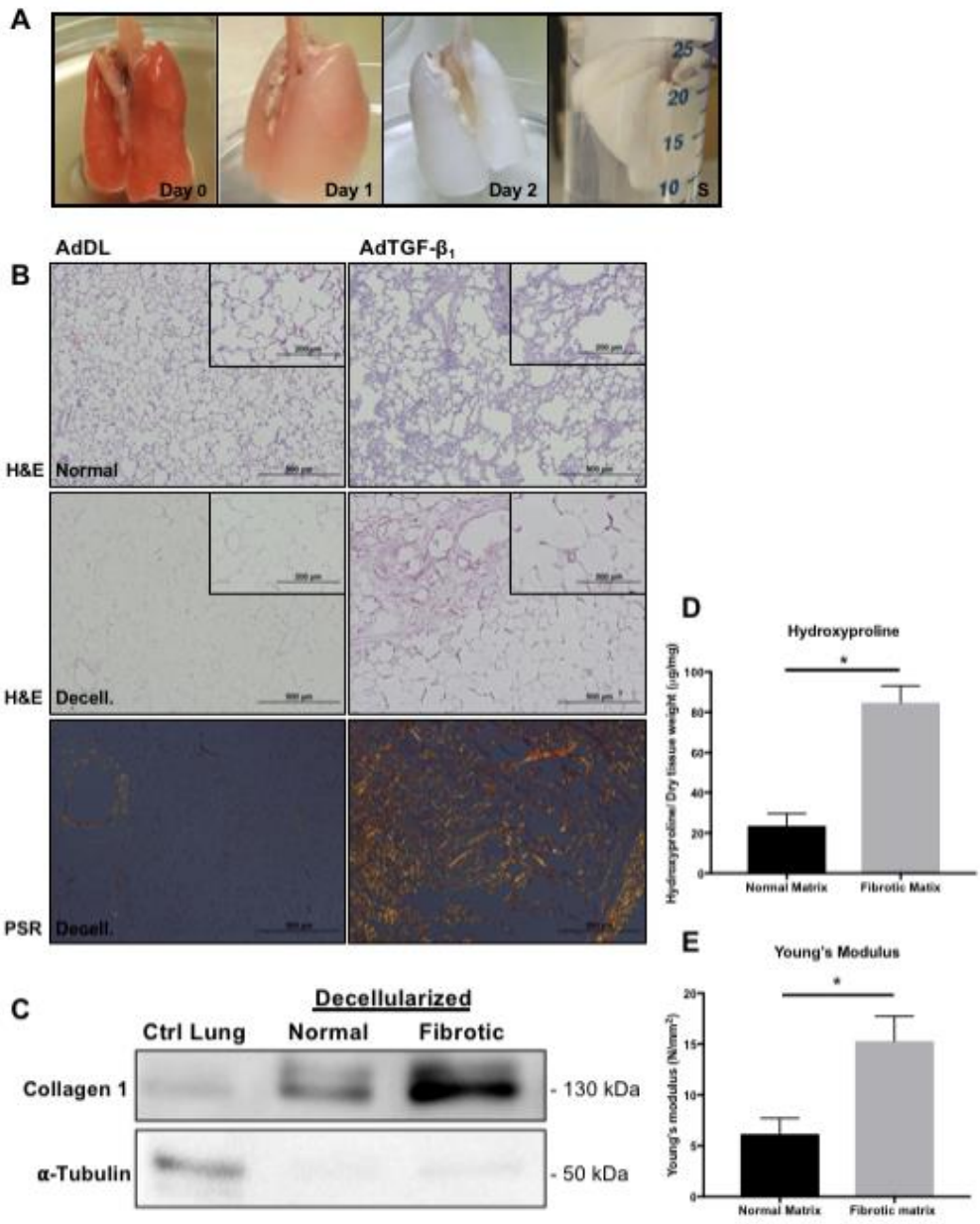
A
Day 0
Day 1
Day 2
25
20
15
10
S
B
AdDL
AdTGF-β1
H&E Normal
H&E Decell.
PSR Decell.
C
Decellularized
Ctrl Lung
Normal
Fibrotic
Collagen 1
- 130 kDa
α-Tubulin
- 50 kDa
D
Hydroxyproline
*
Hydroxyproline/ Dry tissue weight (µg/mg)
100
80
60
40
20
0
Normal Matrix
Fibrotic Matix
E
Young's Modulus
*
Young's modulus (N/mm²)
20
15
10
5
0
Normal Matrix
Fibrotic matrix

Figure 2

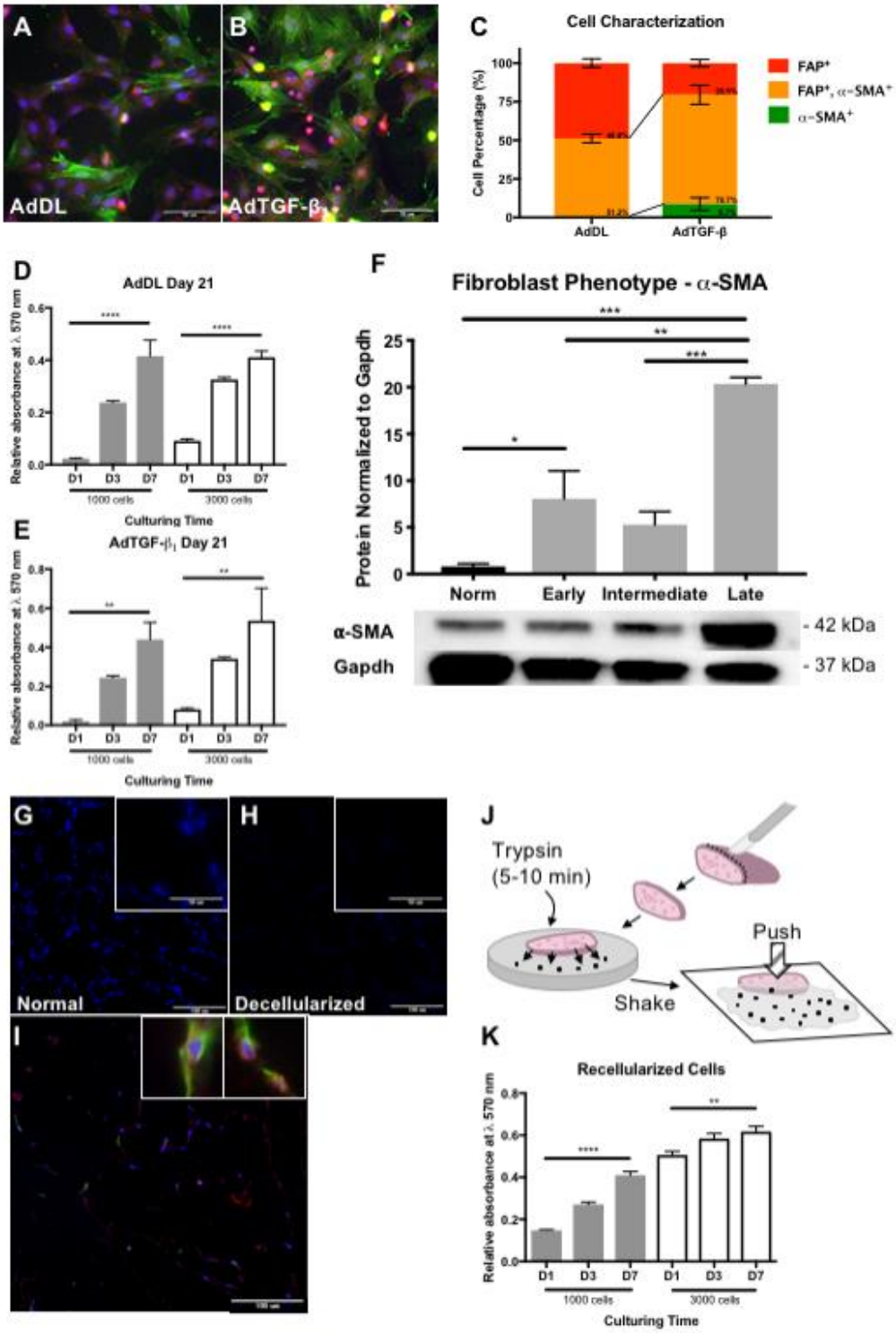
A
AdDL
B
AdTGF-β
C
Cell Characterization
Cell Percentage (%)
FAP+
FAP+, α-SMA+
α-SMA+
AdDL
AdTGF-β
D
AdDL Day 21
Relative absorbance at λ 570 nm
D1 D3 D7 D1 D3 D7
1000 cells
3000 cells
Culturing Time
E
AdTGF-β1 Day 21
F
Fibroblast Phenotype - α-SMA
Protein Normalized to Gapdh
Norm
Early
Intermediate
Late
α-SMA
Gapdh
- 42 kDa
- 37 kDa
G
Normal
H
Decellularized
I
J
Trypsin
(5-10 min)
Push
Shake
K
Recellularized Cells

Figure 3

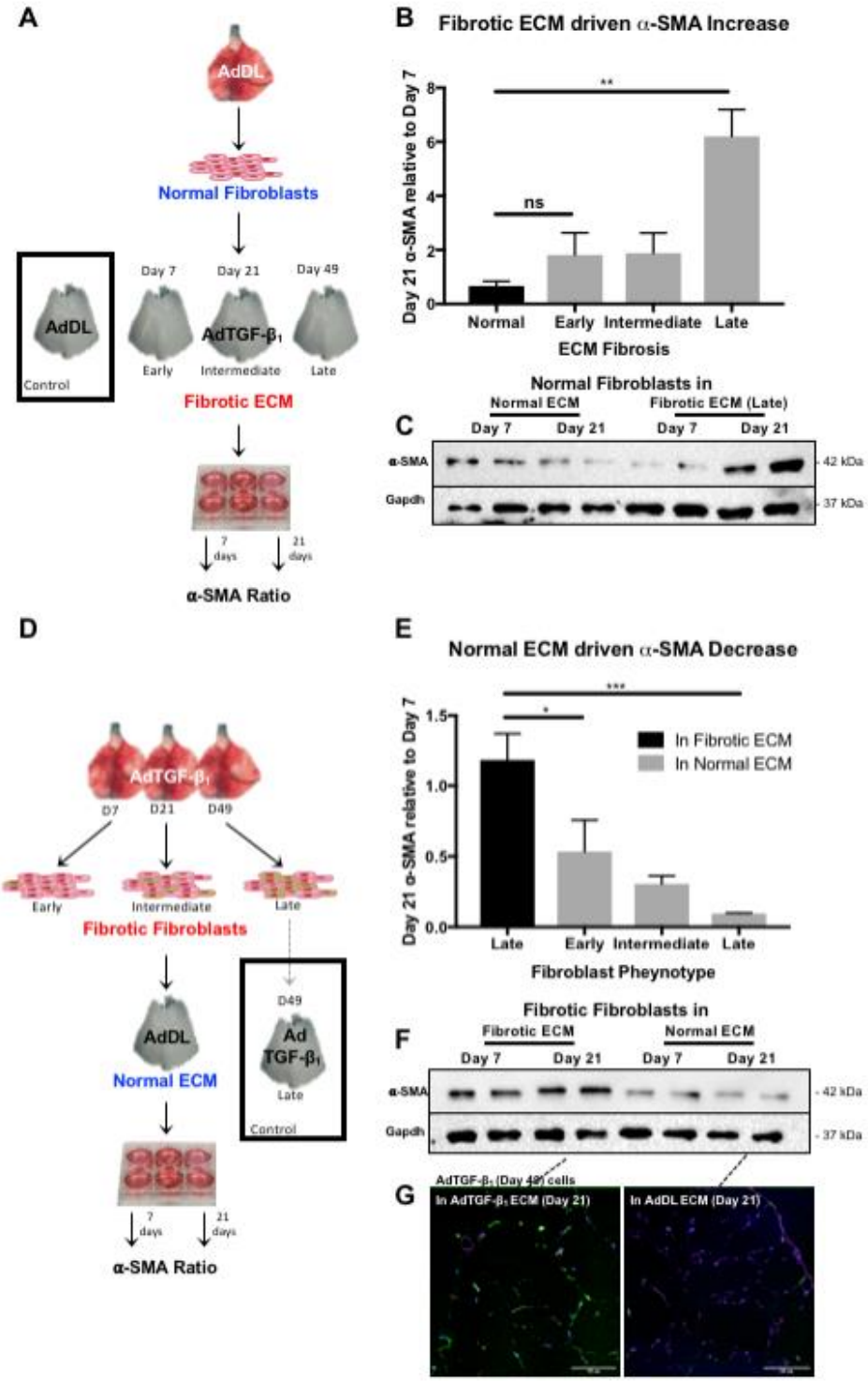
A
AdDL
Normal Fibroblasts
Day 7
Day 21
Day 49
AdDL
AdTGF-β1
Control
Early
Intermediate
Late
Fibrotic ECM
7 days
21 days
α-SMA Ratio
B
Fibrotic ECM driven α-SMA Increase
Day 21 α-SMA relative to Day 7
**
ns
Normal
Early
Intermediate
Late
ECM Fibrosis
C
Normal Fibroblasts in
Normal ECM
Fibrotic ECM (Late)
Day 7
Day 21
Day 7
Day 21
α-SMA
Gapdh
42 kDa
37 kDa
D
AdTGF-β1
D7
D21
D49
Early
Intermediate
Late
Fibrotic Fibroblasts
D49
AdDL
Ad TGF-β1
Late
Control
Normal ECM
7 days
21 days
α-SMA Ratio
E
Normal ECM driven α-SMA Decrease
***
*
In Fibrotic ECM
In Normal ECM
Day 21 α-SMA relative to Day 7
Late
Early
Intermediate
Late
Fibroblast Pheynotype
F
Fibrotic Fibroblasts in
Fibrotic ECM
Normal ECM
Day 7
Day 21
Day 7
Day 21
α-SMA
Gapdh
42 kDa
37 kDa
G
AdTGF-β1 (Day 49) cells
In AdTGF-β1 ECM (Day 21)
In AdDL ECM (Day 21)

Figure 4

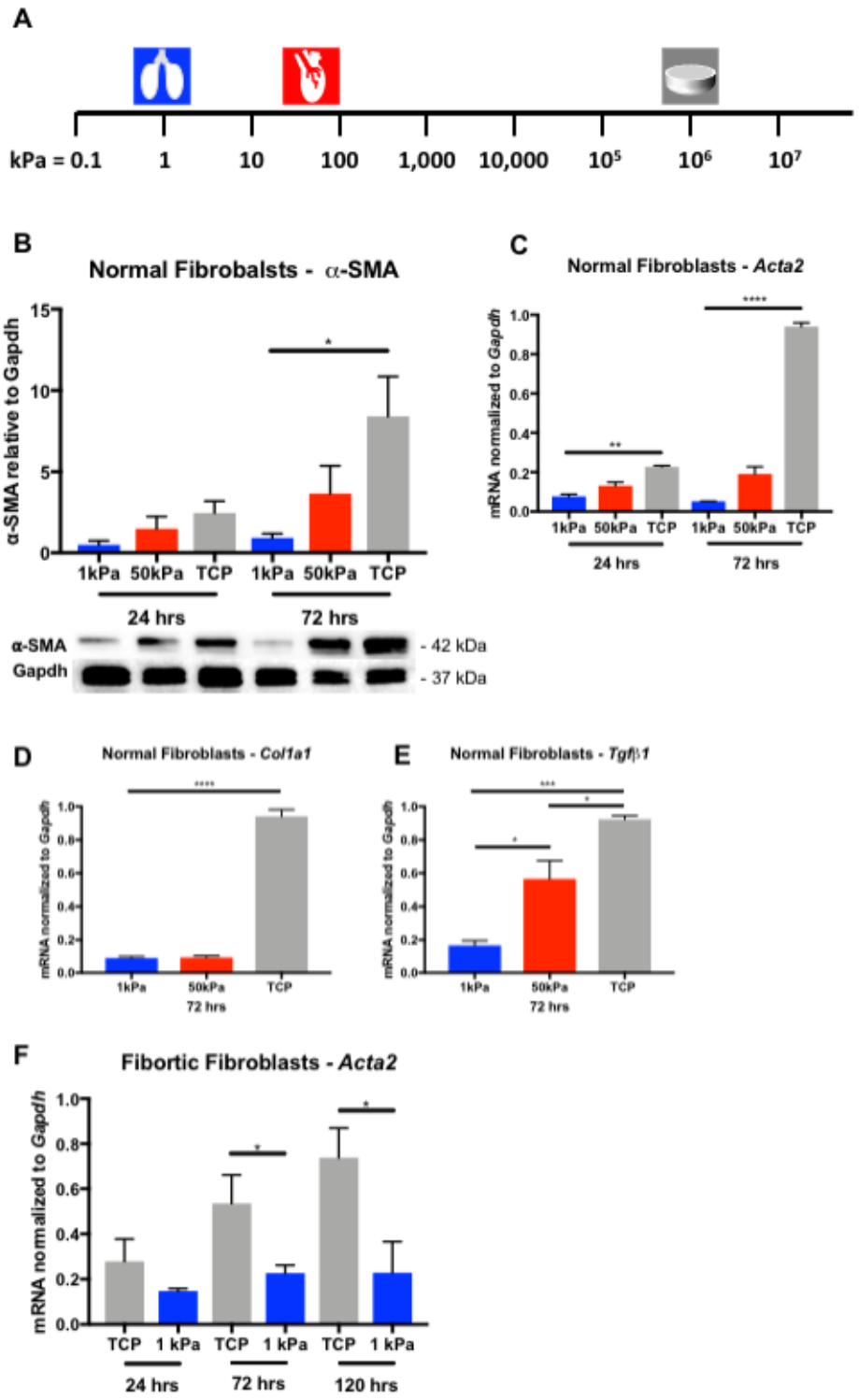
A
kPa = 0.1
1
10
100
1,000
10,000
10^5
10^6
10^7
B
Normal Fibrobalsts - α-SMA
α-SMA relative to Gapdh
1kPa 50kPa TCP 1kPa 50kPa TCP
24 hrs
72 hrs
α-SMA
Gapdh
- 42 kDa
- 37 kDa
C
Normal Fibroblasts - Acta2
mRNA normalized to Gapdh
1kPa 50kPa TCP 1kPa 50kPa TCP
24 hrs
72 hrs
D
Normal Fibroblasts - Col1a1
mRNA normalized to Gapdh
1kPa
50kPa
TCP
72 hrs
E
Normal Fibroblasts - Tgfb1
mRNA normalized to Gapdh
1kPa
50kPa
TCP
72 hrs
F
Fibortic Fibroblasts - Acta2
mRNA normalized to Gapdh
TCP 1 kPa TCP 1 kPa TCP 1 kPa
24 hrs
72 hrs
120 hrs

Figure 5

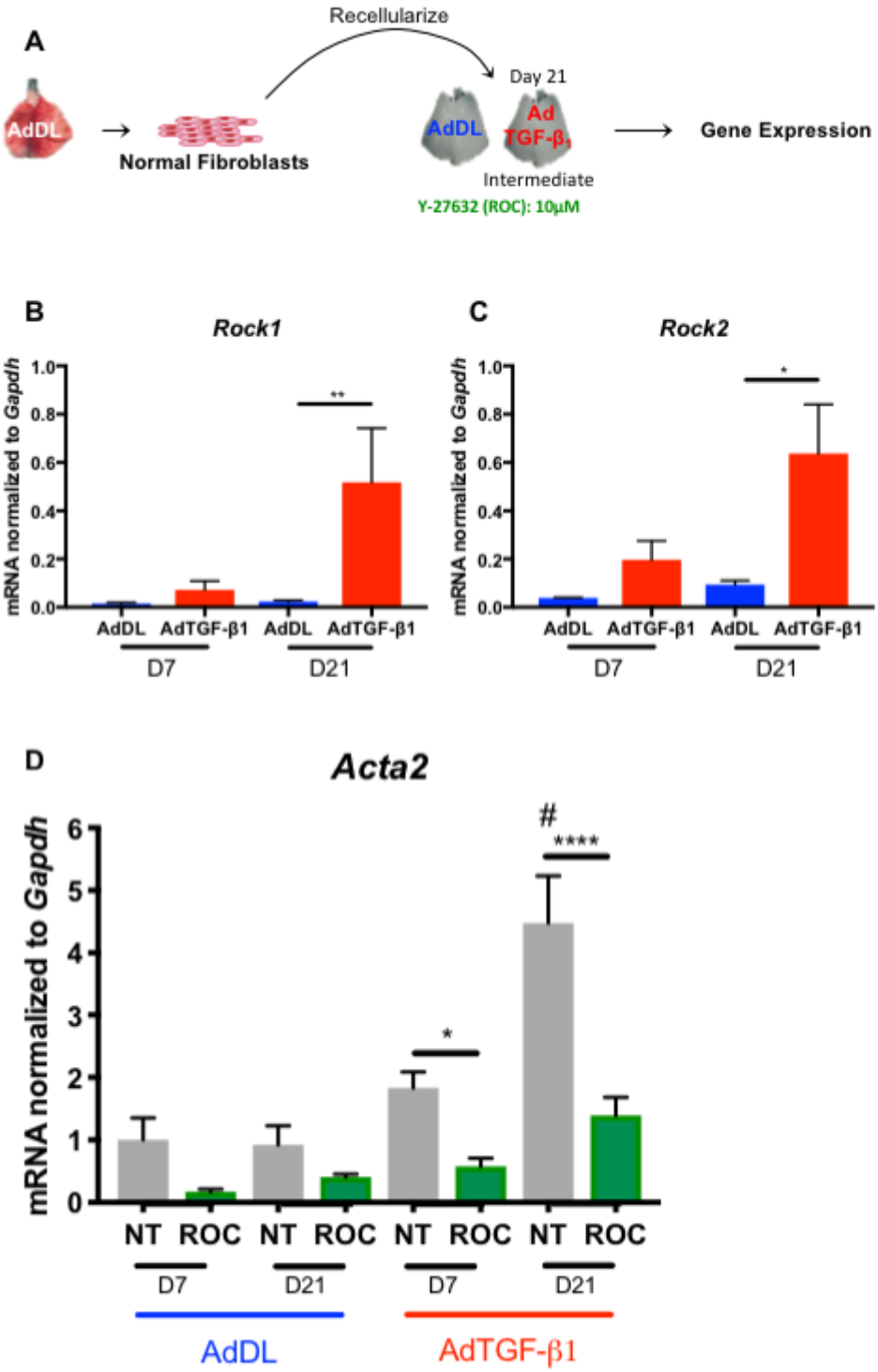
A
Recellularize
Day 21
AdDL
Normal Fibroblasts
AdDL
Ad TGF-β1
Intermediate
Y-27632 (ROC): 10μM
Gene Expression
B
Rock1
mRNA normalized to Gapdh
AdDL AdTGF-β1 AdDL AdTGF-β1
D7 D21
C
Rock2
mRNA normalized to Gapdh
AdDL AdTGF-β1 AdDL AdTGF-β1
D7 D21
D
Acta2
mRNA normalized to Gapdh
NT ROC NT ROC NT ROC NT ROC
D7 D21 D7 D21
AdDL
AdTGF-β1

Figure 6

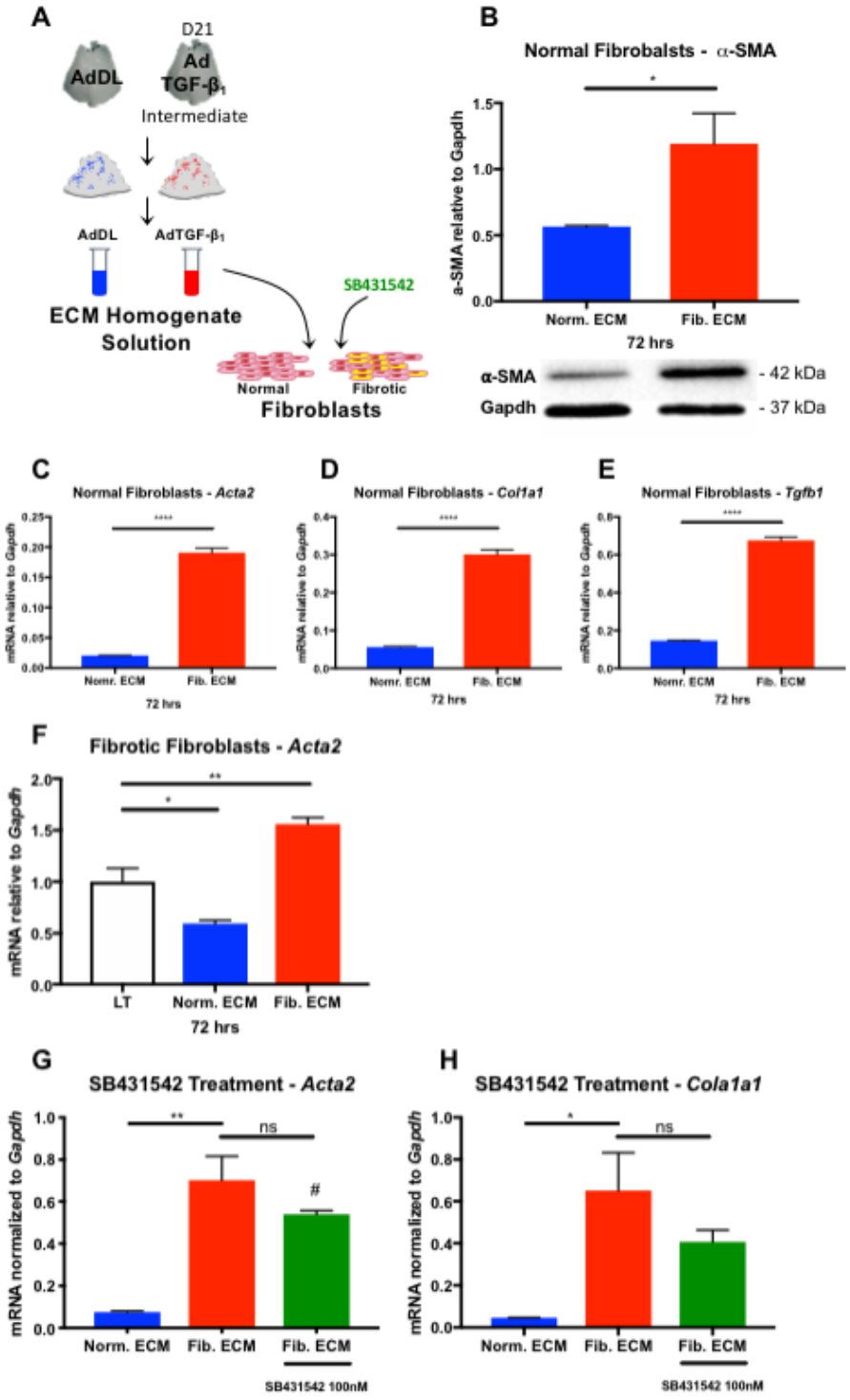
A
D21
AdDL
Ad TGF-β1
Intermediate
AdDL
AdTGF-β1
SB431542
ECM Homogenate Solution
Normal
Fibrotic
Fibroblasts
B
Normal Fibrobalsts - α-SMA
a-SMA relative to Gapdh
Norm. ECM
Fib. ECM
72 hrs
α-SMA
Gapdh
- 42 kDa
- 37 kDa
C
Normal Fibroblasts - Acta2
D
Normal Fibroblasts - Col1a1
E
Normal Fibroblasts - Tgfb1
mRNA relative to Gapdh
Nomr. ECM
Fib. ECM
72 hrs
F
Fibrotic Fibroblasts - Acta2
mRNA relative to Gapdh
LT
Norm. ECM
Fib. ECM
72 hrs
G
SB431542 Treatment - Acta2
H
SB431542 Treatment - Cola1a1
mRNA normalized to Gapdh
ns
Norm. ECM
Fib. ECM
Fib. ECM
SB431542 100nM

REFERENCE

1. Gross TJ, Hunninghake GW. Idiopathic Pulmonary Fibrosis. *New England Journal of Medicine* 2001; 345: 517–525.

2. Idiopathic Pulmonary Fibrosis: Diagnosis and Treatment. *Am J Respir Crit Care Med* 2000; 161: 646–664.

3. Nalysnyk L, Cid-Ruzafa J, Rotella P, Esser D. Incidence and prevalence of idiopathic pulmonary fibrosis: review of the literature. *Eur Respir Rev* 2012; 21: 355–361.

4. Raghu G, Selman M. Nintedanib and Pirfenidone. New Antifibrotic Treatments Indicated for Idiopathic Pulmonary Fibrosis Offer Hopes and Raises Questions. *Am J Respir Crit Care Med* 2015; 191: 252–254.

5. Moore MW, Herzog EL. Regulation and Relevance of Myofibroblast Responses in Idiopathic Pulmonary Fibrosis. *Curr Pathobiol Rep* 2013; 1: 199–208.

6. Mouw JK, Ou G, Weaver VM. Extracellular matrix assembly: a multiscale deconstruction. *Nat Rev Mol Cell Biol* 2014; 15: 771–785.

7. McWhorter FY, Davis CT, Liu WF. Physical and mechanical regulation of macrophage phenotype and function. *Cell Mol Life Sci* 2015; 72: 1303–1316.

8. Stegemann JP, Hong H, Nerem RM. Mechanical, biochemical, and extracellular matrix effects on vascular smooth muscle cell phenotype. *Journal of Applied Physiology* 2005; 98: 2321–2327.

9. Upagupta C, Shimbori C, Alsilmi R, Kolb M. Matrix abnormalities in pulmonary fibrosis. *European Respiratory Review* 2018; 27: 180033.

10. Parker MW, Rossi D, Peterson M, Smith K, Sikström K, White ES, Connett JE, Henke CA, Larsson O, Bitterman PB. Fibrotic extracellular matrix activates a profibrotic positive feedback loop. *J. Clin. Invest.* 2014; 124: 1622–1635.

11. Blaauboer ME, Boeijen FR, Emson CL, Turner SM, Zandieh-Doulabi B, Hanemaaijer R, Smit TH, Stoop R, Everts V. Extracellular matrix proteins: A positive feedback loop in lung fibrosis? *Matrix Biology* 2014; 34: 170–178.

12. Sime PJ, Xing Z, Graham FL, Csaky KG, Gauldie J. Adenovector-mediated gene transfer of active transforming growth factor-beta1 induces prolonged severe fibrosis in rat lung. *J. Clin. Invest.* 1997; 100: 768–776.

13. Woessner JF. The determination of hydroxyproline in tissue and protein samples containing small proportions of this imino acid. *Archives of Biochemistry and Biophysics* 1961; 93: 440–447.

14. Froese AR, Shimbori C, Bellaye P-S, Inman M, Obex S, Fatima S, Jenkins G, Gauldie J, Ask K, Kolb M. Stretch-induced Activation of Transforming Growth Factor-β1 in Pulmonary Fibrosis. *Am. J. Respir. Crit. Care Med.* 2016; 194: 84–96.

15. Crapo PM, Gilbert TW, Badylak SF. An overview of tissue and whole organ decellularization processes. *Biomaterials* 2011; 32: 3233–3243.

16. Gilpin A, Yang Y. Decellularization Strategies for Regenerative Medicine: From Processing Techniques to Applications. *Biomed Res Int* [Internet] 2017 [cited 2019 Feb 1]; 2017Available from: https://www.ncbi.nlm.nih.gov/pmc/articles/PMC5429943/.

17. Seluanov A, Vaidya A, Gorbunova V. Establishing Primary Adult Fibroblast Cultures From Rodents. *J Vis Exp* [Internet] 2010 [cited 2019 Feb 11]; Available from: https://www.ncbi.nlm.nih.gov/pmc/articles/PMC3185624/.

18. Booth AJ, Hadley R, Cornett AM, Dreffs AA, Matthes SA, Tsui JL, Weiss K, Horowitz JC, Fiore VF, Barker TH, Moore BB, Martinez FJ, Niklason LE, White ES. Acellular normal and fibrotic human lung matrices as a culture system for in vitro investigation. *Am. J. Respir. Crit. Care Med.* 2012; 186: 866–876.

19. Hinz B. The extracellular matrix and transforming growth factor-β1: Tale of a strained relationship. *Matrix Biology* 2015; 47: 54–65.

20. Balestrini JL, Chaudhry S, Sarrazy V, Koehler A, Hinz B. The mechanical memory of lung myofibroblasts. *Integr Biol (Camb)* 2012; 4: 410–421.

21. Huang X, Yang N, Fiore VF, Barker TH, Sun Y, Morris SW, Ding Q, Thannickal VJ, Zhou Y. Matrix stiffness-induced myofibroblast differentiation is mediated by intrinsic mechanotransduction. *Am. J. Respir. Cell Mol. Biol.* 2012; 47: 340–348.

22. Asano S, Ito S, Takahashi K, Furuya K, Kondo M, Sokabe M, Hasegawa Y. Matrix stiffness regulates migration of human lung fibroblasts. *Physiol Rep* [Internet] 2017 [cited 2019 Feb 8]; 5Available from: https://www.ncbi.nlm.nih.gov/pmc/articles/PMC5430127/.

23. Shimbori C, Upagupta C, Bellaye P-S, Ayaub EA, Sato S, Yanagihara T, Zhou Q, Ognjanovic A, Ask K, Gauldie J, Forsythe P, Kolb MRJ. Mechanical stress-induced mast cell degranulation activates TGF-β1 signalling pathway in pulmonary fibrosis. *Thorax* 2019; .

24. Wells RG. The role of matrix stiffness in regulating cell behavior. *Hepatology* 2008; 47: 1394–1400.

25. Blakney AK, Swartzlander MD, Bryant SJ. The effects of substrate stiffness on the in vitro activation of macrophages and in vivo host response to poly(ethylene glycol)-based hydrogels. *J Biomed Mater Res A* 2012; 100: 1375–1386.

26. Evans RA, Tian YC, Steadman R, Phillips AO. TGF-beta1-mediated fibroblast-myofibroblast terminal differentiation-the role of Smad proteins. *Exp. Cell Res.* 2003; 282: 90–100.

27. Bayreuther K, Rodemann HP, Hommel R, Dittmann K, Albiez M, Francz PI. Human skin fibroblasts in vitro differentiate along a terminal cell lineage. *Proc Natl Acad Sci U S A* 1988; 85: 5112–5116.

28. Garrison G, Huang SK, Okunishi K, Scott JP, Kumar Penke LR, Scruggs AM, Peters-Golden M. Reversal of myofibroblast differentiation by prostaglandin E(2). *Am. J. Respir. Cell Mol. Biol.* 2013; 48: 550–558.

29. Hecker L, Jagirdar R, Jin T, Thannickal VJ. Reversible differentiation of myofibroblasts by MyoD. *Experimental Cell Research* 2011; 317: 1914–1921.

30. Marinković A, Liu F, Tschumperlin DJ. Matrices of physiologic stiffness potently inactivate idiopathic pulmonary fibrosis fibroblasts. *Am. J. Respir. Cell Mol. Biol.* 2013; 48: 422–430.

31. Bellaye P-S, Shimbori C, Upagupta C, Sato S, Shi W, Gauldie J, Ask K, Kolb M. Lysyl Oxidase-Like 1 Protein Deficiency Protects Mice from Adenoviral Transforming Growth Factor-β1-induced Pulmonary Fibrosis. *Am. J. Respir. Cell Mol. Biol.* 2018; 58: 461–470.

32. Xiao Q, Ge G. Lysyl oxidase, extracellular matrix remodeling and cancer metastasis. *Cancer Microenviron* 2012; 5: 261–273.

33. Humphrey JD, Dufresne ER, Schwartz MA. Mechanotransduction and extracellular matrix homeostasis. *Nature Reviews Molecular Cell Biology* 2014; 15: 802–812.

34. Maldonado M, Luu RJ, Ico G, Ospina A, Myung D, Shih HP, Nam J. Lineage- and developmental stage-specific mechanomodulation of induced pluripotent stem cell differentiation. *Stem Cell Res Ther* [Internet] 2017 [cited 2019 Feb 11]; 8Available from: https://www.ncbi.nlm.nih.gov/pmc/articles/PMC5622562/.

35. Watanabe K, Ueno M, Kamiya D, Nishiyama A, Matsumura M, Wataya T, Takahashi JB, Nishikawa S, Nishikawa S, Muguruma K, Sasai Y. A ROCK

inhibitor permits survival of dissociated human embryonic stem cells. *Nature Biotechnology* 2007; 25: 681–686.

36. Ishizaki T, Uehata M, Tamechika I, Keel J, Nonomura K, Maekawa M, Narumiya S. Pharmacological properties of Y-27632, a specific inhibitor of rho-associated kinases. *Mol. Pharmacol.* 2000; 57: 976–983.

37. Knipe RS, Tager AM, Liao JK. The Rho Kinases: Critical Mediators of Multiple Profibrotic Processes and Rational Targets for New Therapies for Pulmonary Fibrosis. *Pharmacol Rev* 2015; 67: 103–117.

38. Htwe SS, Cha BH, Yue K, Khademhosseini A, Knox AJ, Ghaemmaghami AM. Role of Rho-Associated Coiled-Coil Forming Kinase Isoforms in Regulation of Stiffness-Induced Myofibroblast Differentiation in Lung Fibrosis. *Am. J. Respir. Cell Mol. Biol.* 2017; 56: 772–783.

39. Akhmetshina A, Dees C, Pileckyte M, Szucs G, Spriewald BM, Zwerina J, Distler O, Schett G, Distler JHW. Rho-associated kinases are crucial for myofibroblast differentiation and production of extracellular matrix in scleroderma fibroblasts. *Arthritis Rheum.* 2008; 58: 2553–2564.

40. Itoh K, Yoshioka K, Akedo H, Uehata M, Ishizaki T, Narumiya S. An essential part for Rho-associated kinase in the transcellular invasion of tumor cells. *Nat. Med.* 1999; 5: 221–225.

41. Igishi T, Mikami M, Murakami K, Matsumoto S, Shigeoka Y, Nakanishi H, Yasuda K, Gutkind JS, Hitsuda Y, Shimizu E. Enhancement of cisplatin-induced cytotoxicity by ROCK inhibitor through suppression of focal adhesion kinase-independent mechanism in lung carcinoma cells. *Int. J. Oncol.* 2003; 23: 1079–1085.

42. Averill F, Albertson T e., Baratz D m., Chaudhary S, Mobin S, O'Brien T, Scholand M b., Whelan T p. m., Poyurovsky M, Schueller O, Ryan J, Gibson K f. A Phase 2 Trial of KD025 to Assess Efficacy, Safety and Tolerability in Patients with Idiopathic Pulmonary Fibrosis. *C97. DIFFUSE PARENCHYMAL LUNG DISEASES: EVALUATION, OUTCOMES, AND TRIALS* [Internet] American Thoracic Society; 2018 [cited 2019 Feb 1]. p. A5927–A5927Available from: https://www.atsjournals.org/doi/abs/10.1164/ajrccm-conference.2018.197.1_MeetingAbstracts.A5927.

43. Cox TR, Erler JT. Remodeling and homeostasis of the extracellular matrix: implications for fibrotic diseases and cancer. *Dis Model Mech* 2011; 4: 165–178.

44. Neve A, Cantatore FP, Maruotti N, Corrado A, Ribatti D. Extracellular Matrix Modulates Angiogenesis in Physiological and Pathological Conditions. *Biomed Res*

Int [Internet] 2014 [cited 2019 Feb 4]; 2014Available from: https://www.ncbi.nlm.nih.gov/pmc/articles/PMC4052469/.

45. Schultz GS, Wysocki A. Interactions between extracellular matrix and growth factors in wound healing. *Wound Repair and Regeneration* 2009; 17: 153–162.

SUPPLEMENTARY MATERIAL

Rat model of TGF-β1 adenovirus vector-induced pulmonary fibrosis

Female Sprague-Dawley rats (225-250 g; Charles River, Wilmington, MA, USA) were maintained in 12-hours light, 12-hours dark cycles with free access to food and water. Rats were given intratracheal instillation of TGF-β1 adenovirus (AdTGF-β1223/225) or control virus (AdDL) as previously described [12]. Rats intratracheally received 5.0 $x10^8$ plaque-forming units (PFU) of virus in 300 µl sterile saline and were culled on days 7, 21, or 49 after administration by terminal anaesthesia. Lungs were either decellularized to prepare ECM scaffolds or used for primary culturing fibroblasts. All work was conducted under the Canadian Council on Animal Care guidelines and approved by the Animal Research Ethics Board of McMaster University under protocol #13.12.48.

Antibodies and regents

The used antibodies for western blot were α-smooth muscle actin (α-SMA) (ab7817, Abcam) and Glyceraldehyde 3-phosphate dehydrogenase (GAPDH) (#5174, Cell signalling Technology). Anti-rabbit HRP linked IgG (#7074, Cell Signaling Technology), Anti-mouse IgG HRP-linked Antibody (#7076, Cell Signaling Technology). For fluorescence microscopy, we used goat or donkey secondary antibody conjugated with Alexa Fluor-488 and Alexa Fluor-555 (Abcam).

Primary culturing fibroblasts from rat lungs

Single cell suspensions were created by mincing and 1 hr collagenase treatment of harvested rat lungs. Cells were cultured in 10% Fetal Bovine Serum and 1% pen-strep (Gibco, Life Technologies) in Dulbecco's modified Eagle Medium (Biowhittaker

Reagents, Lonza) and cultured at 37°C, 5% CO^2 in T150 Falcon flasks for 7 days or till confluency and used for experiments/analysis. Due to the stiff culturing conditions and plasticity of primary cultured fibroblasts, cells were used within 14 days or passage 3. Fibroblast populations harvested at 7, 21 and 49 days following AdTGF-β1 treatment were considered Early, Intermediate, and Late fibrotic fibroblast populations respectively. 1kPa and 50 kPa collagen coated hydrogel plates (Softwell, Martigel) were used for *in vitro* 2D stiffness experiments.

Decellularization and Recellularization of Rat Lungs

Decellularization was performed through manual lung perfusion (10 ml each time) and incubation with 50 ml of: TritonX (0.1%; overnight), Sodium Deoxycholate (2%; overnight), NaCl (1 M; 1 hr), and stored in PBS supplemented with Penicillin Streptomycin (1%; max 3 months). Lungs were washed with sterile H_2O between each solution during decellularization to ensure there was no mixing of wash solutions. To investigate fibrosis in a kinetic manner, lungs were harvested at three different times points: 7, 21 and 49 days after AdTGF-β1 administration. Lungs from the different timepoints were termed Early (day 7), Intermediate (day 21), and Late (day 49) fibrotic ECMs, and were selected since in the AdTGF-β1 model they represent the initial, active and persistent fibrosis respectively. Lungs harvested at 7, 21 and 49 days following AdTGF-β1 treatment were considered early, intermediate, and late fibrotic ECMs respectively. Left lobe recellularization was performed by first tying off the right lobes leaving only the left lobe open. The left lobe was perfused with 5 ml of fibroblasts ($1*10^6$ cells/ml) in 2% low melting agarose. Lungs were briefly left to solidify at room temperature and the left lobe was

sectioned into horizontal slices of ~3 cm and immersed in 10% Fetal Bovine Serum and 1% pen-strep (Gibco, Life Technologies) in Dulbecco's modified Eagle Medium (Biowhittaker® Reagents, Lonza) and incubated at 37°C, 5% CO^2 for 7 and 21 days. The remaining right lobes were stored for hydroxyproline and histological analysis.

Preparation of ECM homogenate solutions

Normal and fibrotic lungs were harvested at day 49 following vector administration. Lungs were decellularized to produce ECM scaffolds, which were then lyophilized and lysed. The lyses buffer was removed from the resulting ECM homogenate solutions via 3.5K dialysis cassettes (Slide-A-lyzer Dialysis Cassette G2, Thermo Scientific), and supplemented into the culturing media at 1 µg/ml.

Western blotting

Proteins from crushed lung strips was extracted with lysis buffer (Hepes 50 mM pH 7.4, NaCl 150 mM, EDTA 5 mM, Triton X-100 0.5%) using a mechanical homogenizer (Omni International, Waterbury CT), and the collected supernatant was used for western blotting. 20 µg of total protein were separated on a 12% SDS Polyacrylamide Electropheresis gels. Proteins were transferred to a PVDF membrane (Bio-Rad Laboratories, Hercules CA) using a wet transfer apparatus and blocked at room temperature for 1 hour using 8% skim milk. Western blots were used to detect α-SMA (Abcam biotechnology company, Cambridge UK) and normalized to Glyceraldehyde 3-phosphate dehydrogenase (GAPDH) (Cell signalling Technology, Danvers, MA). Protein detection was performed using the SuperSignal West Pico chemiluminescent system (Thermo Fischer Scientific) and read in

a ChemiDoc XRS Imaging System Software. Samples were normalized to a control sample when studies required more than one bolt.

Histology and immunofluorescence

Paraffin sections were prepared at 4 μm and processed at the core histology facility at St Joseph's Healthcare Hamilton. Lung slides were stained with haematoxylin and eosin (H&E) or Picrosirius red (PSR). Images were collected using the Olympus microscope (Olympus BX41, Olympus, ON, Canada) equipped with DP Controller software (Olympus, ON, Canada). PSR pictures were taken using polarized detection. Immunofluorescence staining of α-SMA (Abcam, ON, Canada) and FAP (ab53066, Abcam) was performed on formalin-fixed cells or rat lung tissue sections. In brief, following deparaffinization and antigen retrieval process with a citric acid buffer, and saturation of non-specific sites with BSA (5%, 30 min), sections were incubated with primary antibodies overnight in a humidified chamber at 4°C. Conjugated secondary antibodies were used at a dilution of 1:2000 (Abcam). Slides were mounted in ProLong-Gold with DAPI (ProLong® Gold antifade reagent with DAPI; Thermo Fisher Scientific). Pictures were taken using an epifluorescence microscope (Olympus IX81, Olympus) with the same setting and exposure time for all images.

ELISA

Active TGF-β1 levels in normal and fibrotic ECM homogenate solutions were detected using mouse/rat/porcine/canine TGF-β1-specific ELISA kit (R&D Systems, Minneapolis, MN), according to the manufacturer's recommendations.

Isolation of mRNA and gene expression

Total RNA was extracted from frozen rat lung tissue and *in vitro* cultured cells using TRIzol® reagent (Invitrogen). 1 µg of total RNA was reverse-transcribed using qScript cDNA Super Mix (Quanta Bioscience, Gaithersburg, MD, USA). The cDNA was amplified by a Fast 7500 real-time PCR system (AB Applied Biosystems) using TaqMan® Universal PCR Master Mix and predesigned primer pairs: *Gapdh* (Rn01775763_g1), *Acta2* (Rn01759928_g1), *Col1a1* (Rn00801649_g1), and *Tgfb1* (Rn00572010_m1) (Thermo Fisher Scientific, ON, Canada).

Alamar blue assay

Cell viability and proliferation was assessed for primary cultured fibroblasts before and after ECM recellularization using the Alamar blue dye (Invitrogen) according to the manufacturer's guidelines.

Hydroxyproline assay

Hydroxyproline content in decellularized rat lung samples was determined by a colorimetric assay as described previously [13]. Briefly, lung lobes were frozen in liquid nitrogen and crushed to produce a finely ground powder and immediately homogenized in RIPA buffer. The homogenized lung tissue was centrifuged and the pellet was resuspended in PBS and frozen at -80°C. The pellet was then lyophilized for at least 24 hours using a freezer dryer apparatus (Modulyod Freezer Dryer, Thermo Electron Corporation). Next, 10% TCA solution was added to samples and centrifuged, followed by 6 ml of 6N HCl to hydrolyze the pellet, in a 110°C dry bath incubator. Samples were then brought to a pH of 7 using NaOH and incubated with 0.05M Chloramine T reagent for 20 minutes. The

Chloramine T reagent was then destroyed by using 70% perchloric acid and samples were finally incubated for 20 minutes in a 55-65°C water bath after adding Ehrlich's reagent solution. The absorbance of the final reaction was measured at 550 nm and hydroxyproline contractions were determined using a standard curve. Hydroxyproline concentrations were expressed as μg of hydroxyproline/mg dry lung weight using hydroxyproline standards (Sigma Chemicals) and expressed as fold increase over untreated decellularized lung tissue.

Young's modulus

Using a similar set up as described previously by our group [14], a force transducers and a servo-control arm used in tandem with a digital controller interface (Models 400A, 322C, 604C; Aurora Scientific Inc., Aurora, Canada) were used to exert 5 mN of force onto transversely cut rat lung tissues strips of 10 x 2 x 2 mm sections for 10 to 15 seconds. The resulting change in length of the strips was measured to determine the respective Young's modulus of the lung tissues. This was calculated using the formula:

$$E = \frac{F/Ao}{\Delta L/Lo}$$

E = Young's Modulus

F = force exerted on strip;

A_0 = original cross-sectional area of strip;

ΔL = change in length of strip;

L_0 = original length of strip

Due to the standardized strip dimensions and exerted force:

F = 5 mN, $A_0 = 4\ mm^2$ and $L_0 = 10$ mm

Statistical analysis

The statistically significant differences were determined using a Student's *t*-test for paired samples or a one-way ANOVA followed by a Bonferroni post-hoc test for multiple comparisons. Data sets were normally distributed as determined by the Shapiro-Wilk test. The strength of association between continuous variables was tested with the Pearson correlation (*P*). *P* values of less than 0.05 were considered to be significant. GraphPad Prism program Ver. 8.02 (*GraphPad* Software Inc.) was used for statistical analyses.

SUPPLEMENTARY FIGURE LEGEND

Supplemental Figure 1. Active TGF-β1 ELISA of ECM homogenate solutions. Homogenate solutions prepared from decellularized ECM scaffolds harvested 21 days after adDL (Norm. ECM) or adTGFβ1 (Fib. ECM) vector administration. Kit provided control.

Supplementary Figure 1

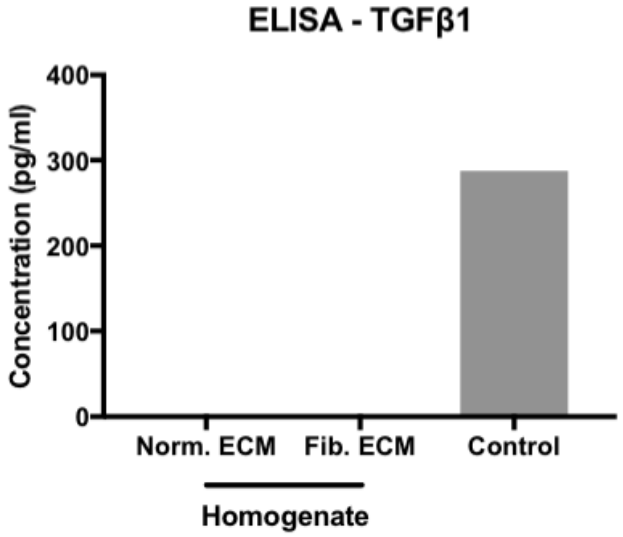

Chapter 4

The Importance of Interventional Timing in the Bleomycin Model of Pulmonary Fibrosis.

Summary and Significance

Idiopathic Pulmonary Fibrosis (IPF) is a complex disease of unknown etiology, however, the lack of effective models that reproduce the disease's pathobiology has made drug development incredibly challenging. Intratracheal administration of bleomycin is one of the most commonly used models to study the pathobiology and test therapeutic efficacy in IPF. The bleomycin model works by inducing an early inflammatory phase which transitions into fibrosis after 5-7 days. As seen in Chapter 2 and 3, existing fibrosis in the fibrotic ECM can promote further scarring and disease progression. Therefore, interventions must be started during the fibrotic phase, when ECM fibrosis is established, and the intervention's therapeutic efficacy can be truly assessed. A study published by our group in 2008 showed surprisingly suboptimal use of the bleomycin model to study anti-fibrotic efficacy, due to poor timing of interventions. The paper advocated for more awareness into the difference between the inflammation and fibrotic phases of the bleomycin model, and appropriate intervention timing for its effective use. Seeing as to how the use of bleomycin in the field has drastically increased over the past decade, we decided to re-evaluate its quality of use in the field. A total of 1009 PubMed-available studies using the bleomycin model to study pulmonary fibrosis between 2008 and 2019 were included. In this study, we see that since 2008, there has been a notable improvement in the number of effectively timed therapeutic studies in this model of 37.1%, compared to the low 5% prior to 2008. In the preventative studies, however, only about 19% of studies characterized early inflammation. This information is important to assess an intervention's preventative capacity, and also gather insight into potential immunological drivers of

fibrosis. Furthermore, since bleomycin-induced lung fibrosis is a commonly used preclinical model for IPF, the collected publicly available studies were cross-referenced with major clinical trials for IPF, to assess the availability of preclinical rational. Surprisingly, very little information was available, and only 28% of clinical trials had accompanying preclinical-bleomycin data available on PubMed. In conclusion, this study highlights that while a positive shift in effective therapeutic timing is observed, further actions such as improved characterization of early inflammation in preventative studies and more transparency in preclinical data for IPF are still needed. This will facilitate effective utilization of the bleomycin model to potentially yield more fruitful preclinical drug development for IPF.

The Importance of Interventional Timing in the Bleomycin Model of Pulmonary Fibrosis.

Philipp Kolb[1*], Chandak Upagupta[1*], Kjetil Ask[1], Ehab Ayaub[1], Pierre-Simon Bellaye[1], Jack Gauldie[1], Chiko Shimbori[1], Mark Inman[1], Martin RJ Kolb[1]

*These authors contributed equally to this work.

1. Firestone Institute for Respiratory Health, Department of Medicine, McMaster University, Hamilton, ON, Canada

Running title: Assessment of Appropriate Intervention Timing in the Bleomycin model over the past 11 years.

Conflict of interest: Dr. Martin Kolb was the study PI for the INSTAGE study. All other authors declare no conflicts of interest.

Status of the work: Prepared for submission to "European Respiratory Journal"

Author contributions: Conception and design: CU, PK, KA, JG, MK. Performed experiments: CU, PK, EA, PSB, CS; Analysis and interpretations: CU, PK, KA, AU, MK; Drafting the manuscript: CU, PK, KA, JG, MK.

Corresponding author: Dr. Martin Kolb, Department of Medicine, McMaster University and The Research Institute of St. Joe's Hamilton, Firestone Institute for Respiratory Health, 50 Charlton Ave East, Room T2120, Hamilton, Ontario, Canada L8N 4A6, Ph. (905) 522.1155 ext. 33683; Fax (905) 521.6183; E-mail: kolbm@mcmaster.ca

ABSTRACT

Idiopathic Pulmonary Fibrosis (IPF) is a complex disease of unknown etiology. Intratracheal administration of bleomycin is standard for studying disease biology of IPF and preclinical efficacy of novel drugs for IPF. The model works by inducing an early inflammatory phase which transitions into fibrosis after 5-7 days. This initial inflammation makes therapeutic timing crucial. To accurately assess anti-fibrotic efficacy, the intervention should inhibit fibrosis without impacting early inflammation.

Studies published between 2008 and 2019 using the bleomycin model to investigate pulmonary fibrosis were retrieved from PubMed, and study characteristics were analyzed. Intervention based studies were classified as either preventative (starting <7 days after bleomycin installation) or therapeutic (>7 days). Studies were also cross-referenced with current major clinical trials to assess the availability of preclinical rational.

A total of 1009 publications were evaluated. 758 investigated potential therapies, of which 464 (61.2%) were preventative alone, 172 (22.7%) therapeutic alone, and 109 (14.4%) were both. Of the 464 preventative studies, only 78 (16.8%) characterized inflammation during the model's early inflammatory phase. Of the reported 145 IPF clinical trials investigating 93 compounds/combinations, only 26 (28.0%) had any PubMed-available preclinical data in bleomycin.

Since 2008, there has been an improvement in the effective timing of therapeutic studies in the bleomycin model. While this shift is encouraging, more characterization of early inflammation and appropriate preclinical therapeutic testing are still needed. This may

facilitate the development of more therapeutic strategies for patient with this devastating disease.

Key words: Idiopathic Pulmonary Fibrosis, Pulmonary Fibrosis, Bleomycin, Inflammatory phase, Fibrotic Phase, Preventative efficacy, Therapeutic efficacy, Clinical Trials

INTRODUCTION

Idiopathic Pulmonary Fibrosis (IPF) is a devastating lung disease in which abnormal wound healing causes a scarring of the pulmonary interstitium and distortion of the lung architecture [1]. This causes impaired gas exchange as well as increased lung stiffness; which eventually leads to respiratory failure. The prognosis of IPF is poor and comparable to aggressive cancers, with a median mortality of 3-5 years post-diagnosis [2]. The epidemiology of IPF has been studied repeatedly in different regions and countries around the world. Recent Canadian data suggests an incidence rate of 18.7 and a prevalence of 41.8 per 100,000 individuals [3]. In populations over 70 years of age, the prevalence can be as high as 200 cases per 100,000 individuals. Similar epidemiological estimates are reported in the United States as well as Europe [4]. While recently two anti-fibrotic medications have been approved for clinical use in treating IPF, neither treatment is curative and efficacy varies across patients. In order to improve patient outcomes and enhance long-term quality of life, additional therapeutic strategies are desperately needed for this progressive disease [5].

Over the past few decades, several animal models have been used to study the biology of IPF [6]. These models serve as tools to test and understand biological the mechanisms of fibrogenesis, and also to test the efficacy of therapeutic interventions. Due to the idiopathic nature of IPF and the highly complex underlying pathobiology, no single model is able to provide a completely robust analysis. Instead, results must be considered across various pre-clinical platforms. Most animal models for pulmonary fibrosis involve injury to the lung, which activates wound healing pathways and eventually excessive scar

formation. Common methods to induce fibrosis include systemic or intratracheal instillation of bleomycin, radiation, intratracheal administration of silica or asbestos, and transgenic mice or gene transfer employing fibrogenic mediators, amongst others.

Of these approaches, intratracheal instillation of bleomycin is the most widely used and best studied [7]. It is a relatively inexpensive system which induces a robust fibrotic response that displays several histological hallmarks seen in IPF patients [8, 9]. These include aberrant fibroblast proliferation and differentiation, excessive deposition of extracellular matrix proteins, and destruction of the alveolar architecture. Histological staining and morphometric analysis of lung tissue, quantification of hydroxyproline, and measurements of lung function are typical metrics to quantify fibrosis in animals. Overall, the bleomycin model has proven invaluable in understanding many of the cellular and molecular pathways in fibrogenesis that are central to the current understanding of IPF pathogenesis. Despite this, the bleomycin model does have limitations. One important limitation is a profound initial inflammatory phase, characterized by up-regulation of acute inflammatory cytokines such as interleukin-1, -6, and tumor necrosis factor-α, together with an influx of neutrophils [10, 11]. This inflammation lasts for approximately 7 days before subsiding into a fibrotic phase which more closely mimics the manifestation of fibrosis present in IPF patients [12]. Spontaneous reversal of fibrosis, particularly in mice, typically occurs 3-4 weeks post intratracheal bleomycin administration [13–16], although several groups have reported non-resolving fibrosis by using multiple intratracheal instillations of bleomycin [17, 18].

These two key features of bleomycin must be critically evaluated when using it to model IPF and assess the efficacy of therapeutic compounds. The fibrotic phase in the bleomycin model is self-limited and eventually reversible, but it mimics some notable aspects of fibrogenesis present in IPF patients. This fibrotic phase is typically no longer than two weeks, starting one week after the initial injury when the acute inflammation subsides, and ending after three weeks when the resolution phase of fibrosis begins [12]. The "window" during which fibrogenic mechanisms can be studied and anti-fibrotic drugs should be tested, is therefore relatively short. When experimental methodologies fail to take this limitation of the bleomycin model into account, the results can be misleading. For example, studies may claim that an intervention has anti-fibrotic effects when in reality it may only interfere with the initial inflammation. This was highlighted in a paper published in 2008 by our group, which described that the vast majority of studies between 1980 and 2006 using the bleomycin model to test antifibrotic efficacy of drugs did not consider the element of appropriate therapeutic timing [19]. Out of 221 studies published during that period, only 10 were designed using a therapeutic treatment regime: starting the administration of an experimental therapy >7 days after bleomycin instillation. This lack of therapeutic testing in this model may have played a role in the slow pace of drug development in the context of IPF. Here, we examine whether the use of the bleomycin model to study antifibrotic effects of compounds has changed since our initial publication in 2008. By advocating for more effective use of this preclinical model, we hope to improve drug development in IPF.

METHODS

A systematic PubMed search was conducted to capture the relevant literature. The search terms "Bleomycin AND Pulmonary Fibrosis" was used to compile a list of publications between January 1st, 2008 and March 10th, 2019. This search yielded 1816 papers to investigate. Papers were included if they used an *in vivo* bleomycin model to study the effect of a particular intervention or transgenic animal on fibrosis. Excluded studies were method papers, review articles, *ex vivo*, or studies aimed to understand changes in gene and protein expression in bleomycin treated animals without intervention or genetic modifications. Non-English papers were not considered. After applying this inclusion and exclusion criteria, a total of 1009 papers were explored in detail (Figure 1) (Supplementary Table 1).

Number of publications per year was determined by downloading the comma-separated values (CSV) files from PubMed (Figure 2a). All studies using mice in pulmonary fibrosis (silver) were identified by the search term "Mice and Pulmonary fibrosis". All bleomycin studies in pulmonary fibrosis were identified by the search term "Bleomycin and Pulmonary fibrosis", and publications per year were plotted before (gray) and after (blue) the above mentioned inclusion and exclusion criteria.

We systematically analyzed these papers and pertinent information was extracted. First, the studies were defined by study type – each paper was described as either exploring fibrogenesis in the context of an intervention, a transgenic animal, or both. In studies used an intervention, the timing of intervention was characterized with respect to bleomycin administration as outlined in Moeller 2008 [19]. Intervention beginning <7 days post

bleomycin were termed preventative. While interventions beginning ≥7 days post-bleomycin were classified as therapeutic.

To adequately understand disease prevention and progression, preventative and transgenic animal studies need to assess inflammatory pathways during the early inflammatory phase in the bleomycin model. Therefore, the characterization of inflammation <7 days post bleomycin was evaluated. Typically, this involved an analysis of the bronchoalveolar lavage fluid through differential cell counts, or an examination of the inflammatory cytokine profile by ELISA or gene expression analysis.

Clinical trials conducted in patients suffering from IPF were also searched to allow comparisons with the available basic science data from preclinical-bleomycin trials. Clinical trial data was obtained from clinicaltrials.gov and the definition of associated publicly available data was defined as searchable and retrievable information available on PubMed.

RESULTS

Overall Study Characterization.

Of the 1009 studies published since 2008 that used the bleomycin model of pulmonary fibrosis, 75.1% (758 publications) investigated the potential of an intervention on fibrogenesis (i.e., small molecule, antibodies, traditional medicine etc.) (Figure 2b). 19.9% (201 publications) of the studies focused on the effect of bleomycin in transgenic animals investigating if certain gene manipulations would increase or decrease susceptibility to fibrosis. The remaining 5.0% (50 publications) investigated transgenic animals or the combination of transgenic animals and interventions.

Intervention Characterization.

Of the 758 intervention studies investigated, 61.2% (464 publications) were classified as preventative, while 22.7% (172 publications) were therapeutic, with intervention begun not earlier than 7 days after bleomycin administration (Figure 2c). 14.4% (109 publications) of the studies investigated both the preventative and therapeutic ability, comprising a complete assessment of intervention efficacy.

Bleomycin Results and the Relationship with Clinical Trials.

When evaluating the human clinical trials for IPF, it is interesting to note that of the 145 trials investigating 93 compounds/combinations, only 26 (28.0%) interventions had any available preclinical-bleomycin data on PubMed (Figure 2d). Of these 26 interventions, 20 had explored drug efficacy in therapeutic models. The remaining 67 (72.0%) compounds had no supporting data available. These results are mirrored in the major late-phase clinical trials for IPF therapies outlined by Ahluwalia et al [20]. Of sixteen major trials, only two

have provided the standard of evidence to become approved clinical therapies for IPF: Nintedanib and Pirfenidone. Interestingly, these two therapies, along with Imatinib and Bosentan are the only interventions tested in major Clinical Trials for IPF which have bleomycin model data published on PubMed (Supplementary Table 3).

Inflammation Characterization.

16.8% (78 publications) of the investigated 464 preventative studies assessed inflammation (ie., inflammatory cytokines profile or cell counts) prior to day 7 following bleomycin administration (Figure 2e). A similar proportion was seen in the transgenic animal studies, where of the 251 publications investigated, 23.1% (58 publications) assessed inflammation in the inflammatory phase (at or before day 7) in the bleomycin model.

DISCUSSION

The administration of bleomycin into the airways of small rodents is the most commonly used experimental system to study disease pathology and test therapeutic efficacy of compounds for IPF [7]. There is controversy in the appropriateness of using bleomycin to model pulmonary fibrosis, however, this model makes up a large portion of all murine models used to study pulmonary fibrosis, and its use has been increasing over the past decade (Figure 2a). Therefore, despite the model's limitations, it is important that we evaluate and propose improvements so that researchers that use this model do so as effectively as possible.

Our analysis revealed a total of 1009 reported studies using bleomycin between January 2008 and March 2019. Of these, 758 studies were conducted to test the effectiveness of a particular intervention, and 201 investigated mechanistic questions in genetically modified animals (Figure 2b). In order to get the best possible information from experimental models, it is imperative to apply appropriate research methodology that reflects what is seen clinically in IPF patients. Since the bleomycin model is initially characterized by a major inflammatory phase, which lasts for approximately 7 days, the factor of timing becomes particularly important as the clinical response of patients with IPF to anti-inflammatory therapies is negligible [12, 16]. This was highlighted in a previous publication by our group, which advocated for more critical understanding and appropriate use of timing in the bleomycin model [19]. In order to determine whether an intervention is effective through true anti-fibrotic effects, it should be administered after the inflammation subsides. The transition of inflammation and acute injury to fibrogenesis

occurs between 5-10 days post-intra-tracheal bleomycin and separates the model into an inflammatory and a fibrotic phase [12]. After 3 or 4 weeks, resolution/reversal of fibrosis is often seen in the bleomycin model, which narrows the window to studying anti-fibrotic effects [13–15]. The vast majority of studies published between 1980 and 2006 used suboptimal experimental conditions for studying anti-fibrotic therapies [19]. In fact, 95% of the 222 studies published during this time employed a preventative intervention regimen, yet most of the authors claimed they had found a novel therapeutic intervention for IPF. Most of these studies did not examine changes in inflammatory markers to consider the intervention's impact on the initial inflammatory phase. As the number of publications using the bleomycin model continues to rise, it is critical for investigators to incorporate the appropriate timing regiments for animal studies used to understand human IPF. This will optimize the allocation of resources in pre-clinical drug development and contribute to improved patient outcomes.

In this study, we used the same definitions for preventative and therapeutic interventions as in our previous work and evaluated how experimental practice has changed in the last decade [19]. In contrast to the extremely low 5% of studies that were therapeutically timed prior to 2007, in the past decade about 37.1% (281 publications) of intervention studies in the bleomycin model adequately assessed therapeutic efficacy (Figure 2c). This marked shift in how the bleomycin model is being used in work published between 2008 and 2019 compared to the two decades prior to 2007, highlights how researchers are receptive to change and are now more appropriately using the bleomycin model to test therapeutic efficacy of interventions for IPF.

The use of animals for medical research has become an important point of discussion from an ethical and political perspective [21]. The recent ERS Task Force "Optimizing Experimental Research in Respiratory Diseases" has addressed this important issue [22]. It concluded that substantial efforts have been undertaken by the scientific community, including the development and application of the 3Rs principles (Refinement, Reduction, Replacement) that were introduced 60 years ago to establish the highest standards for humane experimentation on animals [23]. The refined use of the bleomycin model of pulmonary fibrosis as described here is a reflection and proof that scientists are willing to learn and apply an improving experimental practice to comply with the 3R principles and animal research ethics. Further success in this context can be achieved by continuing to promote this message.

One of the key questions to experimental scientists is whether their models are useful to predict the success or failure of novel drugs in clinical studies. In theory, pre-clinical models do exactly this, but in reality, this is not so easily quantifiable. With regard to pulmonary fibrosis, the last decade has been filled with debates regarding the most appropriate "end-point" for both clinical trials and experimental studies. From the pre-clinical perspective, it is crucial to use the models as appropriately as possible, and interpret the findings within the limitations of the modeling. Whether data from the bleomycin model is a prerequisite for the progression of a drug candidate into the clinical trial landscape is obviously driven by the institution or company that develops the product. However, it is important for everyone in the field to understand how potential anti-fibrotic therapies work in the biological system. We asked in our analysis, how novel compounds considered for

the treatment of IPF were used in the bleomycin model and how their preclinical "success" compared to their clinical "success". A review by Ahluwalia et al. summarized how recent clinical trials relate to the pathogenesis of IPF and was used as a baseline for our analysis [20]. Ahluwalia et al. highlighted 16 compounds that were tested in clinical phase II and III trials in the last decade. Of these molecules, two have been approved for clinical use in IPF (nintedanib and pirfenidone).

Pirfenidone has by now been approved for the treatment of IPF in most countries [24–26]. The exact mode of action for this small molecule remains elusive, however, evidence from several clinical trials has convincingly shown that this drug reduces FVC decline in patients with progressive IPF [25]. Pre-clinical data for pirfenidone in the bleomycin model is available in both preventative and therapeutic settings, which show this molecule reduces TGF-β levels, fibrocyte migration, and the accumulation of pro-fibrotic myofibroblasts [27–29]. Pirfenidone is also able to reduce the accumulation of hydroxyproline and levels of procollagen I and III in these models [30].

Nintedanib is also approved in many countries and demonstrates a similar potential for slowing FVC decline in patients with IPF [31, 32]. Nintedanib is a potent intracellular inhibitor of the receptor tyrosine kinases PDGFR, FGFR, and vascular VEGFR as well as non-receptor tyrosine kinases from the Src family [33, 34]. This small molecule attenuates processes that are essential for fibrosis such as TGF-β-induced deposition of collagen and histological fibrosis in the bleomycin model. The literature provides many examples of Nintedanib's efficacy in both preventative and therapeutically designed bleomycin animal trials.

The success of these drugs in the therapeutically timed bleomycin models followed by clinical trials and FDA approval, suggests that there are overlaps in the underlying mechanisms of fibrosis in IPF and in the mouse model of bleomycin exposure. Therefore, while we may not have great insight into the mechanisms of IPF or bleomycin-induced fibrosis, this overlap provides considerable impetus for continued efforts to find new efficacious therapeutic applications in the bleomycin model.

Sildenafil is another drug that showed efficacy in both therapeutic and preventative versions of the bleomycin model. Although the STEP-IPF trial that tested sildenafil in patients with advanced IPF was labeled as a "negative" trial [35], sildenafil was recently tested in combination with Nintedanib in the INSTAGE trial in patients with advanced IPF [36]. While this trial did not meet its primary endpoint of changing quality of life, it nevertheless showed that patients treated with the combination of nintedanib plus sildenafil had a reduced decline in FVC than patients treated with Nintedanib alone, suggesting additive antifibrotic effects of the combination in this patient population. Another similar trial testing the combination of pirfenidone plus sildenafil for severe IPF is still ongoing (NCT02951429).

Of the 16 recent phase II and III clinical trials outlined by Ahluwalia et al. six have available data on PubMed regarding their efficacy in the bleomycin model (Supplementary Table 3)[20]. Pirfenidone, Nintedanib as well as Bosentan are only three of the sixteen trials with available therapeutic timing results. This data provides support for the notion that potential therapies have a better chance at clinical trial success if they are effective in a therapeutic model of bleomycin. For example, and in contrast to both Pirfenidone and

Nintedanib, the small molecule dual endothelin receptor inhibitor, Bosentan was unsuccessful in two separate phase III clinical trials [37, 38]. In this case, most of the publicly available data for this molecule was preventative, and only recently in 2017 a therapeutic study was published [39–41]. The preventative studies showed an overall decrease in collagen proteins and mRNA, as well as a reduction of α-SMA positive cells in the lung tissue. Several studies have also revealed that preventative bosentan treatment attenuates total and differential inflammatory cell counts [40, 42]. Therefore, bosentan may interfere with the initial bleomycin-induced inflammation, which subsequently prevents pro-fibrotic pathways from being activated. Furthermore, the recent therapeutic study noted that bosentan was effective at inhibiting bleomycin-induced collagen fibers and lung fibrosis only when administered in the preventative, and not the therapeutic phase [41]. Together, these findings illustrate the importance of proper experimental timing in the bleomycin model.

Of course, this conclusion is based on interpretation of publicly available data alone, and it may well be that unpublished data on therapeutic bleomycin studies exist. This issue of unavailable data can be further illustrated by assessing the preclinical literature available for the 145 clinical trials that have tested or are currently testing 93 unique compounds or combinations to treat IPF. Out of these 93 interventions, no associated animal data was found for 67 on PubMed (Figure 2d). Of the 26 interventions with available preclinical data, 20 were assessed therapeutically. Without comprehensive information available to the scientific community, it is impossible to ascertain why certain compounds may have failed in clinical trials and whether this can be attributed to inappropriate use of

pre-clinical models. Better transparency and publication of experimental data, positive and negative has recently been proposed by the ERS Task Force called "Optimizing experimental models of lung diseases" [22]. We support this endeavor and call for increased transparency in IPF focused animal models.

The importance of therapeutic timing in the bleomycin model for drug development in IPF is obvious, but this does not discard the value of interventions during the initial inflammatory phase. Analyzing the impact of interventions during the initiation of fibrosis allows for investigation into fibrotic pathways that may be linked to certain pro-fibrotic aspects of inflammation. This type of understanding is particularly important when considering pro-fibrotic macrophages, fibrocytes, and other bone marrow-derived cells which are not typical of the classical acute inflammatory pathways, and contribute to fibrosis in a major way. For these preventative interventional studies, it is key that inflammation in the early phase is characterized thoroughly by cell differentials and quantification of inflammatory cytokines. We found that of 464 preventative studies, only 78 (16.8%) provided such information (Figure 2e). Many of these studies reported a decrease in global inflammation following the intervention but still claimed to show anti-fibrotic effects. Similar data is seen in studies using transgenic animals, where therapeutic timing is often not a viable option except for inducible genetic knockouts. Between 2008 and 2019, of the 251 reported bleomycin studies in transgenic animals, only 58 (23.1%) characterized inflammation prior to day 7 post bleomycin administration (Figure 2e). The remaining 77% of studies did not investigate or at least not report any inflammation details. This information is critical to understand how a particular gene or pathway may contribute

to fibrogenesis and potentially serve as novel therapeutic targets. Therefore, the scientific community needs to more rigorously assess these basic features in the early inflammatory phase to capitalize on its utility in pre-clinical experimental research.

In conclusion, the bleomycin model of lung fibrosis is still, by far, the most common and growing experimental tool in this field (Figure 2a). In 2018, bleomycin studies comprised 60.6% of all publications that used mice to investigate pulmonary fibrosis, and the number of publications per year using bleomycin to study pulmonary fibrosis has more than doubled since 2008. Bleomycin is widely used for preclinical mechanistic research, and for preclinical studies to test drug efficacy. The basic science methodology of timing drug administration in the bleomycin model has seen a significant shift over the past 11 years compared to the period before. Both currently approved IPF drugs, pirfenidone, and nintedanib have convincing therapeutic efficacy in the bleomycin model. For the majority of compounds that were clinically tested in the past 15 years for the treatment of IPF, only 28.0% had published bleomycin-tested data. While a more thoughtful use of the model throughout the literature is evident, there is still a substantial lack of data sharing in this field. Despite improvements over the last decade, scientists from both private and academic sectors should strive to optimize this experimental model of lung fibrosis, as it will prove imperative to facilitate cutting edge drug development for IPF.

FIGURE LEGEND

Figure 1: Flow chart outlining the inclusion/exclusion criteria for this study.

Figure 2: a) Number of publications per year of mice in pulmonary fibrosis (PF) (silver), and bleomycin in PF studies before (gray) and after (blue) exclusion criteria. **b)** Distribution of investigated studies. **c)** Distribution of intervention studies**. d)** Associated PubMed Data for IPF clinical trials**. e)** Distribution of Inflammation characterization <7 days after bleomycin administration in preventative and transgenic studies**.**

Figure 3: Illustration of the appropriate times to begin intervention within the bleomycin model of pulmonary fibrosis. The upper (earlier) checkered line represents the time of bleomycin exposure and the beginning of a week-long period dominated by inflammation. The second checkered line represents the beginning of a two-week period dominated by fibrotic events. The central panel, with no treatment, features both the inflammatory and fibrotic aspects of the model. With preventative treatment (applied at the time of bleomycin exposure in the left panel), fibrosis is absent as a result of preventing inflammation. With therapeutic treatment (applied after the resolution of inflammation in the right pane) prevention of fibrosis can be attributed to events independent of inflammation.

Figure 1

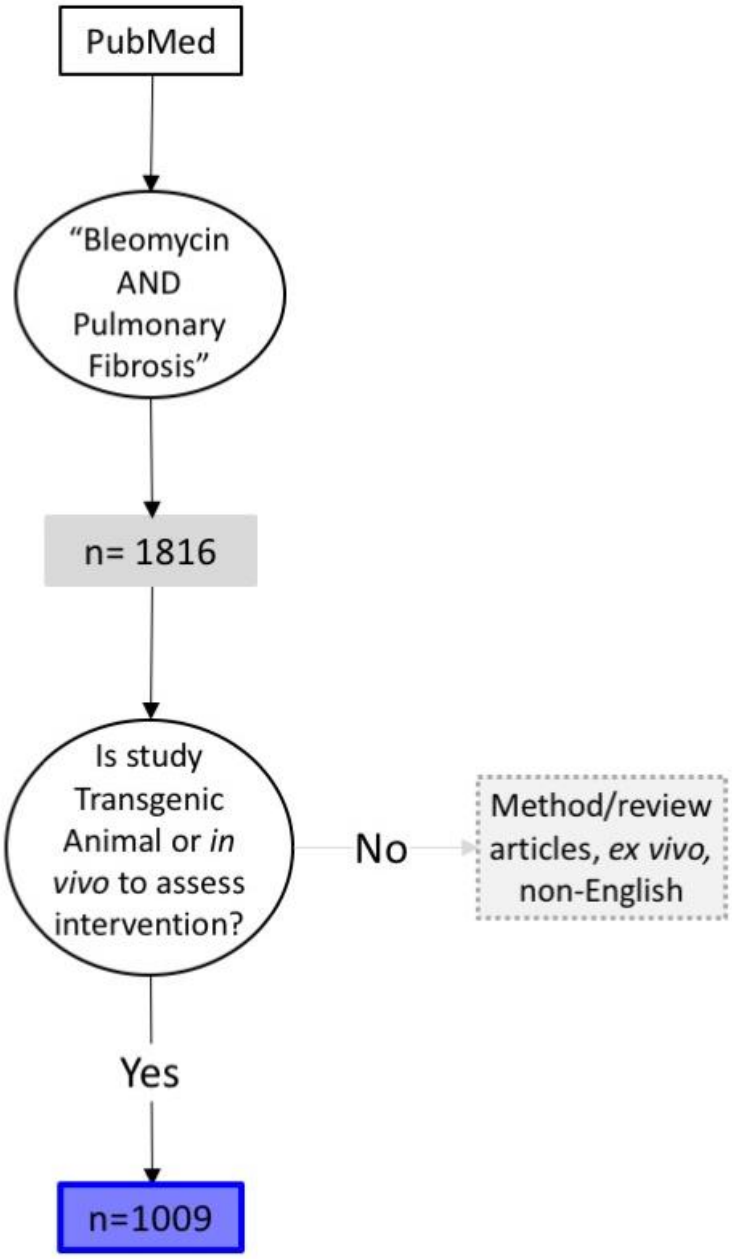
PubMed
"Bleomycin AND Pulmonary Fibrosis"
n= 1816
Is study Transgenic Animal or *in vivo* to assess intervention?
No
Method/review articles, *ex vivo*, non-English
Yes
n=1009

Figure 2

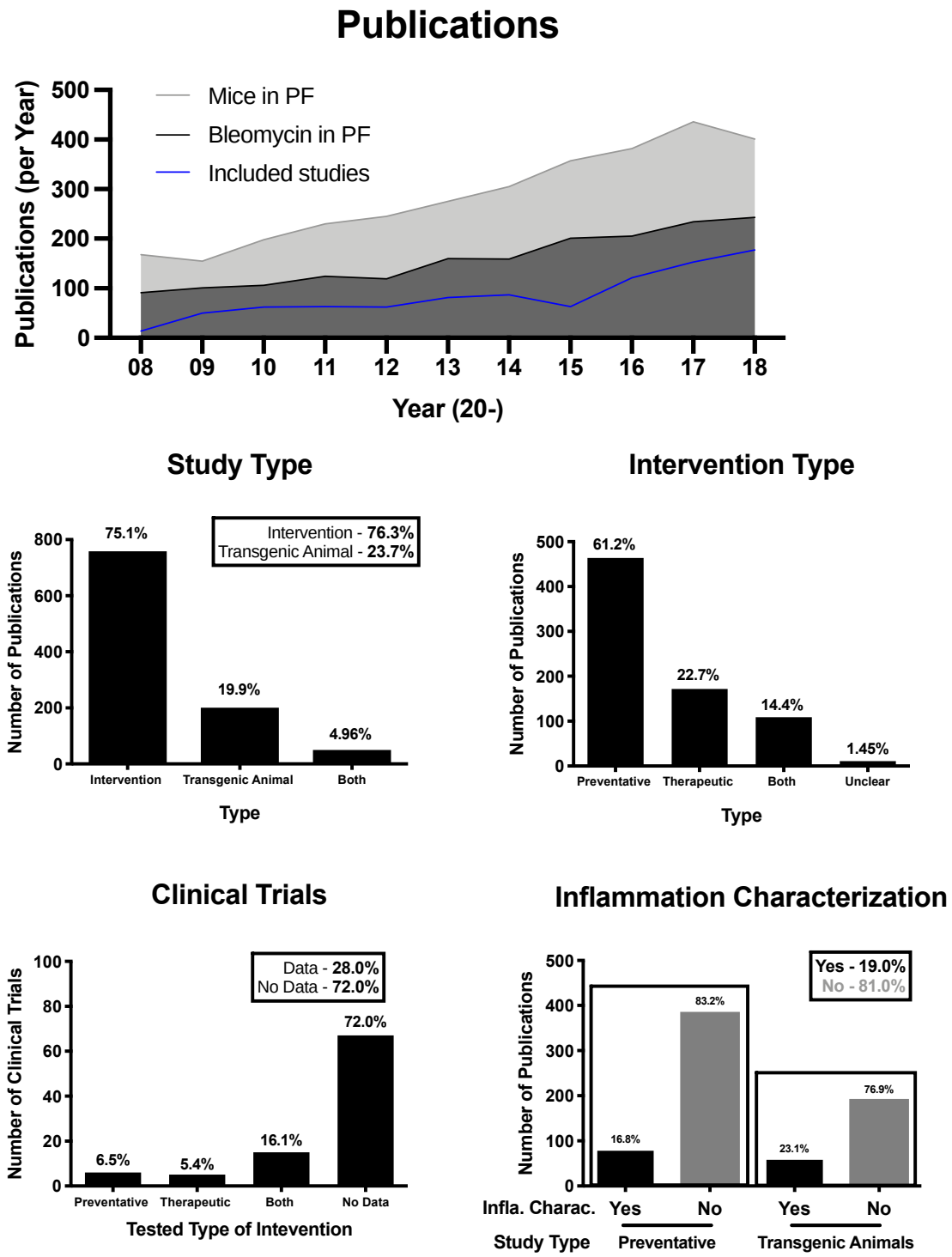
Publications
Publications (per Year)
500
400
300
200
100
0
Mice in PF
Bleomycin in PF
Included studies
08
09
10
11
12
13
14
15
16
17
18
Year (20-)
Study Type
Number of Publications
800
600
400
200
0
75.1%
19.9%
4.96%
Intervention - 76.3%
Transgenic Animal - 23.7%
Intervention
Transgenic Animal
Both
Type
Intervention Type
Number of Publications
500
400
300
200
100
0
61.2%
22.7%
14.4%
1.45%
Preventative
Therapeutic
Both
Unclear
Type
Clinical Trials
Number of Clinical Trials
100
80
60
40
20
0
6.5%
5.4%
16.1%
72.0%
Data - 28.0%
No Data - 72.0%
Preventative
Therapeutic
Both
No Data
Tested Type of Intevention
Inflammation Characterization
Number of Publications
500
400
300
200
100
0
16.8%
83.2%
23.1%
76.9%
Yes - 19.0%
No - 81.0%
Infla. Charac.
Yes
No
Yes
No
Study Type
Preventative
Transgenic Animals

Figure 3

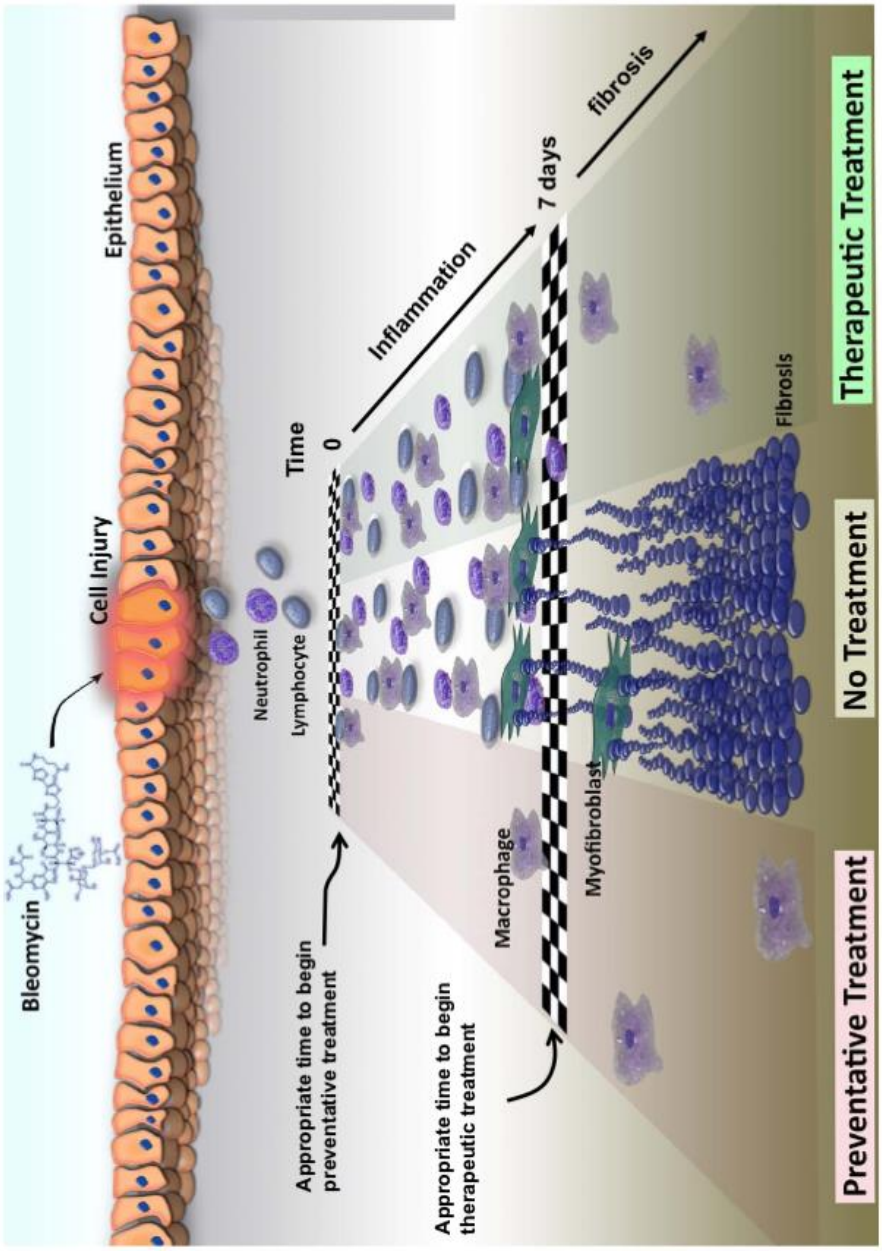
Bleomycin
Cell Injury
Epithelium
Neutrophil
Lymphocyte
Time
0
Inflammation
7 days
fibrosis
Appropriate time to begin preventative treatment
Appropriate time to begin therapeutic treatment
Macrophage
Myofibroblast
Fibrosis
Preventative Treatment
No Treatment
Therapeutic Treatment

SUPPLEMENTAL TABLES

Supplemental table 1. Master list of publications included in this study.

Supplemental table 2. All clinical trials for IPF and accompanying preclinical-bleomycin data.

Supplemental table 3. Major clinical trials assessed in the Ahluwalia et al. publication, with accompanying preclinical-bleomycin data.

Supplemental table 1

Please see attached file (Chapter 4 - Supplemental table 1**)**

Supplemental table 2

Clinical Trials	Available Preclinical Date
[18F]-FBA-A20FMDV2	No Data
[18F]-FBA-A20FMDV2	No Data
aerosol interferon-gamma	No Data
Ambrisentan	No Data
ART-123	Preventative
Autologous mesenchymal stem cells derived from bone marrow	Both
azathioprine	No Data
azathioprine	No Data
BMS-986020	No Data
Bosentan	Both
Bosentan	Both
Bosentan	Both
Bosentan	Both
Carbon Monoxide	Both
CC-90001	No Data
CC-930	No Data
CNTO 888	No Data
Combined Plasma Exchange (PEX), Rituximab, and Corticosteroids	No Data
Adipose-derived mesenchymal stem cells	Preventative
Cotrimoxazole	No Data
Dasatinib, Quercetin	Both
Etanercept	No Data
Fentanyl	No Data
FG-3019	Preventative
FG-3019	Preventative
FG-3019	Preventative
SAR156597	No Data
Fostair	No Data
GBT440	No Data
GBT440	No Data
GC1008	No Data
Gefapixant	No Data
Gefapixant	No Data
GLPG1690	No Data

GS-6624	No Data
GS-6624	No Data
GSK2126458	No Data
HEC585	No Data
Herpesvirus	No Data
hMSC	Both
hMSC	Both
IFN-a	No Data
Iloprost (Ventavis)	Both
Imatinib Mesylate (Gleevec)	Both
Inhaled Nitric Oxide	No Data
inhaled nitric oxide 75 mcg/kg IBW/hr	No Data
Interferon alpha oral lozenge	No Data
Interferon-gamma 1b	No Data
Interferon-gamma 1b	No Data
Interferon-gamma 1b	No Data
Interferon-gamma 1b	No Data
interferon-gamma 1b	No Data
IW001	No Data
KD025	No Data
Lebrikizumab	No Data
Lung stem cells	Both
Macitentan	No Data
Macitentan	No Data
minocycline	No Data
MN-001	No Data
Nintedanib	Both
Nintedanib	Both
Nintedanib	Both
Nintedanib	Both
Nintedanib	Both
Nintedanib	Both
Nintedanib	Both
Nintedanib	Both
octreotide	Both
Omeprazole	No Data
High-dose N-acetylcysteine	Preventative

PBI4050	No Data
Pirfenidone	Both
Pirfenidone	Both
Pirfenidone	Both
Pirfenidone	Both
Pirfenidone	Both
Pirfenidone	Both
Pirfenidone	Both
Pirfenidone	Both
Pirfenidone	Both
Placental MSC	Both
pomalidomide (CC-4047)	No Data
prednisolone	Preventative
Prednisone, Azathioprine, NAC	No Data
PRM-151	No Data
PRM-151	No Data
QAX576	No Data
QAX576	No Data
Rituximab	No Data
Rituximab, Steroids, PEX	No Data
ROTARIX + DPT-HepB-Hib + OPV	No Data
Salbutamol	No Data
SAR156597	No Data
Sildenafil	Both
Sildenafil	Both
Sildenafil	Both
sildenafil	Both
sildenafil	Both
Sildenafil, Losarten	No Data
Simtuzumab	No Data
STX-100	No Data
TD139	Therapeutic
Tetrathiomolybdate	No Data
Thalidomide	Both
Thalidomide	Both
Tralokinumab	No Data
Tralokinumab	No Data

treprostinil	Therapeutic
treprostinil	Therapeutic
VAY736	No Data
Vismodegib	Therapeutic
vismodegib	Therapeutic
Warfarin	No Data
ZL-2102	No Data
Cyclophosphamide; Dapsone	No Data
Iloprost	Both
Ambrisentan	No Data
Tamoxifen	Therapeutic
Rituximab; Cyclophosphamide	No Data
Bevacizumab; Dexamethasone	No Data
CC-90001	No Data
Treprostinil	Therapeutic
Treprostinil	Therapeutic
Treprostinil	Therapeutic
Rituximab; Mycophenolate Mofetil	No Data
iNO	No Data
iNO	No Data
Pirfenidone	Both
BI 1015550	No Data
HEC 68498	No Data
ND-L02-s0201	No Data
BLD-2660	No Data
BG00011	No Data
SM04646	No Data
ZSP1603	No Data
MG-S-2525	No Data
GLPG1690	No Data
GLPG1690	No Data
N-acetyl cysteine	Preventative
GLPG1205	No Data
TRK-250	No Data
BBT-877	No Data
TD139	Therapeutic
GKT137831	Therapeutic

Supplemental table 3

Drug	Mechanisms of action	Outcome	Clinical trial.gov ID	Bleo Results
Ambrisentan	Endothelin receptor antagonist	Negative	NCT00768300	Not Published
BIBF 1120	Inhibitor of VEGF, PDGF, FGF receptor kinases	Positive	NCT00514683	Both
Bosentan	Endothelin receptor antagonist	Negative Negative	NCT00071461 NCT00391443	Both
CNTO-888	Anti-CCL2 antibody	Negative	NCT00786201	Not Published
Etanercept	TNF-α receptor antagonist	Negative	NCT00063869	Not Published
FG-3019	Antibody against CTGF	Results awaited Positive (Phase I) Results awaited	NCT00074698 NCT01262001 NCT01890265	Preventative
GC1008	TGF-β neutalizing antibody	Results awaited	NCT00125385	Not Published
GS6624	Antibody against LOXL2	Results awaited	NCT01362231	Not Published
Imatinib	Tyrosin kinase inhibitor	Negative	NCT00131274	Both
Interferon-g	Anti-inflammatory	Negative Negative	NCT00047645 NCT00075998	Not Published
Macitentan	Endothelin receptor antagonist	Negative	NCT00903331	Not Published
NAC	Anti-oxidant	Negative	NCT00650091	Preventative
NAC, Azathioprine, Prednisone	Anti-oxidant	Positive Negative	NCT00639496 NCT00650091	Not Published
Pirfenidone	Antifibrotic	Positive/Negative Positive Positive	NCT00287716 JAPICCTCI-050121 NCT01366209	Both
QAX576	Anti-IL-13 antibody	Negative	NCT01266135	Not Published
Warfarin	Anticoagulants	Negative	NCT00957242	Not Published

REFERENCES

1. Ley B, Collard HR, King TE. Clinical Course and Prediction of Survival in Idiopathic Pulmonary Fibrosis. *Am J Respir Crit Care Med* 2011; 183: 431–440.

2. American Thoracic Society/European Respiratory Society International Multidisciplinary Consensus Classification of the Idiopathic Interstitial Pneumonias. *Am J Respir Crit Care Med* 2002; 165: 277–304.

3. Hopkins RB, Burke N, Fell C, Dion G, Kolb M. Epidemiology and survival of idiopathic pulmonary fibrosis from national data in Canada. *Eur. Respir. J.* 2016; 48: 187–195.

4. Nalysnyk L, Cid-Ruzafa J, Rotella P, Esser D. Incidence and prevalence of idiopathic pulmonary fibrosis: review of the literature. *Eur Respir Rev* 2012; 21: 355–361.

5. Ogura T, Taniguchi H, Azuma A, Inoue Y, Kondoh Y, Hasegawa Y, Bando M, Abe S, Mochizuki Y, Chida K, Klüglich M, Fujimoto T, Okazaki K, Tadayasu Y, Sakamoto W, Sugiyama Y. Safety and pharmacokinetics of nintedanib and pirfenidone in idiopathic pulmonary fibrosis. *European Respiratory Journal* 2015; 45: 1382–1392.

6. Tashiro J, Rubio GA, Limper AH, Williams K, Elliot SJ, Ninou I, Aidinis V, Tzouvelekis A, Glassberg MK. Exploring Animal Models That Resemble Idiopathic Pulmonary Fibrosis. *Frontiers in Medicine* [Internet] 2017 [cited 2018 May 26]; 4Available from: http://journal.frontiersin.org/article/10.3389/fmed.2017.00118/full.

7. Jenkins RG, Moore BB, Chambers RC, Eickelberg O, Königshoff M, Kolb M, Laurent GJ, Nanthakumar CB, Olman MA, Pardo A, Selman M, Sheppard D, Sime PJ, Tager AM, Tatler AL, Thannickal VJ, White ES, ATS Assembly on Respiratory Cell and Molecular Biology. An Official American Thoracic Society Workshop Report: Use of Animal Models for the Preclinical Assessment of Potential Therapies for Pulmonary Fibrosis. *Am. J. Respir. Cell Mol. Biol.* 2017; 56: 667–679.

8. Degryse AL, Tanjore H, Xu XC, Polosukhin VV, Jones BR, McMahon FB, Gleaves LA, Blackwell TS, Lawson WE. Repetitive intratracheal bleomycin models several features of idiopathic pulmonary fibrosis. *Am. J. Physiol. Lung Cell Mol. Physiol.* 2010; 299: L442-452.

9. Usuki J, Fukuda Y. Evolution of three patterns of intra-alveolar fibrosis produced by bleomycin in rats. *Pathol. Int.* 1995; 45: 552–564.

10. Chaudhary NI, Schnapp A, Park JE. Pharmacologic Differentiation of Inflammation and Fibrosis in the Rat Bleomycin Model. *Am J Respir Crit Care Med* 2006; 173: 769–776.

11. Kim SN, Lee J, Yang H-S, Cho J-W, Kwon S, Kim Y-B, Her J-D, Cho K-H, Song C-W, Lee K. Dose-response Effects of Bleomycin on Inflammation and Pulmonary Fibrosis in Mice. *Toxicol Res* 2010; 26: 217–222.

12. Izbicki G, Segel MJ, Christensen TG, Conner MW, Breuer R. Time course of bleomycin-induced lung fibrosis. *Int J Exp Pathol* 2002; 83: 111–119.

13. Chung MP, Monick MM, Hamzeh NY, Butler NS, Powers LS, Hunninghake GW. Role of Repeated Lung Injury and Genetic Background in Bleomycin-Induced Fibrosis. *Am J Respir Cell Mol Biol* 2003; 29: 375–380.

14. Phan SH, Armstrong G, Sulavik MC, Schrier D, Johnson KJ, Ward PA. A Comparative Study of Pulmonary Fibrosis Induced by Bleomycin and an O2 Metabolite Producing Enzyme System. *CHEST* 1983; 83: 44S-45S.

15. Lawson WE, Polosukhin VV, Stathopoulos GT, Zoia O, Han W, Lane KB, Li B, Donnelly EF, Holburn GE, Lewis KG, Collins RD, Hull WM, Glasser SW, Whitsett JA, Blackwell TS. Increased and prolonged pulmonary fibrosis in surfactant protein C-deficient mice following intratracheal bleomycin. *Am. J. Pathol.* 2005; 167: 1267–1277.

16. Chua F, Gauldie J, Laurent GJ. Pulmonary Fibrosis. *Am J Respir Cell Mol Biol* 2005; 33: 9–13.

17. Limjunyawong N, Mitzner W, Horton MR. A mouse model of chronic idiopathic pulmonary fibrosis. *Physiol Rep* 2014; 2: e00249.

18. Peng R, Sridhar S, Tyagi G, Phillips JE, Garrido R, Harris P, Burns L, Renteria L, Woods J, Chen L, Allard J, Ravindran P, Bitter H, Liang Z, Hogaboam CM, Kitson C, Budd DC, Fine JS, Bauer CMT, Stevenson CS. Bleomycin induces molecular changes directly relevant to idiopathic pulmonary fibrosis: a model for "active" disease. *PLoS ONE* 2013; 8: e59348.

19. Moeller A, Ask K, Warburton D, Gauldie J, Kolb M. The bleomycin animal model: A useful tool to investigate treatment options for idiopathic pulmonary fibrosis? *The International Journal of Biochemistry & Cell Biology* 2008; 40: 362–382.

20. Ahluwalia N, Shea BS, Tager AM. New Therapeutic Targets in Idiopathic Pulmonary Fibrosis. Aiming to Rein in Runaway Wound-Healing Responses. *Am J Respir Crit Care Med* 2014; 190: 867–878.

21. Wadman M. Animal rights: Chimpanzee research on trial. *Nature* 2011; 474: 268–271.

22. Bonniaud P, Fabre A, Frossard N, Guignabert C, Inman M, Kuebler WM, Maes T, Shi W, Stampfli M, Uhlig S, White E, Witzenrath M, Bellaye P-S, Crestani B, Eickelberg O, Fehrenbach H, Guenther A, Jenkins G, Joos G, Magnan A, Maitre B, Maus UA, Reinhold P, Vernooy JHJ, Richeldi L, Kolb M. Optimising experimental research in respiratory diseases: an ERS statement. *European Respiratory Journal* 2018; 51: 1702133.

23. Directive 2010/63/EU of the European Parliament and of the Council of 22 September 2010 on the protection of animals used for scientific purposes Text with EEA relevance [Internet]. 276, 32010L0063 Oct 20, 2010Available from: http://data.europa.eu/eli/dir/2010/63/oj/eng.

24. Raghu G, Collard HR, Egan JJ, Martinez FJ, Behr J, Brown KK, Colby TV, Cordier J-F, Flaherty KR, Lasky JA, Lynch DA, Ryu JH, Swigris JJ, Wells AU, Ancochea J, Bouros D, Carvalho C, Costabel U, Ebina M, Hansell DM, Johkoh T, Kim DS, King TE, Kondoh Y, Myers J, Müller NL, Nicholson AG, Richeldi L, Selman M, Dudden RF, et al. An Official ATS/ERS/JRS/ALAT Statement: Idiopathic Pulmonary Fibrosis: Evidence-based Guidelines for Diagnosis and Management. *Am J Respir Crit Care Med* 2011; 183: 788–824.

25. Noble PW, Albera C, Bradford WZ, Costabel U, Glassberg MK, Kardatzke D, King TE, Lancaster L, Sahn SA, Szwarcberg J, Valeyre D, du Bois RM, CAPACITY Study Group. Pirfenidone in patients with idiopathic pulmonary fibrosis (CAPACITY): two randomised trials. *Lancet* 2011; 377: 1760–1769.

26. Margaritopoulos GA, Vasarmidi E, Antoniou KM. Pirfenidone in the treatment of idiopathic pulmonary fibrosis: an evidence-based review of its place in therapy. *Core Evid* 2016; 11: 11–22.

27. Kakugawa T, Mukae H, Hayashi T, Ishii H, Abe K, Fujii T, Oku H, Miyazaki M, Kadota J, Kohno S. Pirfenidone attenuates expression of HSP47 in murine bleomycin-induced pulmonary fibrosis. *Eur. Respir. J.* 2004; 24: 57–65.

28. Inomata M, Kamio K, Azuma A, Matsuda K, Kokuho N, Miura Y, Hayashi H, Nei T, Fujita K, Saito Y, Gemma A. Pirfenidone inhibits fibrocyte accumulation in the lungs in bleomycin-induced murine pulmonary fibrosis. *Respir Res* 2014; 15: 16.

29. Oku H, Shimizu T, Kawabata T, Nagira M, Hikita I, Ueyama A, Matsushima S, Torii M, Arimura A. Antifibrotic action of pirfenidone and prednisolone: different effects on pulmonary cytokines and growth factors in bleomycin-induced murine pulmonary fibrosis. *Eur. J. Pharmacol.* 2008; 590: 400–408.

30. Iyer SN, Gurujeyalakshmi G, Giri SN. Effects of pirfenidone on procollagen gene expression at the transcriptional level in bleomycin hamster model of lung fibrosis. *J. Pharmacol. Exp. Ther.* 1999; 289: 211–218.

31. Richeldi L, du Bois RM, Raghu G, Azuma A, Brown KK, Costabel U, Cottin V, Flaherty KR, Hansell DM, Inoue Y, Kim DS, Kolb M, Nicholson AG, Noble PW, Selman M, Taniguchi H, Brun M, Le Maulf F, Girard M, Stowasser S, Schlenker-Herceg R, Disse B, Collard HR. Efficacy and Safety of Nintedanib in Idiopathic Pulmonary Fibrosis. *New England Journal of Medicine* 2014; 370: 2071–2082.

32. Case AH, Johnson P. Clinical use of nintedanib in patients with idiopathic pulmonary fibrosis. *BMJ Open Respiratory Research* 2017; 4: e000192.

33. Hilberg F, Roth GJ, Krssak M, Kautschitsch S, Sommergruber W, Tontsch-Grunt U, Garin-Chesa P, Bader G, Zoephel A, Quant J, Heckel A, Rettig WJ. BIBF 1120: triple angiokinase inhibitor with sustained receptor blockade and good antitumor efficacy. *Cancer Res.* 2008; 68: 4774–4782.

34. Hostettler KE, Zhong J, Papakonstantinou E, Karakiulakis G, Tamm M, Seidel P, Sun Q, Mandal J, Lardinois D, Lambers C, Roth M. Anti-fibrotic effects of nintedanib in lung fibroblasts derived from patients with idiopathic pulmonary fibrosis. *Respiratory Research* 2014; 15: 157.

35. A Controlled Trial of Sildenafil in Advanced Idiopathic Pulmonary Fibrosis. *New England Journal of Medicine* 2010; 363: 620–628.

36. Kolb M, Raghu G, Wells AU, Behr J, Richeldi L, Schinzel B, Quaresma M, Stowasser S, Martinez FJ. Nintedanib plus Sildenafil in Patients with Idiopathic Pulmonary Fibrosis. *New England Journal of Medicine* 2018; 379: 1722–1731.

37. King TE, Behr J, Brown KK, du Bois RM, Lancaster L, de Andrade JA, Stähler G, Leconte I, Roux S, Raghu G. BUILD-1: A Randomized Placebo-controlled Trial of Bosentan in Idiopathic Pulmonary Fibrosis. *Am J Respir Crit Care Med* 2008; 177: 75–81.

38. King TE, Brown KK, Raghu G, du Bois RM, Lynch DA, Martinez F, Valeyre D, Leconte I, Morganti A, Roux S, Behr J. BUILD-3: A Randomized, Controlled Trial of Bosentan in Idiopathic Pulmonary Fibrosis. *Am J Respir Crit Care Med* 2011; 184: 92–99.

39. Schroll S, Arzt M, Sebah D, Nüchterlein M, Blumberg F, Pfeifer M. Improvement of bleomycin-induced pulmonary hypertension and pulmonary fibrosis by the endothelin receptor antagonist Bosentan. *Respir Physiol Neurobiol* 2010; 170: 32–36.

40. Chilakapati SR. Amelioration of bleomycin-induced pulmonary fibrosis in a mouse model by a combination therapy of bosentan and imatinib. 2015; 41: 173–188.

41. Zuo W-L, Zhao J-M, Huang J-X, Zhou W, Lei Z-H, Huang Y-M, Huang Y-F, Li H-G. Effect of bosentan is correlated with MMP-9/TIMP-1 ratio in bleomycin-induced pulmonary fibrosis. *Biomedical Reports* 2017; 6: 201–205.

42. Gamze K, Mehmet HM, Deveci F, Turgut T, Ilhan F, Ozercan I. Effect of bosentan on the production of proinflammatory cytokines in a rat model of emphysema. *Exp. Mol. Med.* 2007; 39: 614–620.

Chapter 5

Discussion

In this chapter, the main findings of the previous chapters (2-4) will be discussed in the context of current findings in the literature. The rationale and major findings of the previous three studies have been extensively discussed in their respective chapters. Therefore, the goal of this section is to:

- Articulate the key findings of the thesis in the context of the literature
- Discuss how chapters 2-4 are connected
- State how the work presented in this thesis investigates the lung ECM's role in progressive fibrosis, and uses this knowledge to appropriately model disease and preclinically test antifibrotic therapies to improve identification of pathobiological findings and translation into effective drug development
- Outline future directions for identifying the precise molecular mechanisms to target the ECM as a therapeutic avenue for fibrosis

The Extracellular Matrix-Cell Interaction in ILD

The ECM is synthesized, secreted and deposited by cells to form scaffolding material in organs. The ECM also influences cell phenotype and differentiation in various organ systems [82–84]. In the case of bones, terminal differentiation of osteoblasts is induced by loading forces in collagen-type 1 rich bone matrices [85, 86]. This is also true in the lungs. Chapter 2 of the thesis was written to summarize the current understanding of the ECM – cell interaction in the context of interstitial lung disease. Here, we discuss the drastic structural and compositional changes the lung undergoes during disease progression, which skews the balance between ECM deposition and degradation to cause fibrosis. We discuss how these changes induce profibrotic cellular effects that may drive progressive fibrosis in this disease.

ECM stiffening in the lung imparts mechanical cues that induce intracellular changes in surroundings cells. In this chapter we elaborate on two accepted models of mechanosensing: the tethered and membrane model, and the different machinery (i.e. integrins and GPCRs) through which cells can sense and respond to mechanical cues. We also see that mechanotransduction induces intracellular changes much faster than ligand-stimulated second-messenger based pathways [50, 51]. Diverse cell types such as epithelial cells, mesenchymal cells, and inflammatory cells all possess integrins. GPCRs are also abundantly found in almost all cell types. Therefore, most cells have the machinery to respond to the increased stiffness present in fibrotic lungs, and this interaction needs to be further investigated to understand its role in driving fibrosis.

To do this, the second portion of the chapter is focused on summarizing the current literature on how the structural and compositional ECM changes in ILD influence cell phenotype. Numerous studies have emphasized how increasing 2D stiffness promotes profibrotic changes in cells such as fibroblasts, epithelial cells, and mast cells, all of which have been implicated in fibrosis [46, 47]. At the compositional level, drastic changes in proteoglycans, glycosaminoglycans, fibrillar collagen, elastin fibers, and glycoproteins such as fibronectin, have been shown to mediate profibrotic ECM-cell interactions, and promote myofibroblast differentiation [42–45]. Soluble ECM fragments such as hyaluronan and collagen seem to also have bioactive properties, and promote a profibrotic phenotype in different cells [64, 65]. Lastly, we discuss the complexity in the *in vivo* system where the structural and compositional changes seldom work individually. Instead, they work in concert, with one example being the mechanical stretch-induced activation of TGFβ1. In this process, the increased stiffness caused by structural changes exert more mechanical stretch that activates a compositional ECM component, the growth factor.

This chapter highlights the dynamic interplay between different ECM characteristics, and how the fibrotic ECM in ILD can influence profibrotic cellular changes. Despite this amount of information, there is still a considerable gap in the mechanistic knowledge of how exactly, and to what extent the ECM can influence cell behavior and drive the progression of pulmonary fibrosis.

The 3D lung ECM's effect on fibroblast phenotype

The importance of ECM-cell interaction in the context of pulmonary fibrosis was highlighted in Chapter 2. Currently, most studies investigate this interaction under 2D

conditions, where the intricate 3D architecture of the microenvironment is lost. The 3D context, however, is important to appropriately study cell behaviour as cells behave differently under different culture conditions. Fibroblasts, for example, migrate in different ways depending on if they are cultured in 3D collagen matrices as opposed to cell-derived matrices [87]. YAP mediated mechanotransduction is also different under 2D vs 3D conditions [88]. Human lung cancer cells also produce MMPs when cultured in 3D *ex vivo* models, but not in 2D culture systems [89]. The 3D microenvironment also confers heterogeneity in exposure to nutrients and oxygen depending on their location, something that is lost in homogeneous 2D culture plates [90, 91]. The 2D culture conditions also enforce an apical-basal polarity and restricts cell adhesions to the x-y plane. These factors are not representative of the *in vivo* system, and the 3D architecture needs to be reproduced to appropriately investigate the ECM-cell relationship and its role in fibrosis.

To address the issue of models, researchers have developed interesting approaches to study lung function. One example is the lung on a chip, which is a small functional unit that recreates the biochemistry, function and mechanical strain lung and capillary cells would experience in the air sac of the lung [92]. Mechanical forces such as stretch can also be induced in these units to represent breathing. Though this provides a novel platform to study lung function, the lung on a chip does not address the 3D ECM aspect and the pathological changes in fibrosis. Nanofabrication of substrates on the other hand is another novel technique, where scaffolds are carefully arranged to create culturing platforms for cells [93]. This technique offers robust control over the ECM substrate and arrangements, to study the substrate's effect on cell behaviour. In IPF, however, the lung's intricate

microstructure makes artificially constructing 3D culturing systems of physiological and pathological states challenging, especially since the pathobiological undertesting of fibrosis is still incomplete. Creating ECM scaffolds via lung decellularization provides a unique approach to address this issue. Booth et al. were one of the first to use decellularized lung scaffolds to illustrate the effect of the IPF ECM to promote fibroblast to myofibroblast differentiation [94]. Their model system used scaffolds of one mm in width and cells were seeded using a dropwise technique directly onto the scaffolds. Fibroblasts successfully attached to the ECM, however, due to the thin size, much of the 3D architecture was lost in this technique. The scaffolds were also derived from patient samples, which provide real *in vivo* conditions, however, are difficult to standardize; and without the whole lung architecture (trachea, bronchioles) difficult to achieve full lung/lobe recellularization. In the study in Chapter 3, by decellularizing whole rat lungs we were able to successfully perform complete lobe recellularization and culture cells in ~3 cm wide horizontal lung sections. Researchers have reported cell "memory" in fibroblasts, where prolonged exposure to a certain environment has lasting effects on phenotype that persist for up to 2 weeks [95]. Therefore, we cultured cells in the ECM scaffolds for 7 and 21 days to ensure complete changes in fibroblast phenotype were observed in response to the new microenvironments. The AdTGF-β1 model of pulmonary fibrosis was used to create scaffolds with different levels of fibrosis. Together, this *ex vivo* system allowed us to recapitulate the 3D fibrotic and nonfibrotic ECM microenvironments, to gather mechanistic insight into the ECM components that drive cell behavior and differentiation.

The results suggest that the fibrotic ECMs promote a profibrotic phenotype in recellularized normal rat fibroblasts, which is in line with the findings of Booth et. al. [94]. Interestingly, recellularizing fibrotic fibroblasts into nonfibrotic ECMs seemed to significantly attenuate their profibrotic behavior. This was surprising since initially for many years researchers believed that fibroblast to myofibroblast differentiation was an irreversible process, and therefore an unsuccessful avenue for IPF therapy [96, 97]. Recent data indicates that myofibroblast dedifferentiation is possible and can be induced by prostaglandin E2 or down-regulation of MyoD [98, 99]. Furthermore, plating IPF fibroblasts on physiologically soft plates *in vitro* also decreases cell contractility, suggesting an attenuation in their fibrotic function [55]. However, this is one of the first studies to directly show this effect induced sole by the 3D nonfibrotic ECMs, suggesting an anti-fibrotic capacity worth investigating.

To gather more mechanistic understanding of the ECM components driving these observed effects, we assessed the ECM stiffness and composition individually. Similar to what is seen in the literature, here too we see that increasing *in vitro* stiffness induced a fibrotic phenotype in normal fibroblasts, while decreased stiffness attenuated the fibrotic phenotype in fibrotic fibroblasts [72, 100]. At the compositional level, homogenized ECM proteins from a fibrotic ECM promoted profibrotic differentiation in normal fibroblasts, while the homogenized ECM proteins from a nonfibrotic ECM attenuated profibrotic behavior in fibrotic fibroblasts. These effects were present despite inhibition of TGFβ signaling, suggesting that they were induced by compositional changes between fibrotic and nonfibrotic ECMs. These findings highlight the duel influence of the ECM in inducing

both profibrotic and antifibrotic effects on fibroblasts, and that the changes in ECM stiffness and composition can individually cause these observed effects. This is in accordance with the growing body of research that supports the notion of a vicious cyclical relationship between the fibrotic ECM and lung fibroblasts; which may drive progressive fibrosis [44, 101, 102]. Since our model directly investigates the ECM driven fibroblast phenotype, our results provide support for this theory. Furthermore, these findings provide credence for current research that targets the ECM structure as a potential therapy for IPF. One example is the LOX family of enzymes, which catalyze the cross-linking of collagen and elastin [103, 104]. By developing more effective drugs that restructure the fibrotic ECM, we may be able to utilize the ECM as a tool in the fight against fibrosis, rather than it being an active player in its progression.

Along with providing insight into the pathobiology of pulmonary fibrosis, this ECM scaffold system also serves as a preclinical model to assess an intervention's effect at interfering with the profibrotic ECM-cell interaction. In this chapter we see that ROCK1 and 2 expressions are significantly upregulated in normal fibroblasts recellularized into fibrotic ECMs. Since mechanotransduction seems to play a key role in the profibrotic effect of fibrotic ECMs, we tested the effect of inhibiting mechanotransduction using the pan ROCK inhibitor Y27632. Inhibiting mechanotransduction in this *ex vivo* model significantly attenuated the fibrotic ECM induced *Acta2* expression in normal fibroblasts. This is one of the first studies to show the efficacy of inhibiting mechanotransduction directly within the 3D fibrotic ECM – fibroblast relationship. This may explain the success of KD025 - a ROCK inhibitor that recently passed through a phase IIA clinical trial for

patients with IPF [105]. These mechanotransduction inhibitors may intervene in the vicious positive feedback cycle, that is driving the progression of pulmonary fibrosis. Along with illustrating the efficacy of this particular intervention, this study, more importantly highlights the use of this *ex vivo* system as a preclinical model. Preclinical models are crucial for researchers to translate findings of disease pathology into novel therapeutic interventions. Therefore, such models represent the last and maybe most important phase of drug development, prior to clinical testing.

The importance of interventional timing in the bleomycin model of pulmonary fibrosis

Different preclinical models are available for pulmonary fibrosis, however, none are as well characterize and widely used as the bleomycin model. Briefly, bleomycin injures the lung to induce inflammation, which progresses to fibrosis. The initial inflammatory phase lasts for approximately 7 days before subsiding into a fibrotic phase which is marked by drastic ECM deposition and lung scarring. The fibrotic phase in the bleomycin model mimics the fibrogenesis in IPF patients [77]. Spontaneous reversal of fibrosis, however, can occur 3-4 weeks post intratracheal bleomycin administration [78–81]. Therefore, the fibrotic phase is no longer than two weeks [12], and therapeutic interventions need to be administered within this "window" if true anti-fibrotic efficacy is to be tested. This is in accordance with the findings from chapter 2 and 3, which highlight the role of the fibrotic ECM in driving progressive fibrosis. It is therefore important that the pathological ECM is established so that an intervention's anti-fibrotic efficacy can be truly assessed in the model.

The bleomycin model makes up a large portion of all murine models used to study pulmonary fibrosis, and its use has been constantly increasing. In 2008, our team assessed the use of the model in the field, and found surprisingly poor appropriate therapeutic intervention timing (intervention starting >7 days after bleomycin administration) in studies published between 1980 and 2008 [106]. Here, we reassessed all PubMed available publications that used the bleomycin model to test interventions for pulmonary fibrosis between January 2008 and March 2019. This totaled 1009 papers, which were analyzed to assess appropriate intervention timing. Of these 1009 publications, 758 studies tested interventions, while the remaining 201 investigated mechanistic questions in genetically modified animals. 32.5% (281 publications) of the 758 interventions studies appropriately assessed therapeutic efficacy by initiating the intervention during the fibrotic phase of the model. This is a drastic improvement since the 2008 assessment where only 5% of studies had appropriately timed therapeutic interventions. This highlights how researchers are receptive to change and are now more effectively using the bleomycin model to study IPF.

Therapeutic timed interventions are important to assess the preclinical efficacy of drugs, however, this does not discredit the value of interventions during the initial inflammatory phase of the bleomycin model. Analyzing the impact of interventions during this inflammatory phase offers insight into pathways that may be linked to certain pro-fibrotic aspects of inflammation. To do this, however, it is important that the inflammation in the early phase is thoroughly characterized by either cell differentials or quantification of inflammatory cytokines. In our analysis, of the 464 preventatively timed studies, only 78 (16.8%) provided such information. Many of these studies reported a decrease in global

inflammation following the intervention, but still went on to claim anti-fibrotic effects of the intervention when in fact the drugs may have only interfered with the initial inflammatory process. Similar data is seen in studies using transgenic animals, where therapeutic timing is often not a viable option except for inducible genetic knockouts. Between 2008 and 2019, of the 251 reported bleomycin studies in transgenic animals, only 58 (23.1%) characterized inflammation prior to day 7 post bleomycin administration. The vast majority did not investigate or at least not report any inflammation details. This information is critical to understand how a particular gene or pathway may contribute to fibrogenesis, and potentially serve as targets for future therapeutics.

The ability to accurately predict the success or failure of a drug in clinical studies defines the usefulness of a preclinical model. Therefore, we assessed how novel compounds for IPF were tested in the bleomycin model and how their preclinical "success" compared to their clinical "success". A review by Ahluwalia et al. summarized how recent clinical trials relate to the pathogenesis of IPF and was used as a baseline for our analysis [107]. Ahluwalia et al. highlighted 16 compounds that were tested in clinical phase II and III trials in the last decade. Of these molecules, only four had publicly available preventative and therapeutic assessments in the bleomycin model. Two of these four drugs: nintedanib and pirfenidone also happened to be the only two currently approved for clinical use in IPF. Bosentan was another drug that also had available therapeutically tested results. Most of the publicly available preclinical data for this molecule was preventative, and only recently in 2017, a therapeutic study was published [108–110]. The preventative studies showed an overall decrease in collagen proteins and mRNA, as well as a reduction of α-SMA positive

cells in the lung tissue. Several studies have also revealed that preventative bosentan treatment attenuates total and differential inflammatory cell counts [109, 111]. Therefore, it seems that bosentan interferes with the initial bleomycin-induced inflammation, which subsequently prevents pro-fibrotic pathways from being activated. The recent therapeutic study also noted that bosentan was effective at inhibiting bleomycin-induced collagen fibers and lung fibrosis only when administered in the preventative, and not the therapeutic phase [110]. Unsurprisingly, in contrast to pirfenidone and nintedanib, bosentan was unsuccessful in two separate phase III clinical trials [112, 113]. These findings suggest that when used appropriately, interventions that are effective in the therapeutic phase of the bleomycin model have a better chance at clinical trial success in the future.

Open access to preclinical information to the general scientific community facilitates collaboration and more effective drug development. Therefore, we assessed the availability of preclinical bleomycin data on PubMed for the 145 clinical trials that have tested or are currently testing a total of 93 unique compounds or combinations for the treatment of IPF. Out of these 93 interventions, no associated animal data was found for 67 (72%) on PubMed. Of the 26 interventions with available preclinical data, 20 were assessed therapeutically. Without comprehensive information available to the scientific community, it is impossible to understand why certain compounds may have failed in clinical trials and whether this can be attributed to inappropriate use of preclinical models. Therefore, better transparency and publication of both positive and negative experimental data is needed in pulmonary fibrosis focused animal models.

It is important to note that the bleomycin model has some notable limitations, which include the spontaneous reversal of fibrosis seen in young mice at around 21 to 24 days following injury. Despite the limitations of the model, it remains the best characterized and most commonly used preclinical model for IPF. The preclinical therapeutic success in the bleomycin model of nintedanib and pirfenidone, which later went on to be clinically approved for IPF, suggests the usefulness of this model at predicting clinical success. Therefore, identifying and advocating for ways in which this model can be more effectively used will facilitate better translation of basic science findings into fruitful drug development for pulmonary fibrosis. In this current analysis of the field, while a more thoughtful use of the model throughout the literature is evident, there is still a substantial lack of data sharing. Therefore, continued improvement of appropriate therapeutic timing, a thorough characterization of inflammation in preventatively timed studies, and more transparency in preclinical data are needed. This will further optimize the use of this regularly used preclinical model, and may facilitate cutting edge drug development for pulmonary fibrosis.

Concluding remarks

The research discussed in Chapters 2-4 include: 1) a summary of the current knowledge on ECM-cell interactions and their role in ILD; 2) establishing a novel decellularization system to create nonfibrotic and fibrotic 3D ECM scaffolds to directly study the physiological and pathological ECM – fibroblast interactions that dictate fibrosis; and 3) evaluate the utility and use of the bleomycin model as a preclinical model for pulmonary fibrosis.

The role of the ECM as an active driver in the progression of pulmonary fibrosis is an idea that is gaining more acceptance in recent years. In this thesis, we see that the 3D ECM alone can drive both profibrotic and antifibrotic differentiation in fibroblasts. These effects are present at the structural level, and inhibiting mechanotransduction of cues from the stiff ECM attenuates the fibrotic ECM's profibrotic effect on fibroblasts. The ECM's influence on cells seems to also be present at the compositional level, where the soluble ECM proteins can also induce pro- and anti-fibrotic cellular changes. Investigating the specific ECM components driving these effects would be an integral next step to develop viable therapeutic targets for pulmonary fibrosis. Furthermore, in this chapter, we established a novel 3D *ex vivo* system to model nonfibrotic and fibrotic ECM states and used this model to study the ECM's effect on fibroblasts. As discussed, fibroblasts are not the only precursor of myofibroblasts and cellular contributors to ECM fibrosis. Therefore, investigating how other cells such as epithelial, endothelial, and

inflammatory cells will respond to the ECM microenvironments using this *ex vivo* model system is of value.

Lastly, since the ECM plays a key role in progressive fibrosis, we see the importance of establishing the fibrotic ECM to appropriately model progressive pulmonary fibrosis in preclinical models. It is important to note that in the bleomycin model there is overlap between the inflammatory and fibrotic phases, with the initial strong inflammatory response taking up to 10 days post-injury to completely clear. In the study in chapter 4, the 7 day time point is used as a separation between the inflammatory and fibrotic phases. Since there is no clear distinction between the two phases, using the 7 day time point to differentiate between preventative and therapeutic studies is a limitation that needs to be considered. With this in mind, we compared our current results to the initial assessment completed in 2008 which used the same characterization criteria. Over the past decade, there has been a positive shift in effective therapeutic timing. In this current publication, we also advocate for improved inflammation characterization in preventative studies, as well as transparency of preclinical data of clinically tested interventions. Since the use of the bleomycin model to study interventions for pulmonary fibrosis continues to increase, it would be interesting to see how these changes are implemented into the field over the next few years. Through this, we can ensure continued improvements in disease modeling and drug development, which may translate to more effective treatments for this devastating disease in the future.

References for Chapters 1 & 5

1. Selman M, Pardo A. Revealing the Pathogenic and Aging-related Mechanisms of the Enigmatic Idiopathic Pulmonary Fibrosis. An Integral Model. *American Journal of Respiratory and Critical Care Medicine* 2014; 189: 1161–1172.

2. Hopkins RB, Burke N, Fell C, Dion G, Kolb M. Epidemiology and survival of idiopathic pulmonary fibrosis from national data in Canada. *Eur. Respir. J.* 2016; 48: 187–195.

3. Raghu G, Chen S-Y, Yeh W-S, Maroni B, Li Q, Lee Y-C, Collard HR. Idiopathic pulmonary fibrosis in US Medicare beneficiaries aged 65 years and older: incidence, prevalence, and survival, 2001-11. *Lancet Respir Med* 2014; 2: 566–572.

4. Nalysnyk L, Cid-Ruzafa J, Rotella P, Esser D. Incidence and prevalence of idiopathic pulmonary fibrosis: review of the literature. *Eur Respir Rev* 2012; 21: 355–361.

5. Gross TJ, Hunninghake GW. Idiopathic Pulmonary Fibrosis. *New England Journal of Medicine* 2001; 345: 517–525.

6. Raghu G, Selman M. Nintedanib and Pirfenidone. New Antifibrotic Treatments Indicated for Idiopathic Pulmonary Fibrosis Offer Hopes and Raises Questions. *Am J Respir Crit Care Med* 2015; 191: 252–254.

7. Raghu G, Collard HR, Egan JJ, Martinez FJ, Behr J, Brown KK, Colby TV, Cordier J-F, Flaherty KR, Lasky JA, Lynch DA, Ryu JH, Swigris JJ, Wells AU, Ancochea J, Bouros D, Carvalho C, Costabel U, Ebina M, Hansell DM, Johkoh T, Kim DS, King TE, Kondoh Y, Myers J, Müller NL, Nicholson AG, Richeldi L, Selman M, Dudden RF, et al. An official ATS/ERS/JRS/ALAT statement: idiopathic pulmonary fibrosis: evidence-based guidelines for diagnosis and management. *Am. J. Respir. Crit. Care Med.* 2011; 183: 788–824.

8. Bellaye P-S, Kolb M. Why do patients get idiopathic pulmonary fibrosis? Current concepts in the pathogenesis of pulmonary fibrosis. *BMC Med* 2015; 13: 176.

9. Baum J, Duffy HS. Fibroblasts and Myofibroblasts: What are we talking about? *J Cardiovasc Pharmacol* 2011; 57: 376–379.

10. Hinz B, Phan SH, Thannickal VJ, Galli A, Bochaton-Piallat M-L, Gabbiani G. The myofibroblast: one function, multiple origins. *Am. J. Pathol.* 2007; 170: 1807–1816.

11. Moeller A, Gilpin SE, Ask K, Cox G, Cook D, Gauldie J, Margetts PJ, Farkas L, Dobranowski J, Boylan C, O'Byrne PM, Strieter RM, Kolb M. Circulating fibrocytes are an indicator of poor prognosis in idiopathic pulmonary fibrosis. *Am. J. Respir. Crit. Care Med.* 2009; 179: 588–594.

12. Desmoulière A, Redard M, Darby I, Gabbiani G. Apoptosis mediates the decrease in cellularity during the transition between granulation tissue and scar. *Am J Pathol* 1995; 146: 56–66.

13. Cox TR, Erler JT. Remodeling and homeostasis of the extracellular matrix: implications for fibrotic diseases and cancer. *Dis Model Mech* 2011; 4: 165–178.

14. Thannickal VJ, Horowitz JC. Evolving Concepts of Apoptosis in Idiopathic Pulmonary Fibrosis. *Proc Am Thorac Soc* 2006; 3: 350–356.

15. King TE, Schwarz MI, Brown K, Tooze JA, Colby TV, Waldron JA, Flint A, Thurlbeck W, Cherniack RM. Idiopathic pulmonary fibrosis: relationship between histopathologic features and mortality. *Am. J. Respir. Crit. Care Med.* 2001; 164: 1025–1032.

16. Zhang K, Rekhter MD, Gordon D, Phan SH. Myofibroblasts and their role in lung collagen gene expression during pulmonary fibrosis. A combined immunohistochemical and in situ hybridization study. *Am J Pathol* 1994; 145: 114–125.

17. Chapman HA. Epithelial-mesenchymal interactions in pulmonary fibrosis. *Annu. Rev. Physiol.* 2011; 73: 413–435.

18. Lee K, Nelson CM. New insights into the regulation of epithelial-mesenchymal transition and tissue fibrosis. *Int Rev Cell Mol Biol* 2012; 294: 171–221.

19. Keeley EC, Mehrad B, Strieter RM. The role of fibrocytes in fibrotic diseases of the lungs and heart. *Fibrogenesis Tissue Repair* 2011; 4: 2.

20. Bellini A, Mattoli S. The role of the fibrocyte, a bone marrow-derived mesenchymal progenitor, in reactive and reparative fibroses. *Lab. Invest.* 2007; 87: 858–870.

21. Yamaguchi M, Hirai S, Tanaka Y, Sumi T, Miyajima M, Mishina T, Yamada G, Otsuka M, Hasegawa T, Kojima T, Niki T, Watanabe A, Takahashi H, Sakuma Y. Fibroblastic foci, covered with alveolar epithelia exhibiting epithelial-mesenchymal transition, destroy alveolar septa by disrupting blood flow in idiopathic pulmonary fibrosis. *Lab. Invest.* 2017; 97: 232–242.

22. Zeisberg M, Hanai J, Sugimoto H, Mammoto T, Charytan D, Strutz F, Kalluri R. BMP-7 counteracts TGF-β1–induced epithelial-to-mesenchymal transition and reverses chronic renal injury. *Nature Medicine* 2003; 9: 964–968.

23. Zeisberg M, Bottiglio C, Kumar N, Maeshima Y, Strutz F, Müller GA, Kalluri R. Bone morphogenic protein-7 inhibits progression of chronic renal fibrosis associated

with two genetic mouse models. *Am. J. Physiol. Renal Physiol.* 2003; 285: F1060-1067.

24. Féréol S, Fodil R, Pelle G, Louis B, Isabey D. Cell mechanics of alveolar epithelial cells (AECs) and macrophages (AMs). *Respir Physiol Neurobiol* 2008; 163: 3–16.

25. Marmai C, Sutherland RE, Kim KK, Dolganov GM, Fang X, Kim SS, Jiang S, Golden JA, Hoopes CW, Matthay MA, Chapman HA, Wolters PJ. Alveolar epithelial cells express mesenchymal proteins in patients with idiopathic pulmonary fibrosis. *Am. J. Physiol. Lung Cell Mol. Physiol.* 2011; 301: L71-78.

26. Adamson IY, Young L, Bowden DH. Relationship of alveolar epithelial injury and repair to the induction of pulmonary fibrosis. *Am J Pathol* 1988; 130: 377–383.

27. Uhal BD, Joshi I, Hughes WF, Ramos C, Pardo A, Selman M. Alveolar epithelial cell death adjacent to underlying myofibroblasts in advanced fibrotic human lung. *Am. J. Physiol.* 1998; 275: L1192-1199.

28. Jolly MK, Ward C, Eapen MS, Myers S, Hallgren O, Levine H, Sohal SS. Epithelial–mesenchymal transition, a spectrum of states: Role in lung development, homeostasis, and disease. *Developmental Dynamics* 2018; 247: 346–358.

29. Tanjore H, Cheng D-S, Degryse AL, Zoz DF, Abdolrasulnia R, Lawson WE, Blackwell TS. Alveolar epithelial cells undergo epithelial-to-mesenchymal transition in response to endoplasmic reticulum stress. *J. Biol. Chem.* 2011; 286: 30972–30980.

30. Block ER. Pulmonary endothelial cell pathobiology: implications for acute lung injury. *Am. J. Med. Sci.* 1992; 304: 136–144.

31. Kalluri R, Zeisberg M. Fibroblasts in cancer. *Nat. Rev. Cancer* 2006; 6: 392–401.

32. Zeisberg EM, Tarnavski O, Zeisberg M, Dorfman AL, McMullen JR, Gustafsson E, Chandraker A, Yuan X, Pu WT, Roberts AB, Neilson EG, Sayegh MH, Izumo S, Kalluri R. Endothelial-to-mesenchymal transition contributes to cardiac fibrosis. *Nat. Med.* 2007; 13: 952–961.

33. Hashimoto N, Phan SH, Imaizumi K, Matsuo M, Nakashima H, Kawabe T, Shimokata K, Hasegawa Y. Endothelial-mesenchymal transition in bleomycin-induced pulmonary fibrosis. *Am. J. Respir. Cell Mol. Biol.* 2010; 43: 161–172.

34. Armulik A, Genové G, Betsholtz C. Pericytes: developmental, physiological, and pathological perspectives, problems, and promises. *Dev. Cell* 2011; 21: 193–215.

35. Greenhalgh SN, Iredale JP, Henderson NC. Origins of fibrosis: pericytes take centre stage. *F1000Prime Rep* [Internet] 2013 [cited 2019 Apr 20]; 5Available from: https://www.ncbi.nlm.nih.gov/pmc/articles/PMC3768328/.

36. Rock JR, Barkauskas CE, Cronce MJ, Xue Y, Harris JR, Liang J, Noble PW, Hogan BLM. Multiple stromal populations contribute to pulmonary fibrosis without evidence for epithelial to mesenchymal transition. *Proc. Natl. Acad. Sci. U.S.A.* 2011; 108: E1475-1483.

37. Sava P, Ramanathan A, Dobronyi A, Peng X, Sun H, Ledesma-Mendoza A, Herzog EL, Gonzalez AL. Human pericytes adopt myofibroblast properties in the microenvironment of the IPF lung. *JCI Insight* [Internet] [cited 2019 Apr 20]; 2Available from: https://www.ncbi.nlm.nih.gov/pmc/articles/PMC5752282/.

38. Mori L, Bellini A, Stacey MA, Schmidt M, Mattoli S. Fibrocytes contribute to the myofibroblast population in wounded skin and originate from the bone marrow. *Exp. Cell Res.* 2005; 304: 81–90.

39. Abe R, Donnelly SC, Peng T, Bucala R, Metz CN. Peripheral Blood Fibrocytes: Differentiation Pathway and Migration to Wound Sites. *The Journal of Immunology* 2001; 166: 7556–7562.

40. Heukels P, van Hulst JAC, van Nimwegen M, Boorsma CE, Melgert BN, van den Toorn LM, Boomars KAT, Wijsenbeek MS, Hoogsteden H, von der Thüsen JH, Hendriks RW, Kool M, van den Blink B. Fibrocytes are increased in lung and peripheral blood of patients with idiopathic pulmonary fibrosis. *Respiratory Research* 2018; 19: 90.

41. Rangarajan S, Locy ML, Luckhardt TR, Thannickal VJ. Targeted therapy for idiopathic pulmonary fibrosis: where to now? *Drugs* 2016; 76: 291–300.

42. Kulkarni T, O'Reilly P, Antony VB, Gaggar A, Thannickal VJ. Matrix Remodeling in Pulmonary Fibrosis and Emphysema. *Am J Respir Cell Mol Biol* 2016; 54: 751–760.

43. Kuhn C, Boldt J, King TE, Crouch E, Vartio T, McDonald JA. An immunohistochemical study of architectural remodeling and connective tissue synthesis in pulmonary fibrosis. *Am. Rev. Respir. Dis.* 1989; 140: 1693–1703.

44. Blaauboer ME, Boeijen FR, Emson CL, Turner SM, Zandieh-Doulabi B, Hanemaaijer R, Smit TH, Stoop R, Everts V. Extracellular matrix proteins: A positive feedback loop in lung fibrosis? *Matrix Biology* 2014; 34: 170–178.

45. Serini G, Bochaton-Piallat ML, Ropraz P, Geinoz A, Borsi L, Zardi L, Gabbiani G. The fibronectin domain ED-A is crucial for myofibroblastic phenotype induction by transforming growth factor-beta1. *J. Cell Biol.* 1998; 142: 873–881.

46. Wells RG. The role of matrix stiffness in regulating cell behavior. *Hepatology* 2008; 47: 1394–1400.

47. Blakney AK, Swartzlander MD, Bryant SJ. The effects of substrate stiffness on the in vitro activation of macrophages and in vivo host response to poly(ethylene glycol)-based hydrogels. *J Biomed Mater Res A* 2012; 100: 1375–1386.

48. Kung C. A possible unifying principle for mechanosensation. *Nature* 2005; 436: 647–654.

49. Cantor RS. Lateral Pressures in Cell Membranes: A Mechanism for Modulation of Protein Function. *The Journal of Physical Chemistry B* 1997; 101: 1723–1725.

50. Na S, Collin O, Chowdhury F, Tay B, Ouyang M, Wang Y, Wang N. Rapid signal transduction in living cells is a unique feature of mechanotransduction. *Proceedings of the National Academy of Sciences* 2008; 105: 6626–6631.

51. Mitrossilis D, Fouchard J, Pereira D, Postic F, Richert A, Saint-Jean M, Asnacios A. Real-time single-cell response to stiffness. *Proceedings of the National Academy of Sciences* 2010; 107: 16518–16523.

52. Sukharev S, Sachs F. Molecular force transduction by ion channels – diversity and unifying principles. *Journal of Cell Science* 2012; 125: 3075–3083.

53. Eisenberg JL, Safi A, Wei X, Espinosa HD, Budinger GS, Takawira D, Hopkinson SB, Jones JC. Substrate stiffness regulates extracellular matrix deposition by alveolar epithelial cells. *Res Rep Biol* 2011; 2011: 1–12.

54. Balestrini JL, Chaudhry S, Sarrazy V, Koehler A, Hinz B. The mechanical memory of lung myofibroblasts. *Integr Biol (Camb)* 2012; 4: 410–421.

55. Marinković A, Liu F, Tschumperlin DJ. Matrices of physiologic stiffness potently inactivate idiopathic pulmonary fibrosis fibroblasts. *Am. J. Respir. Cell Mol. Biol.* 2013; 48: 422–430.

56. Huang X, Yang N, Fiore VF, Barker TH, Sun Y, Morris SW, Ding Q, Thannickal VJ, Zhou Y. Matrix stiffness-induced myofibroblast differentiation is mediated by intrinsic mechanotransduction. *Am. J. Respir. Cell Mol. Biol.* 2012; 47: 340–348.

57. Brown AC, Fiore VF, Sulchek TA, Barker TH. Physical and chemical microenvironmental cues orthogonally control the degree and duration of fibrosis-associated epithelial-to-mesenchymal transitions. *J. Pathol.* 2013; 229: 25–35.

58. Heise RL, Stober V, Cheluvaraju C, Hollingsworth JW, Garantziotis S. Mechanical stretch induces epithelial-mesenchymal transition in alveolar epithelia via hyaluronan activation of innate immunity. *J. Biol. Chem.* 2011; 286: 17435–17444.

59. Leight JL, Wozniak MA, Chen S, Lynch ML, Chen CS. Matrix rigidity regulates a switch between TGF-β1-induced apoptosis and epithelial-mesenchymal transition. *Mol. Biol. Cell* 2012; 23: 781–791.

60. Patel NR, Bole M, Chen C, Hardin CC, Kho AT, Mih J, Deng L, Butler J, Tschumperlin D, Fredberg JJ, Krishnan R, Koziel H. Cell Elasticity Determines Macrophage Function. *PLOS ONE* 2012; 7: e41024.

61. Fowlkes V, Wilson CG, Carver W, Goldsmith EC. Mechanical loading promotes mast cell degranulation via RGD-integrin dependent pathways. *J Biomech* 2013; 46: 788–795.

62. Shimbori C, Upagupta C, Bellaye P-S, Ayaub EA, Sato S, Yanagihara T, Zhou Q, Ognjanovic A, Ask K, Gauldie J, Forsythe P, Kolb MRJ. Mechanical stress-induced mast cell degranulation activates TGF-β1 signalling pathway in pulmonary fibrosis. *Thorax* 2019; .

63. Neve A, Cantatore FP, Maruotti N, Corrado A, Ribatti D. Extracellular Matrix Modulates Angiogenesis in Physiological and Pathological Conditions. *Biomed Res Int* [Internet] 2014 [cited 2019 Feb 4]; 2014Available from: https://www.ncbi.nlm.nih.gov/pmc/articles/PMC4052469/.

64. Veidal SS, Karsdal MA, Vassiliadis E, Nawrocki A, Larsen MR, Nguyen QHT, Hägglund P, Luo Y, Zheng Q, Vainer B, Leeming DJ. MMP Mediated Degradation of Type VI Collagen Is Highly Associated with Liver Fibrosis – Identification and Validation of a Novel Biochemical Marker Assay. Gullberg D, editor. *PLoS ONE* 2011; 6: e24753.

65. Collins SL, Black KE, Chan-Li Y, Ahn Y-H, Cole PA, Powell JD, Horton MR. Hyaluronan Fragments Promote Inflammation by Down-Regulating the Anti-inflammatory A2a Receptor. *Am J Respir Cell Mol Biol* 2011; 45: 675–683.

66. Schultz GS, Wysocki A. Interactions between extracellular matrix and growth factors in wound healing. *Wound Repair and Regeneration* 2009; 17: 153–162.

67. Froese AR, Shimbori C, Bellaye P-S, Inman M, Obex S, Fatima S, Jenkins G, Gauldie J, Ask K, Kolb M. Stretch-induced Activation of Transforming Growth Factor-β1 in Pulmonary Fibrosis. *Am. J. Respir. Crit. Care Med.* 2016; 194: 84–96.

68. Iwasaki H, Eguchi S, Ueno H, Marumo F, Hirata Y. Mechanical stretch stimulates growth of vascular smooth muscle cells via epidermal growth factor receptor. *Am. J. Physiol. Heart Circ. Physiol.* 2000; 278: H521-529.

69. Border WA, Noble NA. Transforming growth factor beta in tissue fibrosis. *N. Engl. J. Med.* 1994; 331: 1286–1292.

70. Westergren-Thorsson G, Hernnäs J, Särnstrand B, Oldberg A, Heinegård D, Malmström A. Altered expression of small proteoglycans, collagen, and transforming growth factor-beta 1 in developing bleomycin-induced pulmonary fibrosis in rats. *J. Clin. Invest.* 1993; 92: 632–637.

71. Khalil N, O'Connor RN, Unruh HW, Warren PW, Flanders KC, Kemp A, Bereznay OH, Greenberg AH. Increased production and immunohistochemical localization of transforming growth factor-beta in idiopathic pulmonary fibrosis. *Am. J. Respir. Cell Mol. Biol.* 1991; 5: 155–162.

72. Asano S, Ito S, Takahashi K, Furuya K, Kondo M, Sokabe M, Hasegawa Y. Matrix stiffness regulates migration of human lung fibroblasts. *Physiol Rep* [Internet] 2017 [cited 2019 Feb 8]; 5Available from: https://www.ncbi.nlm.nih.gov/pmc/articles/PMC5430127/.

73. Booth AJ, Hadley R, Cornett AM, Dreffs AA, Matthes SA, Tsui JL, Weiss K, Horowitz JC, Fiore VF, Barker TH, Moore BB, Martinez FJ, Niklason LE, White ES. Acellular Normal and Fibrotic Human Lung Matrices as a Culture System for In Vitro Investigation. *Am J Respir Crit Care Med* 2012; 186: 866–876.

74. Tashiro J, Rubio GA, Limper AH, Williams K, Elliot SJ, Ninou I, Aidinis V, Tzouvelekis A, Glassberg MK. Exploring Animal Models That Resemble Idiopathic Pulmonary Fibrosis. *Frontiers in Medicine* [Internet] 2017 [cited 2018 May 26]; 4Available from: http://journal.frontiersin.org/article/10.3389/fmed.2017.00118/full.

75. B. Moore B, Lawson WE, Oury TD, Sisson TH, Raghavendran K, Hogaboam CM. Animal Models of Fibrotic Lung Disease. *Am J Respir Cell Mol Biol* 2013; 49: 167–179.

76. Bellaye P-S, Yanagihara T, Granton E, Sato S, Shimbori C, Upagupta C, Imani J, Hambly N, Ask K, Gauldie J, Iglarz M, Kolb M. Macitentan reduces progression of TGF-β1-induced pulmonary fibrosis and pulmonary hypertension. *Eur. Respir. J.* 2018; 52.

77. Izbicki G, Segel MJ, Christensen TG, Conner MW, Breuer R. Time course of bleomycin-induced lung fibrosis. *Int J Exp Pathol* 2002; 83: 111–119.

78. Chung MP, Monick MM, Hamzeh NY, Butler NS, Powers LS, Hunninghake GW. Role of Repeated Lung Injury and Genetic Background in Bleomycin-Induced Fibrosis. *Am J Respir Cell Mol Biol* 2003; 29: 375–380.

79. Phan SH, Armstrong G, Sulavik MC, Schrier D, Johnson KJ, Ward PA. A Comparative Study of Pulmonary Fibrosis Induced by Bleomycin and an O2 Metabolite Producing Enzyme System. *CHEST* 1983; 83: 44S-45S.

80. Lawson WE, Polosukhin VV, Stathopoulos GT, Zoia O, Han W, Lane KB, Li B, Donnelly EF, Holburn GE, Lewis KG, Collins RD, Hull WM, Glasser SW, Whitsett JA, Blackwell TS. Increased and prolonged pulmonary fibrosis in surfactant protein C-deficient mice following intratracheal bleomycin. *Am. J. Pathol.* 2005; 167: 1267–1277.

81. Chua F, Gauldie J, Laurent GJ. Pulmonary Fibrosis. *Am J Respir Cell Mol Biol* 2005; 33: 9–13.

82. Bonnans C, Chou J, Werb Z. Remodelling the extracellular matrix in development and disease. *Nature Reviews Molecular Cell Biology* 2014; 15: 786–801.

83. Lu P, Takai K, Weaver VM, Werb Z. Extracellular Matrix Degradation and Remodeling in Development and Disease. *Cold Spring Harbor Perspectives in Biology* 2011; 3: a005058–a005058.

84. Rozario T, DeSimone DW. The extracellular matrix in development and morphogenesis: A dynamic view. *Developmental Biology* 2010; 341: 126–140.

85. Papachroni KK, Karatzas DN, Papavassiliou KA, Basdra EK, Papavassiliou AG. Mechanotransduction in osteoblast regulation and bone disease. *Trends in Molecular Medicine* 2009; 15: 208–216.

86. Sittichockechaiwut A, Scutt AM, Ryan AJ, Bonewald LF, Reilly GC. Use of rapidly mineralising osteoblasts and short periods of mechanical loading to accelerate matrix maturation in 3D scaffolds. *Bone* 2009; 44: 822–829.

87. Petrie RJ, Yamada KM. At the leading edge of three-dimensional cell migration. *J Cell Sci* 2012; 125: 5917–5926.

88. Lee JY, Chang JK, Dominguez AA, Lee H-P, Nam S, Chang J, Varma S, Qi LS, West RB, Chaudhuri O. YAP-independent mechanotransduction drives breast cancer progression. *Nat Commun* 2019; 10: 1848.

89. Mishra DK, Sakamoto JH, Thrall MJ, Baird BN, Blackmon SH, Ferrari M, Kurie JM, Kim MP. Human Lung Cancer Cells Grown in an Ex Vivo 3D Lung Model

Produce Matrix Metalloproteinases Not Produced in 2D Culture. Tsilibary EC, editor. *PLoS ONE* 2012; 7: e45308.

90. Erler JT, Weaver VM. Three-dimensional context regulation of metastasis. *Clin. Exp. Metastasis* 2009; 26: 35–49.

91. Edmondson R, Broglie JJ, Adcock AF, Yang L. Three-Dimensional Cell Culture Systems and Their Applications in Drug Discovery and Cell-Based Biosensors. *Assay Drug Dev Technol* 2014; 12: 207–218.

92. Huh D, Matthews BD, Mammoto A, Montoya-Zavala M, Hsin HY, Ingber DE. Reconstituting Organ-Level Lung Functions on a Chip. *Science* 2010; 328: 1662–1668.

93. Ermis M, Antmen E, Hasirci V. Micro and Nanofabrication methods to control cell-substrate interactions and cell behavior: A review from the tissue engineering perspective. *Bioactive Materials* 2018; 3: 355–369.

94. Booth AJ, Hadley R, Cornett AM, Dreffs AA, Matthes SA, Tsui JL, Weiss K, Horowitz JC, Fiore VF, Barker TH, Moore BB, Martinez FJ, Niklason LE, White ES. Acellular normal and fibrotic human lung matrices as a culture system for in vitro investigation. *Am. J. Respir. Crit. Care Med.* 2012; 186: 866–876.

95. Balestrini JL, Chaudhry S, Sarrazy V, Koehler A, Hinz B. The mechanical memory of lung myofibroblasts. *Integr Biol (Camb)* 2012; 4: 410–421.

96. Evans RA, Tian YC, Steadman R, Phillips AO. TGF-beta1-mediated fibroblast-myofibroblast terminal differentiation-the role of Smad proteins. *Exp. Cell Res.* 2003; 282: 90–100.

97. Bayreuther K, Rodemann HP, Hommel R, Dittmann K, Albiez M, Francz PI. Human skin fibroblasts in vitro differentiate along a terminal cell lineage. *Proc Natl Acad Sci U S A* 1988; 85: 5112–5116.

98. Garrison G, Huang SK, Okunishi K, Scott JP, Kumar Penke LR, Scruggs AM, Peters-Golden M. Reversal of myofibroblast differentiation by prostaglandin E(2). *Am. J. Respir. Cell Mol. Biol.* 2013; 48: 550–558.

99. Hecker L, Jagirdar R, Jin T, Thannickal VJ. Reversible differentiation of myofibroblasts by MyoD. *Experimental Cell Research* 2011; 317: 1914–1921.

100. Huang X, Yang N, Fiore VF, Barker TH, Sun Y, Morris SW, Ding Q, Thannickal VJ, Zhou Y. Matrix stiffness-induced myofibroblast differentiation is mediated by intrinsic mechanotransduction. *Am. J. Respir. Cell Mol. Biol.* 2012; 47: 340–348.

101. Upagupta C, Shimbori C, Alsilmi R, Kolb M. Matrix abnormalities in pulmonary fibrosis. *European Respiratory Review* 2018; 27: 180033.

102. Parker MW, Rossi D, Peterson M, Smith K, Sikström K, White ES, Connett JE, Henke CA, Larsson O, Bitterman PB. Fibrotic extracellular matrix activates a profibrotic positive feedback loop. *J. Clin. Invest.* 2014; 124: 1622–1635.

103. Bellaye P-S, Shimbori C, Upagupta C, Sato S, Shi W, Gauldie J, Ask K, Kolb M. Lysyl Oxidase-Like 1 Protein Deficiency Protects Mice from Adenoviral Transforming Growth Factor-β1-induced Pulmonary Fibrosis. *Am. J. Respir. Cell Mol. Biol.* 2018; 58: 461–470.

104. Xiao Q, Ge G. Lysyl oxidase, extracellular matrix remodeling and cancer metastasis. *Cancer Microenviron* 2012; 5: 261–273.

105. Averill F, Albertson T e., Baratz D m., Chaudhary S, Mobin S, O'Brien T, Scholand M b., Whelan T p. m., Poyurovsky M, Schueller O, Ryan J, Gibson K f. A Phase 2 Trial of KD025 to Assess Efficacy, Safety and Tolerability in Patients with Idiopathic Pulmonary Fibrosis. *C97. DIFFUSE PARENCHYMAL LUNG DISEASES: EVALUATION, OUTCOMES, AND TRIALS* [Internet] American Thoracic Society; 2018 [cited 2019 Feb 1]. p. A5927–A5927Available from: https://www.atsjournals.org/doi/abs/10.1164/ajrccm-conference.2018.197.1_MeetingAbstracts.A5927.

106. Moeller A, Ask K, Warburton D, Gauldie J, Kolb M. The bleomycin animal model: A useful tool to investigate treatment options for idiopathic pulmonary fibrosis? *The International Journal of Biochemistry & Cell Biology* 2008; 40: 362–382.

107. Ahluwalia N, Shea BS, Tager AM. New Therapeutic Targets in Idiopathic Pulmonary Fibrosis. Aiming to Rein in Runaway Wound-Healing Responses. *Am J Respir Crit Care Med* 2014; 190: 867–878.

108. Schroll S, Arzt M, Sebah D, Nüchterlein M, Blumberg F, Pfeifer M. Improvement of bleomycin-induced pulmonary hypertension and pulmonary fibrosis by the endothelin receptor antagonist Bosentan. *Respir Physiol Neurobiol* 2010; 170: 32–36.

109. Chilakapati SR. Amelioration of bleomycin-induced pulmonary fibrosis in a mouse model by a combination therapy of bosentan and imatinib. 2015; 41: 173–188.

110. Zuo W-L, Zhao J-M, Huang J-X, Zhou W, Lei Z-H, Huang Y-M, Huang Y-F, Li H-G. Effect of bosentan is correlated with MMP-9/TIMP-1 ratio in bleomycin-induced pulmonary fibrosis. *Biomedical Reports* 2017; 6: 201–205.

111. Gamze K, Mehmet HM, Deveci F, Turgut T, Ilhan F, Ozercan I. Effect of bosentan on the production of proinflammatory cytokines in a rat model of emphysema. *Exp. Mol. Med.* 2007; 39: 614–620.

112. King TE, Behr J, Brown KK, du Bois RM, Lancaster L, de Andrade JA, Stähler G, Leconte I, Roux S, Raghu G. BUILD-1: A Randomized Placebo-controlled Trial of Bosentan in Idiopathic Pulmonary Fibrosis. *Am J Respir Crit Care Med* 2008; 177: 75–81.

113. King TE, Brown KK, Raghu G, du Bois RM, Lynch DA, Martinez F, Valeyre D, Leconte I, Morganti A, Roux S, Behr J. BUILD-3: A Randomized, Controlled Trial of Bosentan in Idiopathic Pulmonary Fibrosis. *Am J Respir Crit Care Med* 2011; 184: 92–99.